

Virginia Coastal Resilience Master Plan, Phase II

Appendix A - Flood Hazard Data Development



Table of Contents

A. Introduction	1
B. DCR Planning Scenarios	1
C. Terrain Base Data	2
D. Coastal Flood Hazard Data	3
E. Pluvial Flood Hazard Data	4
E.1 Source	4
E.2 Data Preparation and Products	6
E.2.i Pluvial Planning Scenario Reference Tables	7
E.2.ii Pluvial Recurrence Interval Reference Table	9
E.2.iii Pluvial RAS Plan Reference Table	9
E.2.iv Pluvial Derived Planning Scenario Flood Depth Rasters	10
E.2.v Pluvial Graduated Annual Exceedance Probability (AEP) Rasters	12
E.2.vi Pluvial Storm Duration of Maximum Depth Rasters	13
F. Fluvial Flood Hazard Data	15
F.1 Fluvial flood hazard area	15
F.1.i Source Data	15
F.1.ii Data Processing	15
F.1.iii Items of Interest	17
F.2 Fluvial Multi-Frequency Depth Grids	19
G. Combined Flood Coverages	21
G.1 Data Sources	21
G.2 Flood Type Present	22
G.3 Flood Type Dominant	24
H. References	26
Addendum A: Pluvial Modeling Technical Report	27

Figures and Photos

FIGURE 1: MODEL SUB-BASINS ACROSS CRMP STUDY AREA, SHOWING MODELS WITH TIDAL AND NON-TIDAL BOUNDARY CONDITIONS AS SHOWN IN THE DCR CRMP PLUVIAL MODEL CATALOG APP AVAILABLE ON THE DCR VIRGINIA FLOOD RESILIENCE OPEN DATA PORTAL.	5
FIGURE 2: EXAMPLE OF MARISA CHANGE FACTORS FOR RCP 4.5 (LEFT) AND RCP 8.5 (RIGHT) AT THE 50TH PERCENTILE, AS COMPARED TO THE NOAA ATLAS 14 BASELINE.	8
FIGURE 3: PERCENT INCREASE COMPARED TO NOAA ATLAS 14 BASELINE FOR RCP 4.5 50TH AND 90TH PERCENTILE VALUES, AVERAGED ACROSS EVENT RETURN PERIODS.	8
FIGURE 4: EXAMPLE PLUVIAL DEPTH GRID PRODUCT.	11
FIGURE 5: EXAMPLE OF PLUVIAL GRADUATED AEP RASTER.	13
FIGURE 6: EXAMPLE OF THE PLUVIAL DURATION OF MAXIMUM DEPTH RASTER PRODUCT.	14
FIGURE 7: VISUAL OVERVIEW OF THE EXTENT OF THE FEMA 1% AEP FLUVIAL SPECIAL FLOOD HAZARD AREA ACROSS THE VA CRMP STUDY AREA.	17
FIGURE 8: HUC8 BOUNDARIES EVALUATED FOR THE FLUVIAL MULTI-FREQUENCY CASE STUDY.	19
FIGURE 9: CONCEPTUAL PROCESS OF "PRESENCE" RASTER.	22
FIGURE 10: EXAMPLE OUTPUT OF THE PRESENCE RASTER WITH THE PRODUCTION COLOR SCHEME.	23
FIGURE 11: CONCEPTUAL PROCESS OF "DOMINANCE" RASTER.	24
FIGURE 12: EXAMPLE COMBINED FLOOD "DOMINANCE" PRODUCT.	25

Tables

TABLE 1: OVERVIEW OF SCENARIOS AND ASSOCIATED HAZARD DATA.	2
TABLE 2: ESSENTIAL DATASETS INCLUDED IN THE PLUVIAL MODELS.	4
TABLE 3: RANGES OF PRECIPITATION TOTALS USED IN THE FIXED-INTERVAL APPROACH.	6
TABLE 4: EXAMPLE PLUVIAL RECURRENCE INTERVAL REFERENCE TABLE.	9
TABLE 5: EXAMPLE PLUVIAL RAS PLAN REFERENCE TABLE.	10
TABLE 6: CLASSIFICATION SCHEMA FOR PLUVIAL GRADUATED FLOOD EXTENT RASTERS.	12
TABLE 7: CLASSIFICATION SCHEMA FOR THE DURATION OF MAXIMUM DEPTH RASTERS.	14
TABLE 8: SUMMARY OF SOURCE DATASETS INCLUDED IN THE FLUVIAL 1% AEP REPRESENTATION FOR THE CRMP, PHASE 2.	16
TABLE 9: AREAS WITH LIMITED OR NO DEPTH GRID COVERAGE IN THE FLUVIAL MULTI-FREQUENCY CASE STUDY AREA.	20
TABLE 10: TEST SITES AND ASSOCIATED DEPTHS.	21
TABLE 11: PRESENCE RASTER CLASSIFICATION TYPES AND VALUES.	23
TABLE 12: DOMINANCE RASTER CLASSIFICATION TYPES AND VALUES.	24

Acronyms and Abbreviations

AEP	Annual Exceedance Probability
COG	Cloud-Optimized Geotiffs
CoNED	USGS Coastal National Elevation Database
CRMP	Coastal Resilience Master Plan
DCR	Virginia Department of Conservation and Recreation
DFIRM	Digital Flood Insurance Rate Map
FEMA	Federal Emergency Management Agency
FFRD	Future of Flood Risk Data
HUC	Hydrologic Unit Code
IPCC	Intergovernmental Panel on Climate Change
MARISA	Mid-Atlantic Regional Integrated Sciences and Assessments Program
MHW	Mean High Water
NACCS	North Atlantic Comprehensive Coastal Study
NFHL	National Flood Hazard Layer
NOAA	National Oceanic and Atmospheric Administration
RCP	Representative Concentration Pathway
RSLR	Relative Sea Level Rise
SFHA	Special Flood Hazard Area
SLR	Sea Level Rise
SSURGO	U.S Department of Agriculture, Soil Survey Geographic Database
USACE	U.S. Army Corps of Engineers

A. Introduction

This document provides a technical overview of the data and methods used to develop flood hazard data for Phase II of the Virginia Coastal Resilience Master Plan (CRMP). Phase I of the CRMP included only coastal flood hazard data (Dewberry, 2022). Phase II expands the flood hazards to also include pluvial and fluvial hazards. DCR developed robust multi-frequency pluvial data in response to stakeholder feedback and priorities from Phase I. Over 280 thousand simulations were completed to provide a wide range of existing and future rainfall conditions for the CRMP study area. Several derivative products were created from these simulations to enable use for the CRMP Phase II Impact Assessment.

Fluvial data were represented by the Federal Emergency Management Agency (FEMA) Special Flood Hazard Areas (SFHA). Combined representations of the three flood hazards were also developed to understand the spatial extent of each hazard, where compound flooding exists, and what hazards dominate for major flooding.

Additional changes were made to how the data are represented in terms of planning scenarios to accommodate the additional hazard data and better reflect uncertainty in future climate scenarios. An overview of these aspects is provided in the following text.

B. DCR Planning Scenarios

DCR defined five planning scenarios for the Phase II effort, considering the planning horizon, and relative climate projections (Table 1). Current and future conditions are broken out into these scenarios to help planners and decision-makers prepare for a range of possible future conditions while recognizing the uncertainty that exists in climate forecasts. The planning scenarios were developed specifically for the Coastal Resilience Master Plan with guidance from expert stakeholders, using widely accepted data sources. The planning scenarios are based on the best available data to forecast increasing coastal flood hazards and precipitation.

CRMP Phase I utilized the 2017 Federal Sea Level Rise Intermediate-High scenario as a projection of potential increases in coastal water levels for the state. Updated interagency projections were released in 2022. An essential improvement in the projections was updating the timing of the acceleration of sea levels with observation-based data. The Phase I data remain valid compared to this newer data, as the rise occurs about 10 years later for the same scenario, depending on the location across the state.

Observation-based projections show that regions of Virginia at most risk are already tracking on the mid-range of the projections.¹ In this context, CRMP Phase II has reframed the Phase I projections to better align with the latest federal science and guidance. The science behind

¹ <https://www.vims.edu/research/products/slrc/localities/nova/>

sea level rise projections continually improves, and DCR will review and make appropriate adjustments with each update of the CRMP.

Pluvial and fluvial flood hazards were new to Phase II. The Commonwealth selected the Mid-Atlantic Regional Integrated Sciences and Assessments (MARISA) Program projected intensity-duration-frequency (IDF) curves to model future precipitation conditions. The MARISA curve numbers provide an adjustment factor to NOAA Atlas-14 data, the current standard for planning and design. The adjustment factors are based on the Representative Concentration Pathway (RCP) 4.5 as described by the Intergovernmental Panel on Climate Change (IPCC), a climate scenario in which emissions peak around 2040 and then decline. Alternative emissions scenarios were considered but not included here for planning purposes. Within the RCP 4.5 scenario, the 50th percentile (known as the median or “best estimate”) and 90th percentile (representing higher climatic changes) projections were used across two time horizons: 2020-2070 and 2050-2100. Due to differences in weather patterns and climate models, the projections are not uniform across Virginia.

Table 1: Overview of Scenarios and Associated Hazard Data.

Time Horizon:	Baseline	Near Future		Far Future	
		Moderate	High	Moderate	High
Coastal Sources	CRMP Phase 1 modeling, using NOAA and FEMA water level data and the NOAA 2017 Intermediate-High relative sea level rise scenario				
	2020 Conditions	2040 Projections	2060 Projections	2060 Projections	2080 Projections
Rainfall-Driven Sources	NOAA Atlas-14 precipitation estimates with MARISA RCP 4.5 change factors				
	No Change Factor	2020-2070 50 th Percentile	2020-2070 90 th Percentile	2050-2100 50 th Percentile	2050-2100 90 th Percentile
Riverine Sources	FEMA National Flood Hazard Layer filtered to riverine flooding.				

C. Terrain Base Data

The principal source for terrain data was the composite dataset created for the CRMP Phase I effort. The dataset was primarily composed of the USGS Coastal National Elevation Database (CoNED), augmented with more recently publicly available datasets (Dewberry, 2022). The tiled 10 ft resolution cloud-optimized geotiffs (COGs) were copied from the AWS open dataset at s3://vadcr-frp/rasters/TOPO. A review of the metadata led to the identification of several updated sources (i.e., best available) from the National Elevation Dataset (Figure 2). These data were retrieved and integrated into the base terrain for the CRMP Phase II.

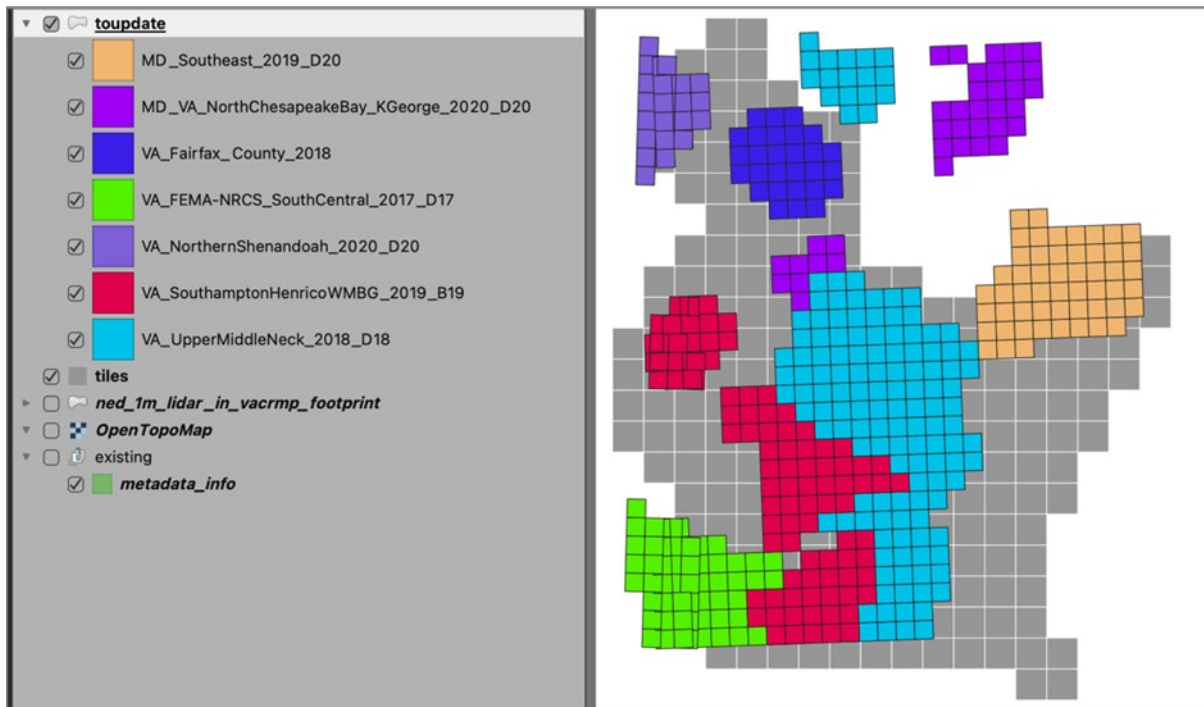


Figure 2: Map of existing coastal topography tiles (gray) and newly available USGS datasets (overlaid) used to create the project-wide DEM for pluvial modeling.

D. Coastal Flood Hazard Data

Coastal flood hazard data were leveraged from Phase I work activities and left unchanged for Phase II. The data consist of various tidal and storm surge flood elevations sourced from the National Oceanic and Atmospheric Administration (NOAA) and the Federal Emergency Management Agency (FEMA), respectively. Adjustments were made to bring the data to 2020 conditions to account for relative sea level rise from the tidal datum epoch of the source data. Future conditions (2040, 2060, 2080, 2100) represented projected sea level rise based on the NOAA 2017 Intermediate High Curve using a spatially variable representation across the state. An amplification factor derived from the U.S. Army Corps of Engineers (USACE) North Atlantic Comprehensive Coastal Study (NACCS) was applied to 2060, 2080, and 2100 conditions to represent non-linear dynamic changes to surge propagation. Data products included flood extents, depth grids, and estimated total water level conditions with wave heights. Complete documentation of the source data and production process can be found in the CRMP Phase I Appendix C – Coastal Flood Hazard Framework Report (Dewberry, 2022).

E. Pluvial Flood Hazard Data

E.1 SOURCE

Pluvial flood hazard data were developed for the CRMP Phase II based on the prioritization of needs from stakeholder feedback from Phase I. The CRMP Phase II pluvial production effort sub-divided coastal Virginia's HUC-12 watersheds into 1,830 smaller sub-catchments. Each sub-catchment represented an area ranging between 3 and 10 square miles to make the models more manageable and support uniform precipitation. The models were created using the USACE HEC-RAS version 6.1 software. The scale of this project required the creation and use of a semi-automated cloud-based system to complete about 300,000 simulations of current and future-condition rainfall events in urban, rural, and suburban communities in coastal Virginia. Each pluvial flood model required foundational input data, which includes topographic data, hydraulic friction values, surface water infiltration values, and precipitation depths, shown in Table 2. Complete documentation of data sources and treatment for model application is provided in the Pluvial Modeling Final Report (Dewberry 2024, Addendum A).

Table 2: Essential datasets included in the pluvial models.

Dataset	Model Use	Source
Topography	Terrain	CRMP Phase I, updated with more recent publicly available data in the National Elevation Dataset
Land Cover	Friction (Manning's n)	2019 National Land Cover Dataset*
Soil Type	Infiltration	U.S Department of Agriculture, Soil Survey Geographic Database (SSURGO)
Land Cover	Infiltration, first priority	2022 Chesapeake Land Use and Land Cover (LULC) Database
	Infiltration, second priority	2016 Virginia State Land Cover Dataset
	Infiltration, third priority	2021 National Land Cover Database

*The 2019 National Land Cover Dataset was used to develop the friction grid; the friction grid was created prior to the availability of the 2021 dataset.

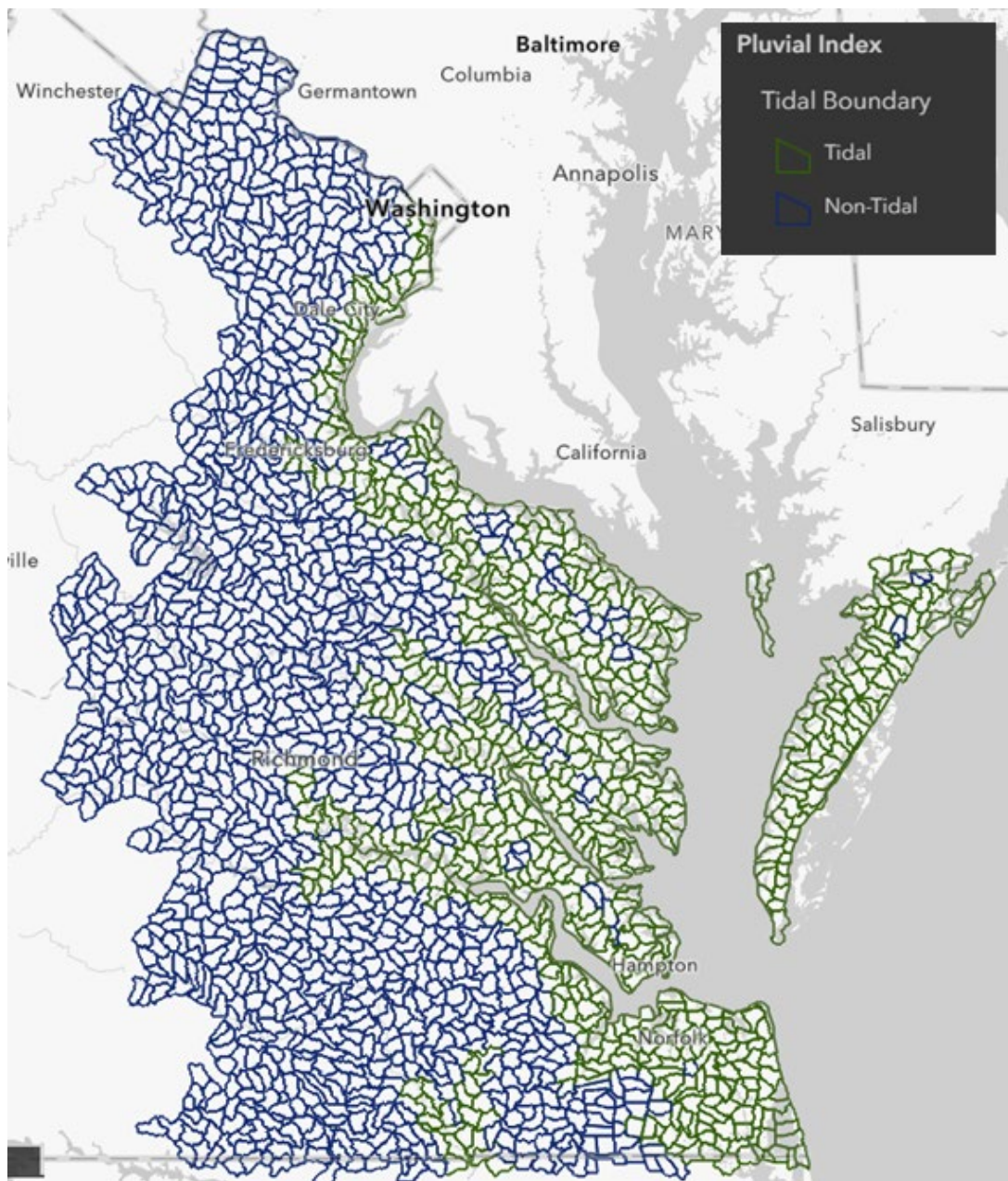


Figure 1: Model sub-basins across CRMP study area, showing models with tidal and non-tidal boundary conditions as shown in the DCR CRMP Pluvial Model Catalog App available on the DCR [Virginia Flood Resilience Open Data Portal](https://crmp.vdcr.hub.arcgis.com/).²

² Department of Conservation and Recreation. Virginia Flood Resilience Open Data Portal. <https://crmp.vdcr.hub.arcgis.com/>.

The model simulations include a wide range of precipitation scenarios at 2-, 6-, and 24-hour durations to cover the current and future conditions due to the projected increase in precipitation intensity-duration-frequency. In contrast to more traditional approaches that rely on volume estimates selected from *Atlas 14*³ at selected frequencies, this study instead developed a pre-defined range of volumes using existing conditions from *Atlas 14* at the lower end and future condition adjusted rainfall volumes using climate factors from the *MARISA*⁴ study at the upper end for each modeled storm duration. The low end of each duration was taken as the lowest 2-year precipitation for current conditions. In contrast, the high end of each duration was taken as the highest extrapolated 500-year precipitation for future conditions when considering the *MARISA* 90th percentile of Representative Concentration Pathway (RCP) 8.5 in the 2050 to 2100 time period.

As shown in Table 2 below, each delivered HEC-RAS model contains 63 pluvial plans that reflect the range of precipitation values. If a model included tidal waters, where Mean High Water (MHW) serves as a boundary condition, additional models were generated to account for increasing tailwater conditions for rising sea level projections out to 2100. In these situations, five sets of simulations totaling 315 RAS plans represent MHW in the years 2020, 2040, 2060, 2080, and 2100, which are sourced from the CRMP coastal hazard data.

Table 3: Ranges of precipitation totals used in the fixed-interval approach.

Storm Duration	Raw <i>Atlas 14</i> Depth (2-yr)	Future RCP8.5 Depth (500-yr)	Starting Rainfall Total (inch)	Ending Rainfall Total (inch)	Depth Interval Between RAS Plans (inch)	Number RAS Plans
2 hours	1.4	11.7	1.0	12.0	0.5	23
6 hours	1.8	16.6	1.0	17.0	1.0	17
24 hours	2.6	23.6	2.0	24.0	1.0	23
Total RAS Plans:						63

E.2 DATA PREPARATION AND PRODUCTS

Two groups of products were produced from the pluvial modeling effort: rainfall-interval-based and scenario-based. The specific rainfall interval-based products were based directly on the model outputs, including the HEC-RAS pluvial models, input data, and depth grid outputs. The scenario-based products are derivatives of the rainfall interval-based products.

³ National Oceanic and Atmospheric Administration. Precipitation Frequency Data Server. Hydrometeorological Design Studies Center. <https://hdsc.nws.noaa.gov/pfds/>.

⁴ Mid-Atlantic Regional Integrated Sciences and Assessments (MARISA) Program. Projected Intensity-Duration-Frequency Curve Data Tool for the Chesapeake Bay Watershed and Virginia. <https://midatlantic-idf.rcc-acis.org/>.

Phase II of the CRMP has adopted a planning framework encompassing five scenarios, as described in Section B. For each scenario, cross-referencing related the rainfall intervals to 2-, 5-, 10-, 25-, 50-, 100-, and 500-year recurrence intervals for each rainfall duration, the process is described in the subsection below.

Descriptions of methods for other derivative products, including depth grids, graduated flood representations, and duration of maximum rainfall depth, are also provided. Note that additional data products such as flow velocity or flood durations can be produced with the HEC-RAS models to support various use cases; however, these products were not created for Phase II of the CRMP.

E.2.i Pluvial Planning Scenario Reference Tables

Two reference tables were established to relate the interval-based modeling to the CRMP Phase II planning scenarios and the desired flood probabilities for each scenario (2-, 5-, 10-, 25-, 50-, 100-, and 500-year recurrence intervals). As mentioned in Section E.1, the models included additional simulations for various tide elevation boundary conditions depending on the scenario. However, the pluvial reference tables are unrelated to tide (only related to precipitation frequency). The final pluvial depth grid mosaic products (described in a later section of this report) did leverage the comprehensive planning scenarios defined by DCR, accounting for these tidal iterations where appropriate.

The cross-referencing approach considered that, for each precipitation frequency, the climate scenarios were defined by a unique permutation of the following variables:

1. MARISA-selected climate epoch: “present”, “2020-2070”, or “2050-2100”.
2. MARISA-selected representative concentration pathway (RCP): “present”, “4.5”, or “8.5”.⁵
3. MARISA-provided confidence interval: 50th percentile (median), or 90th percentile.

Locality-specific MARISA change factors were retrieved and used for each climate epoch, RCP, and confidence interval (an example of averaged percent increases for the factors is shown in Figure 2). A general comparison of the range of 50th and 90th percentile values for RCP 4.5, as averaged across the study area and recurrence intervals, is shown in Figure 3. Readers interested in further detail on the technical approach used by MARISA to develop the change factors should visit the MARISA website (<https://midatlantic-idf.rcc-acis.org/>) or review the technical documentation for the change factors (Miro et al. 2021).

⁵ Note: MARISA data were developed using the Coupled Model Intercomparison Project Phase 5 (CMIP5) climate model data that were used for the Intergovernmental Panel on Climate Change (IPCC) Fifth Assessment Report.

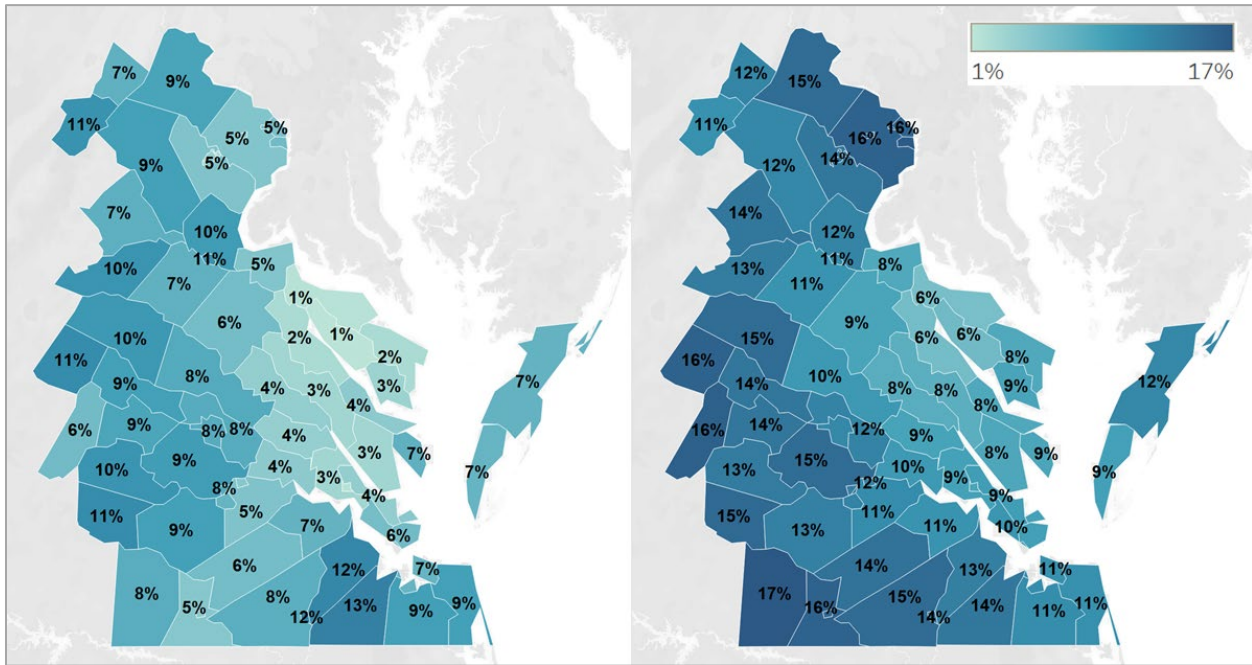


Figure 2: Example of the percent increases derived from MARISA for RCP 4.5 (left) and RCP 8.5 (right) at the 50th percentile, as compared to the NOAA Atlas 14 baseline. These values are converted to change factors by dividing by 100 and adding 1 (e.g., a 6% increase would result in a change factor of 1.06).

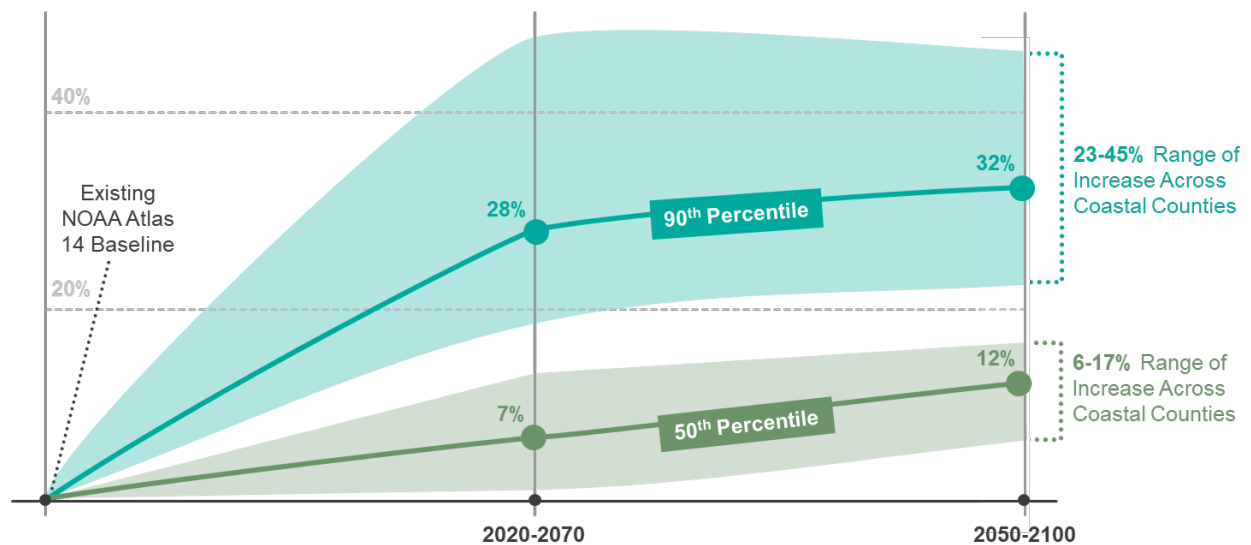


Figure 3: Percent increase compared to NOAA Atlas 14 baseline for RCP 4.5 50th and 90th percentile values, averaged across event return periods.

Two reference tables were produced to relate each RAS plan to statistical return periods, or frequencies, at various climate scenarios. Each modeled RAS plan, or simulation, is defined by a unique permutation of precipitation depth and storm duration, irrespective of location or climate scenario. For example, 3 inches over 2 hours is always plan “p05”, and 7 inches over 24 hours is always plan “p46”. Further, 8 inches of rain over 24 hours may be more frequent in the future than in the present. The two tables leverage the same mathematical relationships and interpolation techniques, but they differ in that they allow the user to apply the relationships to two different use cases.

E.2.ii Pluvial Recurrence Interval Reference Table

Given any RAS plan (or equivalent pair of precipitation depth + storm duration), the recurrence interval reference table can identify the interpolated recurrence interval for a given scenario and storm duration. An example output is provided below for a single location (basin), which shows that RAS plan p46 (7 inches over 24 hours) is expected to occur once every 15.27 years under the climate scenario associated with MARISA epoch 2050-2100 and MARISA RCP 8.5. For this particular table, the recurrence interval column was not rounded.

Table 4: Example Pluvial Recurrence Interval Reference Table.

basin_id	Reference Table Inputs					Reference Table Outputs		
	Storm Duration	Time Horizon	Climate Scenario	CI	ras_plan	Precip., Inches	Recurrence Interval, Years	
020403030501_1	24	2050-2100	8.5	50	p42	3	1.29	
020403030501_1	24	2050-2100	8.5	50	p45	6	8.56	
020403030501_1	24	2050-2100	8.5	50	p46	7	15.27	
020403030501_1	24	2050-2100	8.5	50	p47	8	26.49	
020403030501_1	24	2050-2100	8.5	50	p48	9	42.28	
020403030501_1	24	2050-2100	8.5	50	p50	11	98.20	
020403030501_1	24	2050-2100	8.5	50	p52	13	198.42	
020403030501_1	24	2050-2100	8.5	50	p53	14	281.66	
020403030501_1	24	2050-2100	8.5	50	p55	16	567.58	

E.2.iii Pluvial RAS Plan Reference Table

Given any recurrence interval and storm duration, the RAS Plan reference table can be used to look up the modeled RAS plan that best represents the frequency of storm occurrence. The “closest” RAS plan to the provided recurrence interval was determined by rounding the raw recurrence interval of each plan to the nearest discrete value among choices of 2-, 5-, 10-, 25-, 50-, 100-, and 500-year. A “straight round” was applied, meaning it would round up or round down as needed to the nearest one rather than always rounding up (“ceiling”) or

always rounding down (“floor”). An example output is provided below for a single location (basin), which shows that the 10-year, 24-hour storm, for the present-day conditions, represented in the CRMP as the Baseline Scenario, is best represented by RAS plan p44 (5 inches):

Table 5: Example Pluvial RAS Plan Reference Table.

basin_id	Reference Table Inputs						Reference Table Outputs	
	Storm Duration	Time Horizon	Climate Scenario	CI	Recurrence Interval, Years	ras_plan	Precip., Inches	
020403030501_1	24	present	present	50	2	p42	3	
020403030501_1	24	present	present	50	5	p43	4	
020403030501_1	24	present	present	50	10	p44	5	
020403030501_1	24	present	present	50	25	p46	7	
020403030501_1	24	present	present	50	50	p47	8	
020403030501_1	24	present	present	50	100	p48	9	
020403030501_1	24	present	present	50	500	p52	13	

E.2.iv Pluvial Derived Planning Scenario Flood Depth Rasters

The CRMP Impact Assessment required region-wide coverages of depth rasters. Although depth products were available directly from the individual pluvial models, these outputs had to be related to the discrete set of flood frequencies (e.g., 2-, 5-, 10-, 25-, 50-, 100-, and 500-year recurrence intervals), and aggregated for the Impact Assessment. Additional processing was required to identify the best value from overlapping depth information from both the three independent modeled storm durations and subbasin overlap, since the subbasins were intentionally buffered to ensure adequate coverage and to ensure hydrologic fidelity respective of ridges and other flow boundaries in the input ground elevation surface (DEM). Considerations and processing steps required to create these derivative products to meet this need, described below.

The logic behind the pluvial planning scenario reference table (Section E.2.i) was leveraged to identify the most appropriate HEC-RAS plan for every permutation of MARISA climate epoch, MARISA RCP, MARISA confidence limit, and CRMP tidal epoch for each DCR planning climate scenario, for each recurrence interval. This process was completed using the MARISA change factors for the county intersecting the centroid of each pluvial model subbasin. For each desired storm frequency and CRMP planning scenario, the script looks up the most appropriate HEC-RAS plan associated with that scenario for each subbasin, and then selects the resulting depth grid raster from that HEC-RAS plan. For example, HEC-RAS plan p11 might be the most appropriate for a subbasin near the coast, but HEC-RAS plan p10 might be more appropriate for an inland subbasin, at the same storm frequency and scenario.

DCR desired to use the maximum depth from the three modeled rainfall durations for the planning analysis. Overlapping depth values were addressed by creating new rasters representing the maximum depth at each grid cell location, accounting for all durations and all overlapping subbasins. Depth values less than 0.5 feet were screened out based on input from DCR and the Coastal Resilience Technical Advisory Committee. Key considerations for this decision were model and data uncertainty, as well as a desire to not overcommunicate flood risk for these shallow flooding areas. There were rare instances (less than 0.5% of all depth values assigned to assets for the Impact Assessment) of anomalously high values (depth values greater than 100). Where values were outside the range of [0.5, 100], the high values were screened out and set to 0. This process was completed for all five planning scenarios and the seven recurrence intervals, to produce a total of 35 surfaces. The resultant surfaces were then reprojected into the State Plane Virginia South (U.S. Feet) coordinate system (EPSG:2284) and tiled. “Nearest” sampling was used instead of “bilinear interpolation” sampling.



Figure 4: Example pluvial depth grid product.

E.2.v Pluvial Graduated Annual Exceedance Probability (AEP) Rasters

“Graduated” rasters provide a single classified raster coverage representing the most frequent precipitation recurrence interval that floods a given location. It is similar in concept to a “floodplain” product but is in raster form instead of polygon form. This product consolidates the 35 surfaces into five easy-to-interpret coverages for stakeholders to understand flood risk, one for each of the five DCR planning scenarios.

The table below indicates the raster classification values used. These values match similar class definitions from the Phase I coastal flood analysis.

The maximum value of all overlapping pixels was used at locations of overlap in raw pluvial depth rasters (due to multiple storm durations and/or adjacent buffered subbasins). Pluvial flood depth values outside the range of [0.5, 100] were treated as 0. Since these integer-based products are much smaller than floating-point depth rasters, it was feasible to deliver each study-wide surface as an individual tif mosaic as well as tiled tifs. An example product is provided in Figure 5.

Table 6: Classification schema for pluvial graduated flood extent rasters.

Most-Frequent Pluvial AEP Causing Flood	Raster Value
None	(NoData / Null) 0
0.5 (2-year)	40
0.2 (5-year)	50
0.1 (10-year)	60
0.04 (25-year)	70
0.02 (50-year)	80
0.01 (100-year)	90
0.002 (500-year)	100

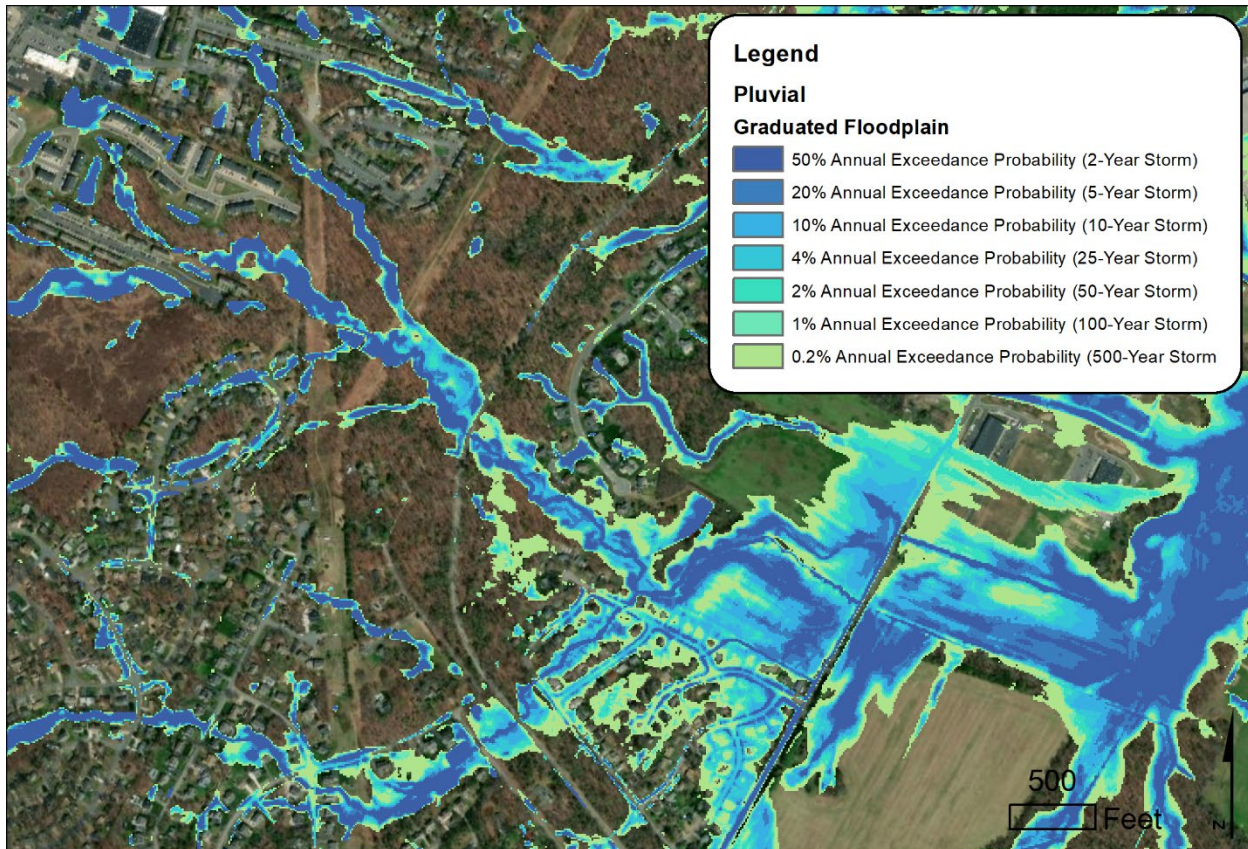


Figure 5: Example of pluvial graduated AEP raster.

E.2.vi Pluvial Storm Duration of Maximum Depth Rasters

The pluvial depth rasters aggregated the maximum flood depth from three different modeled storm durations. However, users may also want to understand which of the storm durations produces the highest depth pluvial flood conditions in their area of interest. A companion raster product was created to represent which modeled pluvial storm duration resulted in the maximum flood depth at any given location.

The pluvial storm duration rasters contain classified values representing the modeled storm duration (2-hour, 6-hour, or 24-hour) that caused the highest flood depth. There are 35 such rasters, one for each pair of climate scenarios (five) and recurrence interval (seven). At most locations, the 24-hour storm caused the most flooding since the 24-hour storm has more total rain volume than the other storms. However, at some locations, the sharper peaks of rain intensity associated with 2-hour and 6-hour storms caused flood depths from those shorter durations to be higher than the 24-hour storm.

A classified raster coverage was created by writing the modeled storm duration of the maximum flood depth to a new raster file for each grid cell in the study area. For locations

that experienced a “tie” between depths of different storm durations, the shorter duration classification was chosen. For example, if the flood depths for the 2-hour, 6-hour, and 24-hour were 6.3 ft, 8.2 ft, and 8.2 ft, respectively, then the 6-hour classification would be assigned.

Table 7: Classification schema for the duration of maximum depth rasters.

Storm Duration Causing Deepest Pluvial Flood	Raster Value
None	(NoData / Null) 0
2-hour	1
6-hour	2
24-hour	3

At locations of overlap in raw pluvial depth rasters due to adjacent buffered subbasins, the maximum value of all overlapping pixels was used. Pluvial flood depth values outside the range of [0.5, 100] were treated as 0. Since these integer-based products are much smaller than floating-point depth rasters, it was feasible to deliver each study-wide surface as an individual tif mosaic and provide a separate tif for each tile from Phase I. An example of the product is shown in Figure 4.

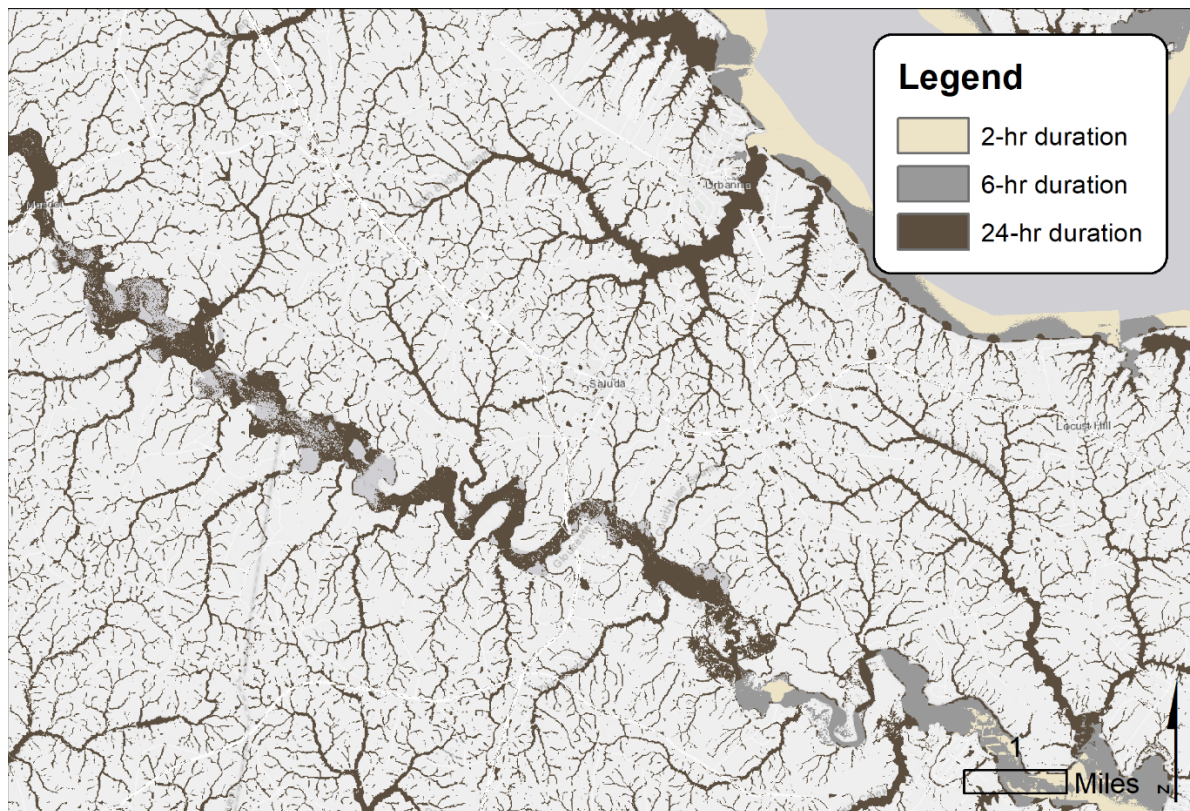


Figure 6: Example of the pluvial duration of maximum depth raster product.

F. Fluvial Flood Hazard Data

F.1 FLUVIAL FLOOD HAZARD AREA

FEMA is the primary resource for existing publicly available riverine (fluvial) flood hazard data. Although multi-frequency fluvial data are preferred, they are not fully available across the study area. Given this, it was decided that CRMP Phase II would use the FEMA Special Flood Hazard Area (SFHA), equivalent to a major flood (1% AEP/100-yr recurrence interval) to represent fluvial flood hazards. FEMA is developing multi-frequency data across Virginia and the nation as part of the Future of Flood Risk Data (FFRD) initiative. These data will be available for future iterations of the CRMP.

A spatial dataset representing the fluvial floodplain for the CRMP study area was partially provided by DCR, with the remaining data obtained directly from the FEMA Map Service Center. The data were merged and filtered, and problem areas were reviewed to prepare the layer for use in the CRMP.

F.1.i Source Data

DCR compiled statewide National Flood Hazard Layer (NFHL) data on January 29, 2024 and provided it to Dewberry on March 12, 2024. In addition to the current NFHL, DCR requested that eight communities with pending effective Flood Insurance Studies (FIS) be incorporated into the dataset. DCR provided pending effective Digital Flood Insurance Rate Map (DFIRM) data for four counties on March 12, 2024: Hanover County (51085C), Falls Church (510054), Chesterfield County (51041C), Henrico County (51087C). Dewberry acquired pending effective DFIRM data from the FEMA MSC for two counties on March 12, 2024: Prince William County (51153C) and Powhatan County (51145C). Two communities requested by DCR, Manassas City and Manassas Park City, were included in the Prince William County DFIRM data, so no additional effort was needed to acquire these communities. In all, current NFHL data and pending effective DFIRM data for six communities were acquired statewide. See Table 8 for a summary.

F.1.ii Data Processing

Data were reviewed to ensure complete coverage of the study area. First, it was confirmed that the flood hazard area data from NFHL layer, S_FLD_HAZ_AR, provided coverage of the Virginia CRMP study area. Flood hazard area data in communities outside of the CRMP were removed. Additionally, it was confirmed that flood hazard area data for the six pending effective communities provided complete coverage within those communities.

All flood hazard areas for Hanover, Falls Church, Chesterfield, Henrico, Prince William, and Powhatan localities were removed from the existing NFHL dataset. These six localities' pending effective floodplain polygons were merged into this layer to create the initial CRMP fluvial coverage. A review was completed to ensure the data merge was complete and successful.

Table 8: Summary of source datasets included in the fluvial 1% AEP representation for the CRMP, Phase 2.

Locality Name	FIPS	Effective Date	Source	Acquired
Statewide	various	various	DCR	Compiled, 1/29/2024; Acquired, 3/12/2024
Chesterfield County	51041	5/8/2024	DCR	3/12/2024
Falls Church		6/6/2024	DCR	3/12/2024
Hanover County	51085	6/20/2024	DCR	3/12/2024
Henrico County	51087	4/25/2024	DCR	3/12/2024
Powhatan County	51145	9/26/2024	FEMA MSC	3/12/2024
Prince William County	51153	9/26/2024	FEMA MSC	3/12/2024
Manassas	51683	9/26/2024	Included within Prince William	
Manassas Park	51685	9/26/2024		

The initial merged CRMP floodplain dataset was reduced by removing flood zones that did not represent flood hazard areas. Specifically, floodplain polygons representing 'D', 'X', 'Area Not Included', and 'Open Water' flood zones were removed. Floodplain polygons representing 'A', 'A.E.', 'A.O.', 'A.H.', and 'VE' flood zones were retained. These remaining polygons represent the 1% AEP floodplain.

The remaining polygons were then classified as riverine (fluvial) or coastal flooding. FEMA flood hazard areas are not designated by flood source (e.g., coastal or riverine). However, these can be initially identified and separated by reviewing the Base Flood Elevation (BFE) attribution in the Special Flood Hazard Area (SFHA) floodplain polygons. The 1% AEP floodplain mapped as Zone 'A' or 'AE' that do not have BFEs are typically riverine dominated areas, as they have BFEs attributed to lines that overlay the polygons. In contrast, areas flooded by the 1% AEP coastal flood have BFEs assigned to the polygons. Given this, floodplain polygons representing 'VE' flood zones and all polygons with a 'STATIC BFE' > -9999 were initially classified as 'coastal', while all remaining polygons with a 'STATIC BFE' = -9999 were initially classified as 'riverine'. All 'A.O.' and 'A.H.' flood zones were individually reviewed and classified as either 'coastal' or 'riverine' based on analyst discretion. Inland water bodies, typically lakes and ponds, with STATIC BFE > -9999 were reviewed and re-classified as 'riverine' where there was no apparent hydraulic connection to tidal waters. After a full review, floodplain polygons classified as 'riverine' were extracted into a final deliverable dataset representing riverine (fluvial) 1% AEP floodplain areas. The extent of the resultant riverine flood coverage is shown in Figure 5.

F.1.iii Items of Interest

During and after the merge, classification, and final extraction of the riverine floodplain data, several items of interest were noted:

- There were no riverine floodplain areas in Accomack County, Northampton County, and in the cities of Norfolk, Poquoson, or Chesapeake.
- There were very few and/or very small riverine floodplain areas in Mathews County and Portsmouth City.
- Many inland AE-zone water bodies appear as coastal (STATIC BFE > -9999) but were retained as riverine. They represent inland lakes, reservoirs, or flood zones isolated without a direct hydraulic connection to tidal waters.

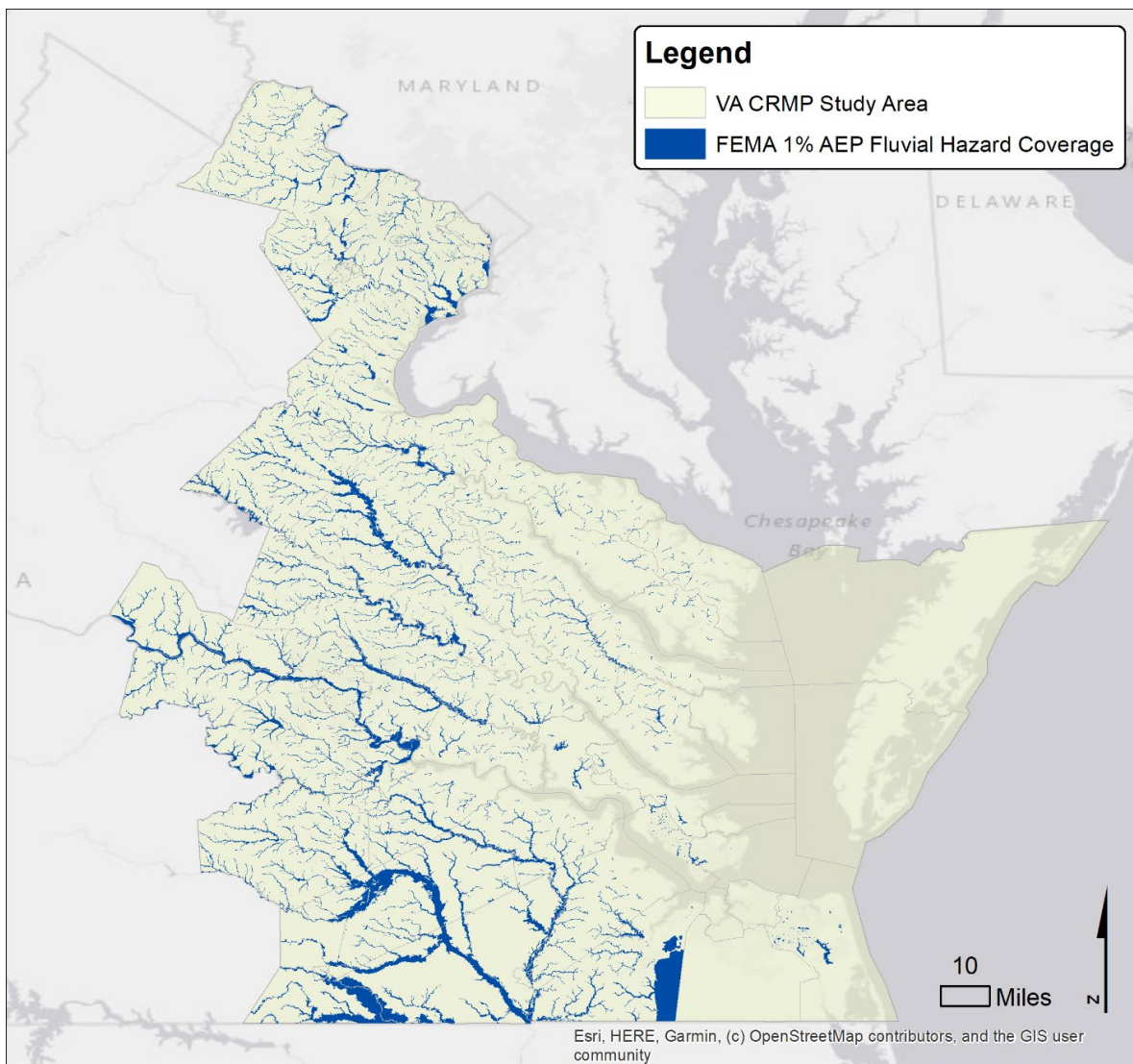


Figure 7: Visual overview of the extent of the FEMA 1% AEP Fluvial Special Flood Hazard Area across the VA CRMP study area.

- The Great Dismal Swamp National Wildlife Refuge is bisected by the Suffolk – Chesapeake County boundary. The refuge is represented by riverine floodplain on the Suffolk side of the boundary but is not represented by any floodplain on the Chesapeake side. This area represents a noticeable hole in the source NFHL/DFIRM data.
- Two areas where the transition from coastal to riverine classification is particularly abrupt but nevertheless correct with respect to the extent of FEMA coastal studies in the CRMP study area:
 - Along the Potomac River at the Fairfax – Prince William County boundary. Fairfax has riverine floodplain along the Potomac, while neighboring Prince William County does not. This difference was interpreted to be a result of the newer Prince William study incorporating the FEMA Region 3 coastal study update, whereas the Fairfax FIRM dates back to 2010, prior to the coastal study update.
 - At the confluence of the James and Appomattox Rivers. Chesterfield County is all riverine floodplain and has no coastal SFHA for the entirety of both rivers. The opposite banks in Hopewell City, as well as portions of Prince George and Charles City counties were classified as coastal floodplain.
- Between some communities, the floodplains on opposite sides of a locality boundary do not match very well, leaving either small gaps or overlaps in the floodplains. No attempt was made to edit or reconcile individual boundary discrepancies, as such issues were not consequential to the intended use of the data in the CRMP Phase 2 impact assessment. In most locations, these differences were minimal; however, there were two locations where these inconsistencies were visually apparent:
 - Along Bull Run, which separates Prince William County from both Fairfax and Loudon Counties. The inclusion of the pending effective data for Prince William County did help lessen these differences but did not completely fix them.
 - In Mathews County, the floodplain polygons do not match the county boundary and do not align with Gloucester County floodplain polygons.
- All A.O. flood zones in the dataset were tucked behind coastal zones and did not contact riverine floodplains. The conclusion is that all A.O. zones represent sheet flow corresponding to coastal flooding and were excluded from the final dataset.
- Two isolated inland A.H. zones exist in Fairfax County. No coastal floodplain polygons exist in the county, so the two A.H. zones were considered riverine and retained in the dataset. Otherwise, all other A.H. zones in the dataset have been associated with coastal flooding and were excluded from the final dataset.
- All pending effective data were considered an upgrade in the floodplain data over the current NFHL in each respective locality. In all cases, the pending data provided a good, if not improved fit to county boundaries and neighboring floodplain polygons.

There were no concerns about the inclusion of the pending effective floodplain data in the final deliverable.

F.2 FLUVIAL MULTI-FREQUENCY DEPTH GRIDS

FEMA is the primary resource for existing publicly available riverine (fluvial) flood hazard data. While multi-frequency fluvial data were unavailable across the study area, DCR had gathered a subset of three HUCs and provided to Dewberry for the Fluvial Multi-frequency Impacts Case Study. Water surface elevation and depth grid data were provided for HUC8 watersheds including 02080102, 02080103, 02080104, 02080105 (Figure 6). Ultimately, HUC 02080103 was not included due to the limited extent in the CRMP study area.

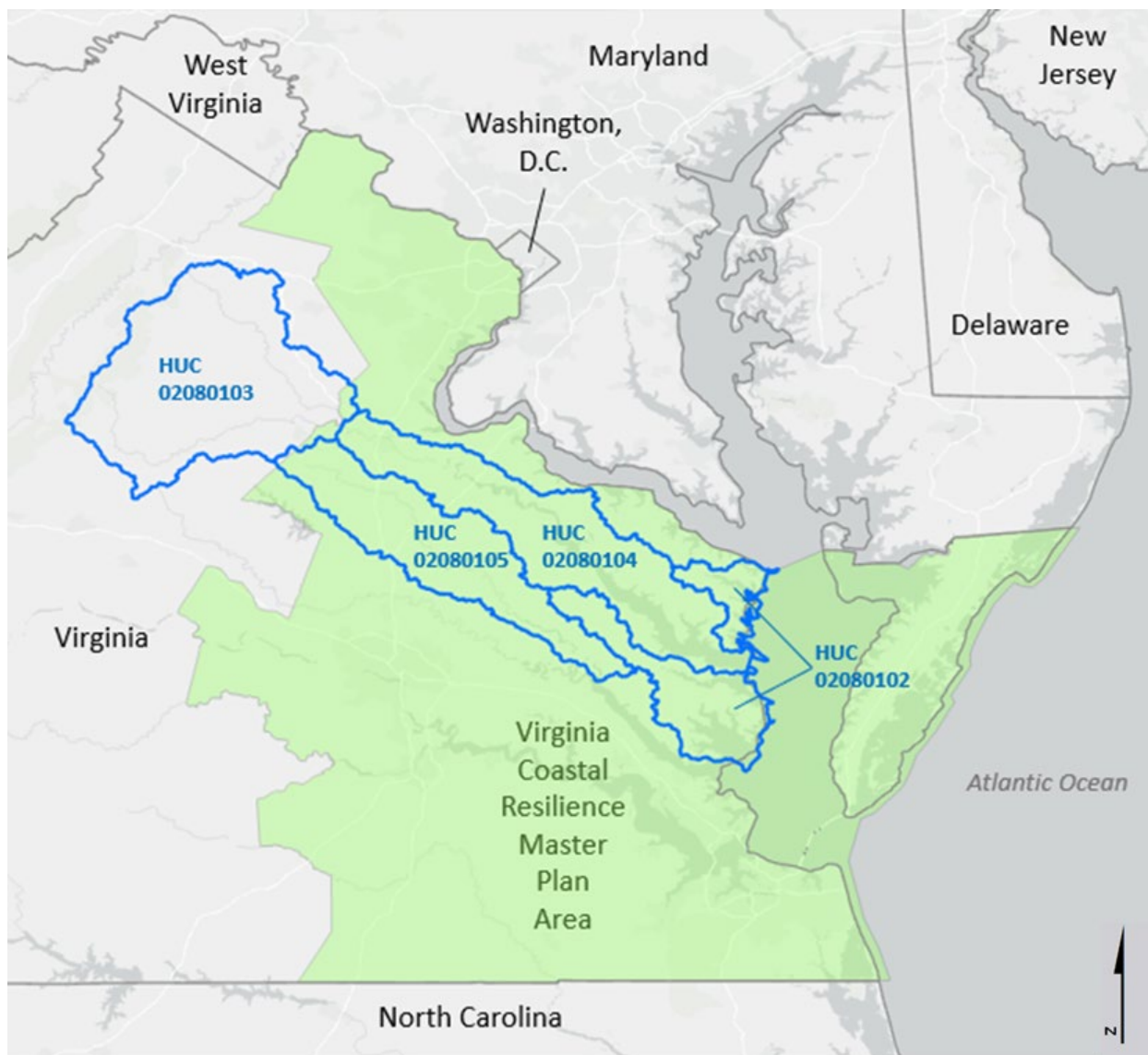


Figure 8: HUC8 Boundaries evaluated for the fluvial multi-frequency case study.

The data were reviewed before use, including a data completeness check and a data consistency check. The data completeness check reviewed for areas with limited or no depth grid coverage, summarized in Table 9.

Table 9: Areas with limited or no depth grid coverage in the Fluvial Multi-frequency case study area.

HUC	Stream	Zone	Stream Area (sq feet)	DG Coverage
02080102	Conrad Pond/Wilton Creek	A	2,205,340	None
02080104	Sturgeon Creek, Woods Creek, and 2 Unnamed tributaries of Rappahannock River @ Deltaville	A	1,075,654	None
02080104	Three unnamed tributaries of Corrotoman River @ Kilmarnock	A	1,915,141	None
02080104	Unnamed tributary of Robinson Creek @ Bethpage.	A	219,743	None
02080104	Three unnamed tributaries of Lancaster Creek @ Simonson	A	1,756,106	None
02080104	Mill Branch @ Haynesville	A	1,396,127	None
02080104	Pecks Creek @ Wellford	A	1,115,529	None
02080104	Jugs Creek @ Warsaw	A	1,863,718	None
02080104	Cliffs Creek and Garlands Creek @ Singerly	A	3,268,769	None
02080104	Unnamed tributary of Troy Creek @ Leedstown	A	761,348	None
02080104	Bristol Mine Run @ Rollins Fork	A	343,387	None
02080104	Portobago Creek @ Daniel Corner	A	1,715,043	Incomplete coverage of 10%, 4% 2%, 1%, 0.2% depth grids
02080105	Unnamed tributary of Aylett Pond @ Aylett Mill. Upstream of Fairwoods Rd	A	4,172,605	Incomplete coverage of 10%, 4% 2%, 1%, 0.2% depth grids

A data consistency check was also performed to ensure that the depth grids had similar values where the HUCS overlapped. Some depth grid inconsistencies exist just below the confluence of the Rapidan and Rappahannock Rivers, where HUC 02080103 transitions into HUC 02080104. These inconsistencies appeared to be localized to the confluence and HUC boundary. The depth grids were sampled in two locations. While differences across the transition appear minimal (differences less than or equal to 1 ft), there were some large differences in the 1% depth grid, about 15 feet, as shown in Table 10. A preliminary investigation of the issue indicates that the probable cause of these large discrepancies is processing issues in the HUC 02080103 portion of the 1% depth grid near the confluence.

This issue did not require correction as HUC 02080103 was dropped from the analysis due to the small footprint inside the CRMP study area.

Table 10: Test sites and associated depths.

Site	0.2% WSE	0.2% Depth	1% WSE	1% Depth	2% WSE	2% Depth	4% WSE	4% Depth	10% WSE	10% Depth
Site 1 Upstream	154.3	27.6	147.8	21.1	145.8	19.1	143.8	17.1	141.2	14.5
Site 1 Downstream	154.3	27.6	133.0	6.3	130.6	3.9	128.5	1.8	125.8	N/A
Site 2 Upstream	141.3	20.4	132.4	11.5	130.1	9.2	127.8	6.9	124.9	4.0
Site 2 Downstream	140.5	20.0	132.8	12.3	130.5	10.0	128.3	7.8	125.5	5.0

G. Combined Flood Coverages

A combined flood coverage was developed to provide a product that would illustrate the spatial extent of each of the three flood hazards considered by the CRMP Phase II effort. Two different combined flood products were created as classified rasters, **both types relied solely on the 1% AEP flood condition.**

- Flood type present: The “presence” coverages show the areas where each of the three flood types occur, as well as areas subject to compound flooding, where two or more flood types occur.
- Flood type dominant: The “dominance” coverages show which flood type is greatest (has the highest flood depth).

G.1 DATA SOURCES

The combined flood hazard rasters include the following flooding source data for the 1% AEP condition:

- Coastal (from CRMP Phase I)
 - Coastal depth grids used include wave height, i.e., “DGWV” products.
- Pluvial/rainfall (from CRMP Phase II)
 - Derived Planning Scenario Flood Depth Rasters (as described in Section E.2.iv).
- Fluvial/riverine (from CRMP Phase II)
 - For “presence”, the fluvial/riverine aspect used FEMA Special Flood Hazard Area (SFHA) polygons associated with the 100-year event (See

Section F.1). This layer is used for all CRMP Phase II scenarios as no future condition data is available at this time.

- For “dominance”, the fluvial/riverine aspect used FEMA nonregulatory depth grids from FEMA, **only used for select pilot HUC8s**, with limited coverage within those HUC8 areas. This layer is used for all CRMP Phase II scenarios as no future condition data is available at this time.

G.2 FLOOD TYPE PRESENT

The flood type present “presence” raster shows which flood hazard type is present for each 10-ft cell in the CRMP study area for each CRMP Phase II scenario. The data sources above were compared at the raster cell level to identify if and what type of flood hazard inundated any raster cell of the CRMP DEM – results are aligned (snapped) to each DEM cell. A conceptual process for this product is shown in Figure 7. Since these integer-based products are much smaller in size than floating-point depth rasters, it was feasible to deliver each study-wide surface as an individual tif mosaic, in addition to providing a separate tif for each tile. Users should note that the fluvial data remains constant for all scenarios. Seven potential classifications were identified depending on if the three hazards occur independently or compound at any particular raster cell. The classification values for the output product are shown in Table 11.

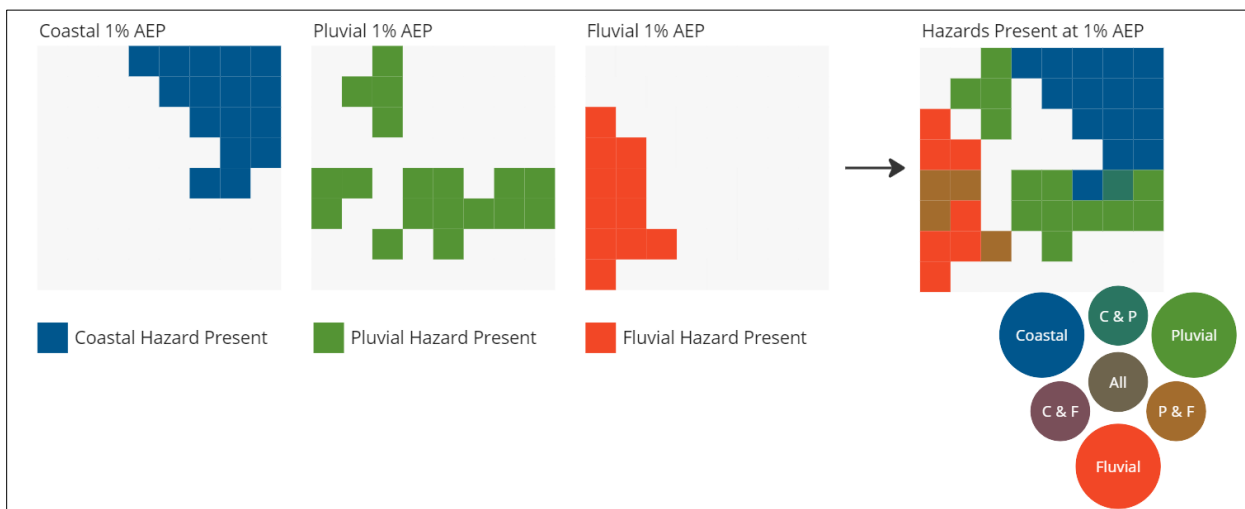


Figure 9: Conceptual process of "presence" raster.

Table 11: Presence raster classification types and values.

Combined Hazard Presence Class	Raster Value
No Hazard	(NoData / Null) 0
Coastal Only	1
Pluvial Only	2
Fluvial SFHA Only	3
Coastal + Pluvial	4
Coastal + Fluvial SFHA	5
Fluvial SFHA + Pluvial	6
Coastal + Pluvial + Fluvial SFHA (all)	7

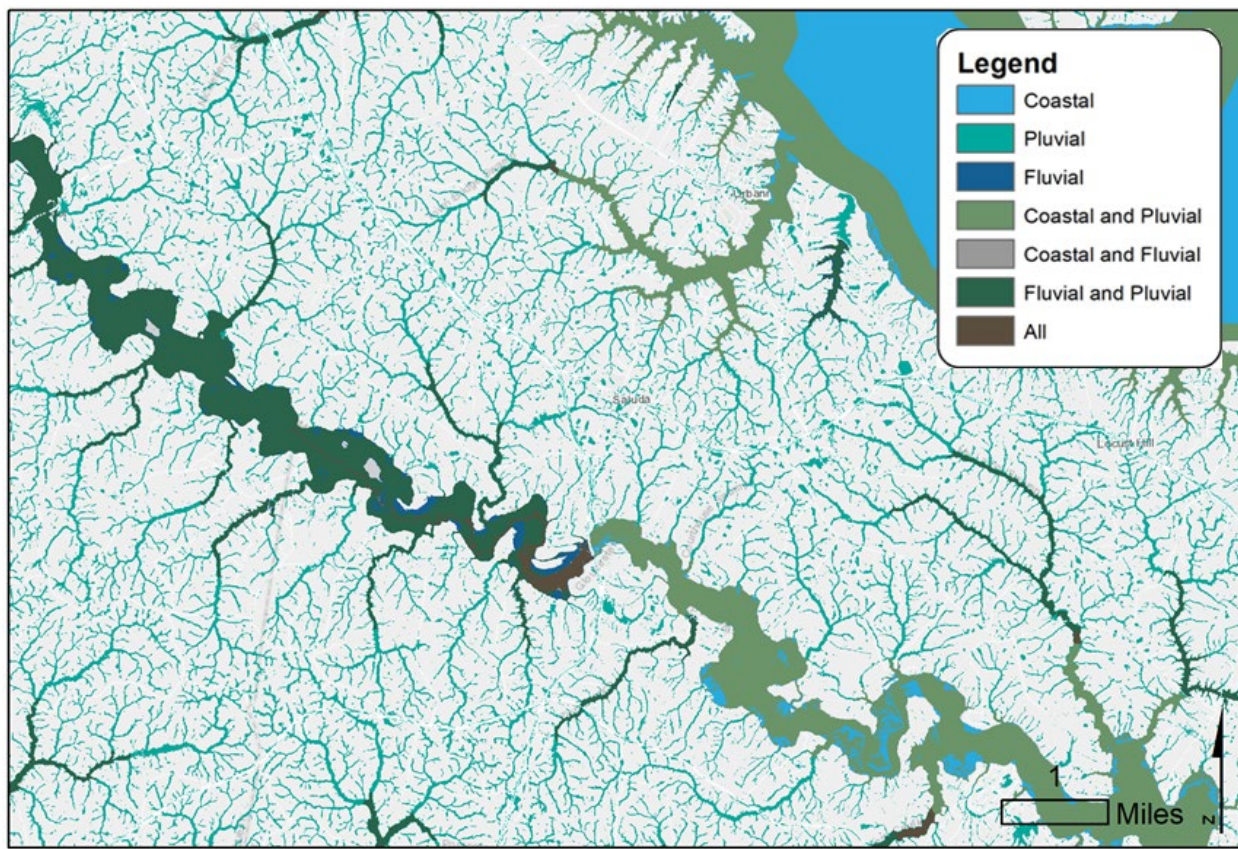


Figure 10: Example output of the presence raster with the production color scheme.

G.3 FLOOD TYPE DOMINANT

The flood type dominant “dominance” raster shows which flood hazard type has the greatest depth for each 10-ft cell in the CRMP study area for each CRMP Phase II scenario. A conceptual process for this product is shown in Figure 9. Results are aligned (snapped) to each DEM cell. Since these integer-based products are much smaller in size than floating-point depth rasters, it was feasible to deliver each study-wide surface as an individual tif mosaic, in addition to providing a separate tif for each tile from Phase I. Users should note that the fluvial data remains constant for all scenarios. Four potential classifications were identified depending on if a cell was flooded and which of the three hazards had the dominant flood depth for any particular raster cell. The classification values for the output product are shown in Table 11.

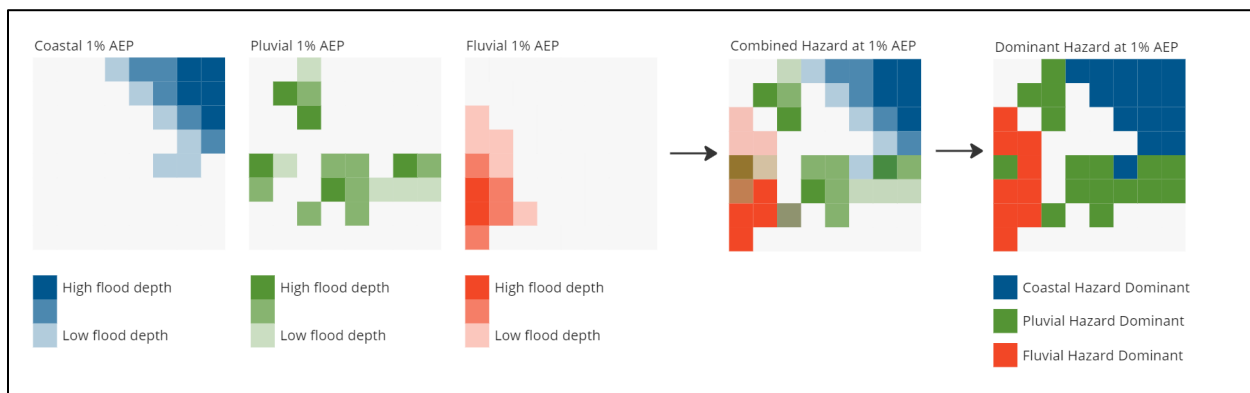


Figure 11: Conceptual process of "dominance" raster.

Table 12: Dominance raster classification types and values.

Combined Hazard Dominance Classification	Raster Value
No Hazard	(NoData / Null) 0
Coastal Depth	1
Pluvial Depth	2
Fluvial Depth	3

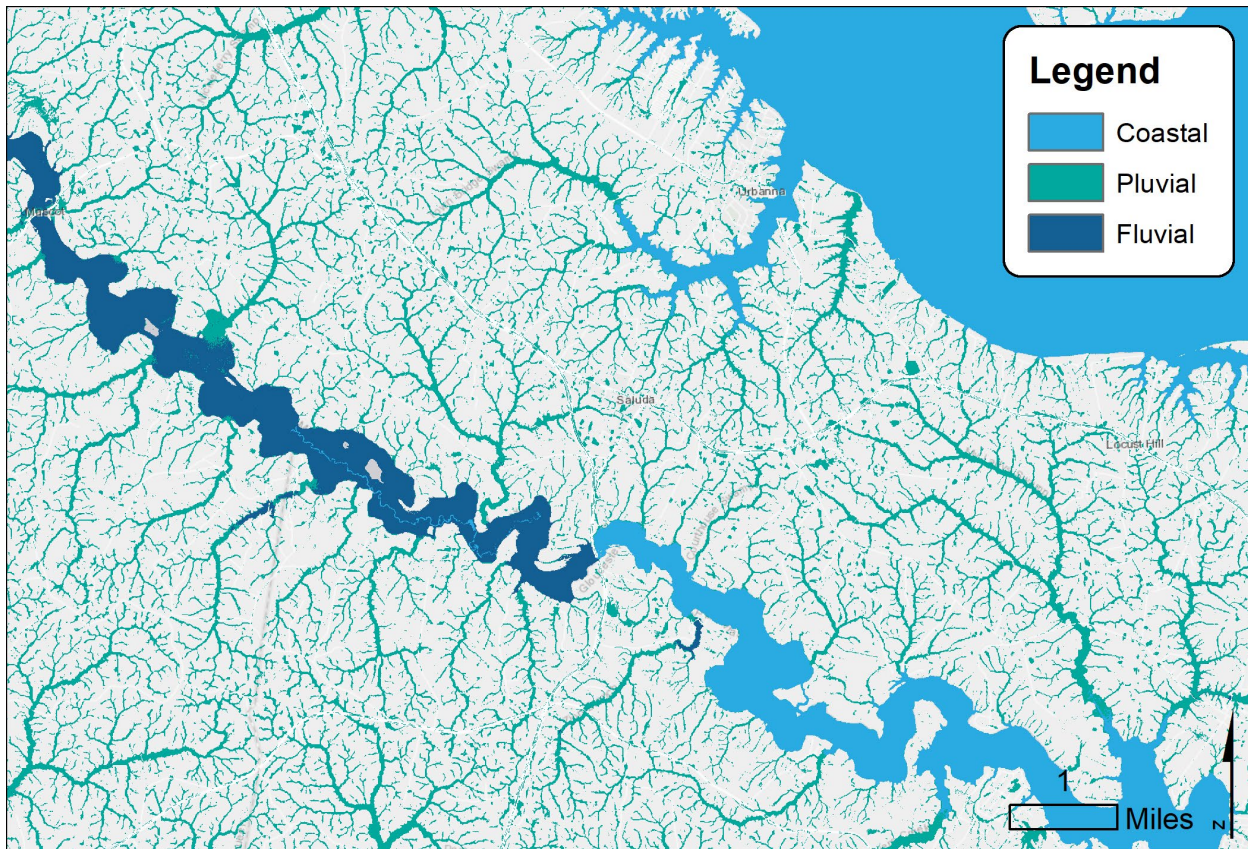


Figure 12: Example combined flood "dominance" product.

H. References

Dewberry. (2022). Virginia Coastal Resilience Master Plan, Task 3: Coastal Flood Hazard Framework. <https://www.dcr.virginia.gov/crmp/document/Appendix-C-Coastal-Flood-Hazard-Framework.pdf>

Dewberry. (2024). Virginia Coastal Resilience Master Plan, CO-8A: Pluvial Modeling Final Report. June 14, 2024. https://vadcr-frp.s3.amazonaws.com/Pluvial_CRMP/VACRMP_PluvialModelingReport_Final_20240614.pdf.

Miro, M., DeGaetano, A., Samaras. C., Romita Grocholski, K., López-Cantú, T., Webber, M., Eck, B. (2021). “Projected Intensity-Duration-Frequency (IDF) Curve Tool for the Chesapeake Bay Watershed and Virginia”. Northeast Regional Climate Center. <https://midatlantic-idf.rcc-acis.org/>

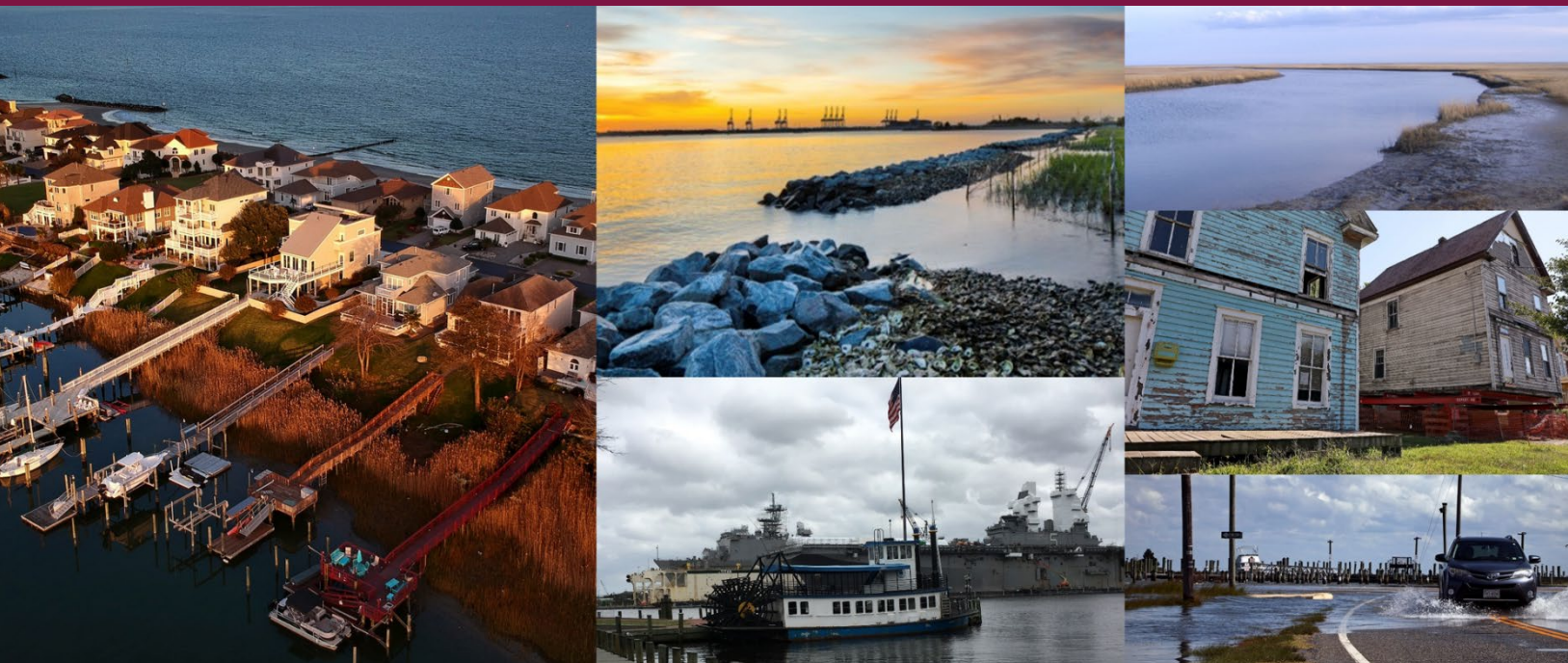
Addendum A - Pluvial Modeling Technical Report

VIRGINIA COASTAL RESILIENCE MASTER PLAN, PHASE II

Appendix A – Flood Hazard Data Development

Addendum A – CO-8A: Pluvial Modeling

JUNE 14, 2024



FINAL REPORT

PREPARED BY

Dewberry Engineers Inc.
4805 Lake Brook Drive, Suite 200
Glen Allen, Virginia 23060

Contract No. E194-89627

SUBMITTED TO

Department of Conservation and Recreation
600 East Main Street
Richmond, Virginia 23219

CONTENTS

LIST OF FIGURES.....	IV
LIST OF TABLES.....	VII
EXECUTIVE SUMMARY	1
INTRODUCTION.....	3
1 TECHNICAL MEMORANDUM 1: MODEL DEVELOPMENT, GEOMETRY, AND PARAMETERIZATION.....	4
1.1 Data Repositories	4
1.2 Foundational datasets.....	5
1.2.1 Topography.....	5
1.2.2 Friction Grid	7
1.2.3 Infiltration Grid	11
1.2.4 Vectors.....	17
1.3 MODEL DEVELOPMENT.....	18
2 TECHNICAL MEMORANDUM 2: MODEL FORCING	19
2.1 Interval-Based Approach.....	19
2.2 Tidal Boundary Conditions	21
2.3 Development of Basin Hyetographs	21
2.3.1 QC Process	22
2.4 Pipeline and Outputs.....	23
2.4.1 HEC-DSS Files with Hyetographs.....	23
2.4.2 Units.....	23
3 TECHNICAL MEMORANDUM 3: MODEL PIPELINE	24
3.1 HUC-12 Reference Model Development.....	24
3.2 Model Domain Delineation	24
3.3 Model Creation	25
3.4 Model Refinement	26
3.4.1 Mesh	26
3.4.2 Terrain.....	27
3.4.3 Outflow Boundary Conditions (OBCs)	28
3.5 Parallel Model Execution and Postprocessing	28

3.6	QA/QC Stages	30
4	TECHNICAL MEMORANDUM 4: PILOT MODELING	31
4.1	Selected Pilot Basins.....	31
4.2	Modeling Process	32
4.2.1	Basin Model Creation	33
4.2.2	Initial Automation.....	33
4.2.3	Model Development.....	34
4.2.4	Model Review	36
4.2.5	Model Simulations.....	36
4.3	Sensitivity Analysis	37
4.3.1	Simulation Time Window	37
4.3.2	Sensitivity Test.....	37
4.3.3	Burnline Testing	41
4.3.4	Model Warm-Up Periods.....	43
4.3.5	Clipped Coastal Model Domains.....	45
4.3.6	Tidal Boundary Conditions.....	49
4.3.7	Hydraulic and Computational Parameters	51
4.3.8	Computation Interval Sensitivity Analysis	53
4.3.9	Boundary Condition Sensitivity Analysis	54
4.4	Pilot Data Deliverables	55
4.4.1	HEC-RAS Models And Depth Grids	55
5	TECHNICAL MEMORANDUM 5: PRODUCTION MODELING	57
5.1	Production Modeling.....	57
5.2	Modeling Process	58
5.2.1	Model Management	58
5.3	Model Review.....	65
5.3.1	Quality Control.....	65
5.4	Automated Unsteady Simulations and Postprocessing	66
5.5	Automated Quality Control.....	67
5.5.1	Input Checks	67
5.5.2	Output Checks	67
5.6	Known Limitations.....	68
5.6.1	Boundary Conditions	68
5.6.2	Stormwater Conveyance	68

5.6.3	Fluvial Processes	68
5.7	Anomaly Review	71
5.7.1	Summary of Production Notes	71
5.7.2	High Volume Accounting Errors	72
5.8	Data Delivery and Documentation	72
5.8.1	Notes on MOSAIC Raster Products	72
5.8.2	Delivered Rasters	74
5.8.3	Delivered RAS Models	75
5.8.4	Metadata and Documentation	77
6	APPENDICES	80
6.1	Appendix A: Anomalous Issues Noted During Production	80
6.2	Appendix B: Precipitation Volume	82
6.3	Appendix C: Quality Plan	84

LIST OF FIGURES

<i>Figure 1. Example datasets stored in PostgreSQL and S3 (bucket named va-pluvial).</i>	5
<i>Figure 2. Map of existing coastal topography tiles (gray) and newly available USGS datasets (overlaid) used to create the project-wide DEM for pluvial modeling.....</i>	6
<i>Figure 3. Representative illustration of differences in depth between models using high resolution (1-meter) friction and NLCD-based datasets. The greatest difference in depths is found in stream channels which are not the focus of the pluvial modeling.</i>	8
<i>Figure 4. Manning's N grid for the project area is shown here (COG).</i>	10
<i>Figure 5. Coverage Area for Land Cover Sources.....</i>	12
<i>Figure 6. CN Grid coverage area and processing tiles.</i>	14
<i>Figure 7. Raw output polygon of the CN tool shown at single tile location.....</i>	15
<i>Figure 8. Final CN grid shown as a COG.</i>	16
<i>Figure 9. Road centerline data used for HEC-RAS breakline development.....</i>	18
<i>Figure 10. Hyetograph records in DSS format.</i>	22
<i>Figure 11. An example HUC-12 basin split into five domains.</i>	25
<i>Figure 12. Breakline effect on 2D model mesh, with zero "near repeat" lines.....</i>	26
<i>Figure 13. HEC-RAS screenshot: burn line parameters and effect on stream profile.....</i>	27
<i>Figure 14. Sample preliminary results for an area demonstrating a 24-hour duration storm. Note that the model identifies flood hazards outside of stream channels in residential areas.</i>	29
<i>Figure 15. A map of the HUC-12s in the study area with locations modeled in the pilot study shown in red.....</i>	32
<i>Figure 16. Basin 020700080301_2 includes rural areas with farmsteads dispersed throughout.</i>	37
<i>Figure 17. 24-hour event simulation hydrographs. The event was run with simulation times of 24, 36, and 48 hours.</i>	38
<i>Figure 18. 6-hour event simulation hydrographs. The event was run with simulation times of 6, 12, and 24 hours.</i>	39

Figure 19. 2-hour event simulation hydrographs. The event was run with simulation times of 2, 12, and 36 hours	39
Figure 20. 2-hour event simulation at simulation times 6 and 12 hours. Pluvial flooding can be seen to peak at around 6 hours.	40
Figure 21. Basin 030102011004_6 includes rural areas with swamp and marshland running throughout.	41
Figure 22. Example of ponding behind structure (left) vs. increased burn width using engineering judgment (right), where flow direction is top to bottom.	42
Figure 23. RAS-generated hydrograph using cut profile line.....	42
Figure 24. Basin 020403040301_1 includes tidal shoreline with tidal streams and estuaries.....	44
Figure 25. Basin 020403040301_2 includes tidal shoreline with tidal streams and estuaries.....	46
Figure 26. Clipped boundary of Basin 020403040301_2.	47
Figure 27. Comparative inundation between clipped and non-clipped coastal basin boundaries.	48
Figure 28. Basin 020403040104_2 includes rural tidal shoreline along with tidally-influenced streams. Note that the open boundary spans approximately 2 miles.	49
Figure 29. Basins 020700080301_0 (A, steep rural), 020802060501_3 (B, urban), and 020700110601_4 (C, tidal rural).	51
Figure 30. Difference in inundation at boundary between default and measured normal depth.	55
Figure 31. Deliverable folder structure once file extraction was complete.	56
Figure 32. Map of the 1,830 modeled basins developed from the 419 coastal HUC 12s in the study area.....	58
Figure 33. Location requiring channel burnline before (left) and after (right) the burnline inclusion. Note the reduction in ponding to the hydraulic connectivity created by the burnline.	60
Figure 34. Default dimensions for channel burnlines used throughout the study.....	60

Figure 35. Example of a burnline removed due to a preexisting cut in the terrain. The automated routine included a small burnline in this large channel that was not needed and was removed from the engineered model.....	61
Figure 36. Breakline along the crest of a small reservoir. Note that no conveyance structure or mechanism was added to the model.....	62
Figure 37. Water surface elevation points used to apply tidal values as boundary conditions for production models in the study.....	63
Figure 38. Flood depth difference for basin 020403040301_2 using the pilot single stage hydrograph approach.	64
Figure 39. Flood depth difference for basin 020403040301_2 using the production (stage hydrograph and normal depth) modeling approach.	65
Figure 40. High velocities where there was steep flow from terrain into the channel (reference HUC 020801040102_4).	69
Figure 41. Higher velocities are being forced upstream by the tidal boundary (reference HUC 020700110601_1).	69
Figure 42. The constriction of flow through the burnline was causing higher velocities. This was within the fluvial channel (reference HUC 020700110601_1).....	70
Figure 43. Fluvial results overlap in the boundary between upstream HUC 020700110601_4 and downstream HUC 020700110601_5 subbasin domains.	71
Figure 44. DCR bucket: Example of depth grids per-basin for RAS plan “p01” (1 inch of rain over 2 hours) at tide height associated with the 2020 CRMP epoch.....	74
Figure 45. DCR bucket: Example of global depth grid VRT for RAS plan “p01”, tide epoch 2020, with absolute paths stored for each TIF (for streaming).	74
Figure 46. DCR bucket: Example of global depth grid VRT for RAS plan “p01”, tide epoch 2020, with relative paths stored for each TIF (for local download).	75
Figure 47. DCR bucket: Example of top-level RAS model files for one basin.	75
Figure 48. Example of the unzipped file tree for RAS model files for one basin, one plan, one epoch (one set of geometry data is shared among all plans and all epochs per basin).....	76

<i>Figure 49. Example STAC item on the left lists all depth grids output from HEC-RAS simulations in the MHW-2020 simulation.....</i>	78
<i>Figure 50. Example STAC item on the left lists HEC-RAS model data for all simulations in the MHW-2020 simulation. Links to the corresponding depth grids (not shown) are also included at the bottom of the item at the bottom.</i>	79

LIST OF TABLES

<i>Table 1. Roughness Lookup Table.</i>	9
<i>Table 2. Sources of Land Cover Data for Development of Infiltration Grid.</i>	11
<i>Table 3. Proposed ranges of precipitation totals for fixed-interval approach.</i>	20
<i>Table 4. Summary of HUC-12s and relevant data used for selection in the pilot.</i>	32
<i>Table 5. Static tide heights for applicable models (all units are feet NAVD88).</i>	34
<i>Table 6. Results from simulation time window sensitivity analysis.</i>	40
<i>Table 7. Burnline Sensitivity Analysis (100 ft grid, 50 ft breakline spacing).</i>	43
<i>Table 8. Results from model warm-up period sensitivity analysis.</i>	45
<i>Table 9. Results from clipped basin boundary sensitivity analysis.</i>	48
<i>Table 10. Results from variable mean high water elevation sensitivity analysis.</i>	50
<i>Table 11. Results from mesh resolution sensitivity test. Please note that A, B, and C refer to specific subbasins and are color coded in the table below.</i>	52
<i>Table 12. Time interval sensitivity analysis results.</i>	53
<i>Table 13. Boundary condition sensitivity analysis results.</i>	54
<i>Table 14. Summary of Anomalous Issues Noted During Production.</i>	80
<i>Table 15. Precipitation Volume Table.</i>	82

EXECUTIVE SUMMARY

The Virginia Department of Recreation and Conservation (DCR) undertook the development of the first iteration (Phase I) of the Coastal Resilience Master Plan (CRMP) in 2021. Phase I focused on existing and future coastal flooding and associated projected impacts on the Commonwealth of Virginia's eight coastal Planning District/Regional Commissions (PDC/RCs). After Phase I, DCR received feedback from both the study Technical Advisory Committee (TAC) and study stakeholders that the hazard framework should be expanded to include consideration of other hazards, with priorities for rainfall-induced (pluvial) and riverine (fluvial) flooding. Discussions with stakeholders and the TAC identified that pluvial hazard data development was the priority, given the lack of data for the hazard. In turn, DCR funded pluvial development for inclusion into CRMP Phase II, which produced a total of 1830 models across the 16,600 square miles of the CRMP study area. The effort provides coastal and pluvial hazard data outputs for inclusion in the CRMP Phase II update to the hazard portfolio and impact assessment and open-source models that stakeholders can retrieve and apply to flood resilience studies. The details of the pluvial model development and products are provided in this document, which is a compilation of Technical Memorandums produced throughout the 1.5-year modeling campaign.

Pluvial, or rainfall-induced flooding, is characterized by localized storage and ponding of high-intensity rain events in areas with lower drainage areas. Pluvial flooding scenarios typically have low velocity and shallow depth relative to riverine flooding scenarios, yet such events have been identified as a significant source of damage and disruption to the public. In addition, pluvial flooding events may occur more frequently than riverine flooding events.

For the CRMP, small independent subbasins (approximately 10 square miles or less) were developed by engineers to simulate highly localized rainfall events, ignoring upstream or downstream riverine influence. Each subbasin modeled in this study was initially modeled at the HUC12 level (using boundaries from the [Watershed Boundary Dataset \(WBD\)](#)) and then subdivided into smaller modeling domains. No transfer of flow was accounted for between adjacent basins. The basins were aligned along ridges where possible, buffered, and assigned a full-perimeter normal depth boundary condition, allowing water to exit anywhere along the perimeter of the domain.

Due to the large number of HEC-RAS models (1,830) required to model Virginia's coastal counties, a semi-automated workflow was developed using steps described in a series of technical memorandum. In 2023, the modeling team completed a pilot modeling phase with the goal of identifying parameters, processes, quality assurance procedures, and data pipelines prior to production modeling. A series of sensitivity analyses were performed to evaluate the impact of various model parameter options such as default mesh spacing, normal depth boundary condition, simulation time step, tidal boundary conditions, model warm-up parameters, roughness and infiltration, and total simulation duration.

Outcomes and results of the pilot modeling phase were then reviewed by DCR and the TAC to provide input and direction to the production modeling campaign. Updates from outcomes of the pilot modeling were incorporated into the production campaign. The semi-automated production process began with engineers reviewing basin splits, evaluating overall model geometry, and adjusting models. Then, the entire set of models was run through the cloud-based computational pipeline, which executed the pre-defined rainfall plans for each basin. As a part of this pipeline, depth grids were also created which represent the final output of the pluvial modeling study. Final products from the production modeling include HEC-RAS model input and output data for each simulation. Input data is comprised of precipitation data, terrain, friction, and infiltration grids. Output data includes HEC-RAS output files (HDF format) containing simulation results and depth grids for each simulation.

INTRODUCTION

As part of pluvial development for CRMP Phase II, a total of 1830 models were produced across the 16,600 square miles and 57 counties within the CRMP study area, including coastal and pluvial hazard data outputs. The details of the pluvial model development and products are provided in this document in five Technical Memorandums (TM) that were produced throughout the modeling campaign. The five TMs included in this report are outlined below:

- **TM #1: Model Development, Geometry, and Parameterization**
 - TM #1 provides an overview of the datasets, processes, and foundational inputs required for a comprehensive pluvial modeling campaign of coastal counties in the Commonwealth of Virginia. The data described in this TM serves as the input data used to develop models via semi-automated pipelines.
- **TM # 2: Model Forcing**
 - TM #2 provides an overview of the datasets, processes, and foundational inputs required for forcing applied to the pluvial models described in TM #1. Whereas TM #1 focuses on ground surface characteristics (basin boundaries, elevation/topography, friction, and infiltration), TM #2 focuses on the hydrometeorological forcing data (precipitation) across an array of simulation scenarios.
- **TM # 3: Model Pipeline**
 - TM #3 describes the steps of the semi-automated workflow used to develop the HEC-RAS models. The input data sources, modeling assumptions and defaults, simulation scenarios, data storage infrastructure, and other considerations are described in TM #1 and TM #2.
- **TM # 4: Pilot Modeling**
 - TM #4 describes the activities and outcomes of the pilot study designed to explore and refine best practices to be used for the technical approach of the production of the pluvial models in the coastal areas of the Commonwealth of Virginia. The pilot effort identified best practices for implementing existing/future condition rainfall scenarios, model setup, and simulation across simple to complex areas within the study area.
- **TM # 5: Production Modeling**
 - TM #5 describes the production processes and outcomes for the pluvial models for the Virginia Coastal Resilience Master Plan.

1 TECHNICAL MEMORANDUM 1: MODEL DEVELOPMENT, GEOMETRY, AND PARAMETERIZATION

TM #1 provides an overview of the datasets, processes, and foundational inputs required for a comprehensive pluvial modeling campaign of coastal counties in the Commonwealth of Virginia. The data described in this TM serves as the input data used to develop models via semi-automated pipelines. The automated processes in the pipeline functioned as extract, transform, and load (ETL) tools that converted the raw inputs described herein into HEC-RAS models. The modeling process itself was directed by engineers who adjusted these components and parameters as needed to ensure quality models were developed for pluvial simulations.

1.1 DATA REPOSITORIES

All data developed for the pluvial modeling campaign was stored in the cloud for access by human and automated processes. Data storage was managed using Amazon Web Services (AWS) S3 (simple storage service) for binary objects (e.g., geotiffs, documents, images, models) and a PostgreSQL RDS (relational database service) for tabular and vector datasets (e.g., watershed boundaries, transportation data) as shown in Figure 1.

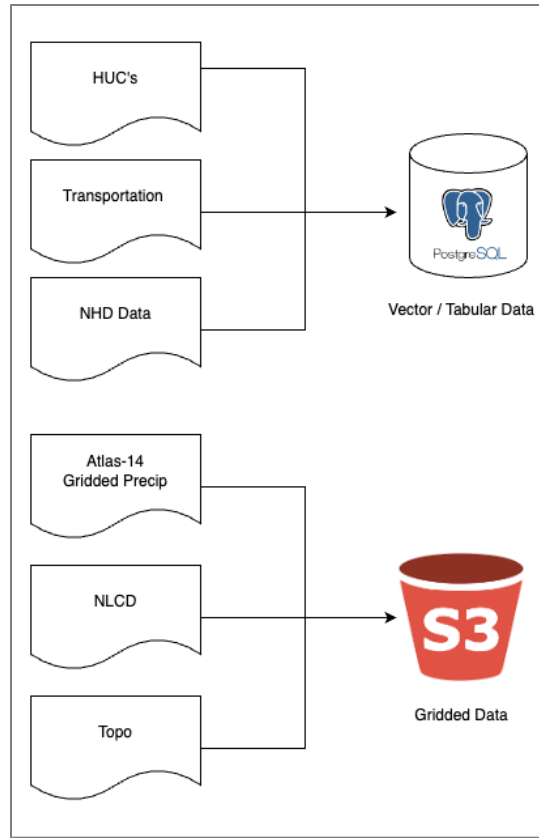


Figure 1. Example datasets stored in PostgreSQL and S3 (bucket named va-pluvial).

1.2 FOUNDATIONAL DATASETS

All pluvial flood models require foundational data, including ground elevation surface (topography), hydraulic friction values, and surface water infiltration values. A Manning's roughness ("N") raster was prepared for friction, while a Natural Resources Conservation Service Curve Number (NRCS, "CN") raster was prepared for infiltration. As Manning's N increases, the surface friction increases. As CN increases, the amount of infiltration decreases (i.e., runoff water increases). The values vary spatially within each basin's model.

1.2.1 TOPOGRAPHY

1.2.1.1 *Sources*

The principal source of ground elevation data is the tiled 10 ft rasters (.tif) developed for Phase I of the Coastal Resilience Master Plan (CRMP). These cloud-optimized geotiffs (COGs) were copied from the publicly available AWS open dataset available at <s3://vadcr-frp/rasters/TOPO>. A review of the data included in the development of that product was then undertaken, and the following new sources (i.e., best available) were identified in the National Elevation Dataset (Figure 2):

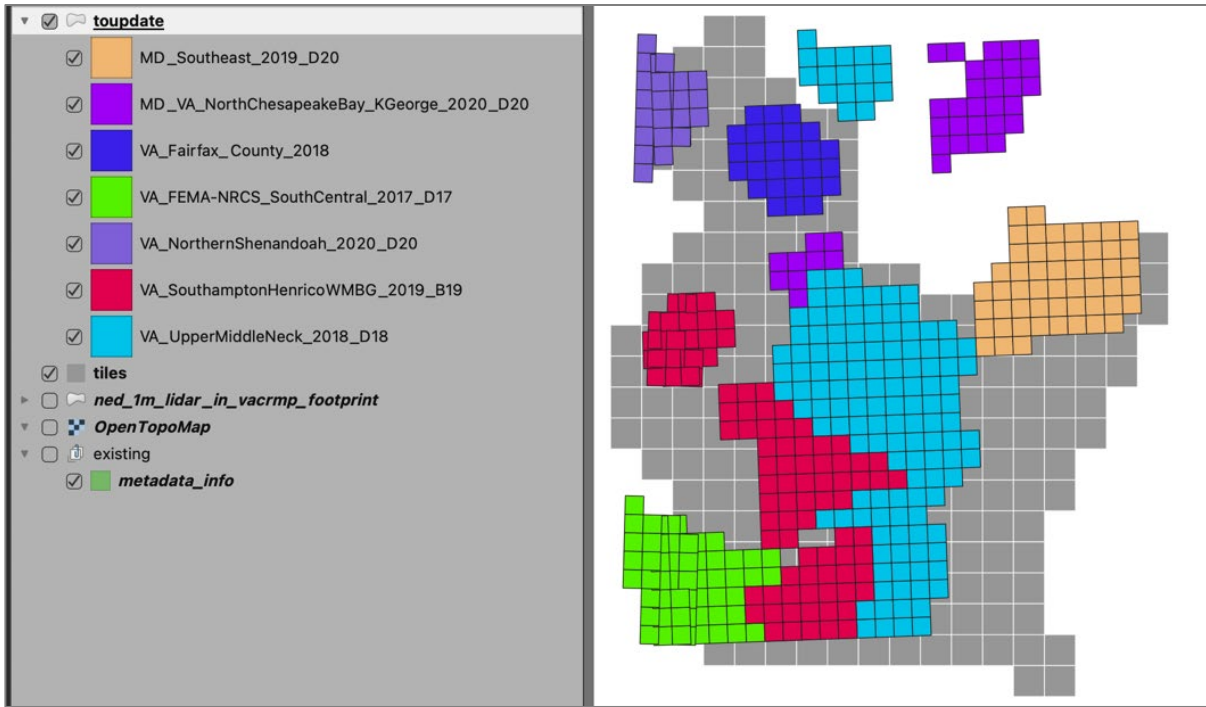


Figure 2. Map of existing coastal topography tiles (gray) and newly available USGS datasets (overlaid) used to create the project-wide DEM for pluvial modeling.

1.2.1.2 Processing

An existing internal tool was used to mosaic each of the newly available datasets into the existing tile grid, preserving the resolution of 10-foot pixels. The process for integrating this data was consistent with the development of the original tile grid, including the projection (EPSG:2284), tile scheme, and horizontal resolution.

1.2.1.3 Results

The results of this process are an expanded set of tiles suitable for use in developing the pluvial model geometry described in the following sections.

1.2.1.4 *Quality Control*

A quality control check was performed on the final set of tiles. The process used to ensure quality was performed by an analyst who was not involved in the development of the tiles themselves. The process for review was consistent with those undertaken for FEMA Flood Insurance Studies.

All tiles were inspected to determine that:

- Horizontal coordinates and units of measurement are in the correct project coordinate system (VA State Plane South), and
- Vertical coordinates, units, and elevations are in the correct project datum and are geocoded (NAVD88, feet).

A 10-20% sample of tiles was inspected to determine that:

- Tiles have elevations consistent with the source data,
- Tiles were correctly snapped to the established raster reference grid and had a resolution of 10 feet,
- Tiles lacked significant gaps not covered by available data sets and/or caused by mosaicking, post-processing, and
- Adjacent tiles maintain edge continuity and do not have poor transitions and/or anomalous elevations.

1.2.2 FRICTION GRID

1.2.2.1 *Sources*

The 2019 National Land Cover Database (NLCD) was downloaded to create the friction surface or Manning's N grid for this study.^{1,2} This dataset was selected for the study because it is the industry standard for developing friction and infiltration data for flood mapping studies. Other datasets containing higher (1 m) resolution data (i.e., the Chesapeake Bay Land Use and Land Cover Database and the Virginia Land Cover Dataset) were considered for developing the friction grid. During the pilot review, an analysis was performed using the higher resolution datasets to determine the impact of high-resolution friction compared to the NLCD.

The study team compared results from nine subbasin models by subtracting the output depths produced using the high-resolution friction with depths produced using the NLCD-based friction. Based on this analysis, it was determined that the average change in depth

¹ <https://www.mrlc.gov/data/nlcd-2019-land-cover-conus>

² https://s3-us-west-2.amazonaws.com/mrlc/nlcd_2019_land_cover_l48_20210604.zip

of pluvial flooding by including high-resolution friction changed depths on average 0.01 feet. Across the nine subbasins, nearly 95% of the resultant depths were within +/- 0.5 ft of the simulation with NLCD data. The areas that were most sensitive to the higher resolution friction grid data were stream channels associated with fluvial flood hazards, which were not the focus of this modeling effort (see Figure 3). Following this analysis, the engineering team opted to use the NLCD data as the source for friction based on the following criteria:

- The US Army Corps of Engineers Hydrologic Engineering Center (HEC) has not published friction values mapped to alternate land cover classifications outside the NLCD.
- High resolution datasets increase the storage size and processing required, while yielding nearly identical results.

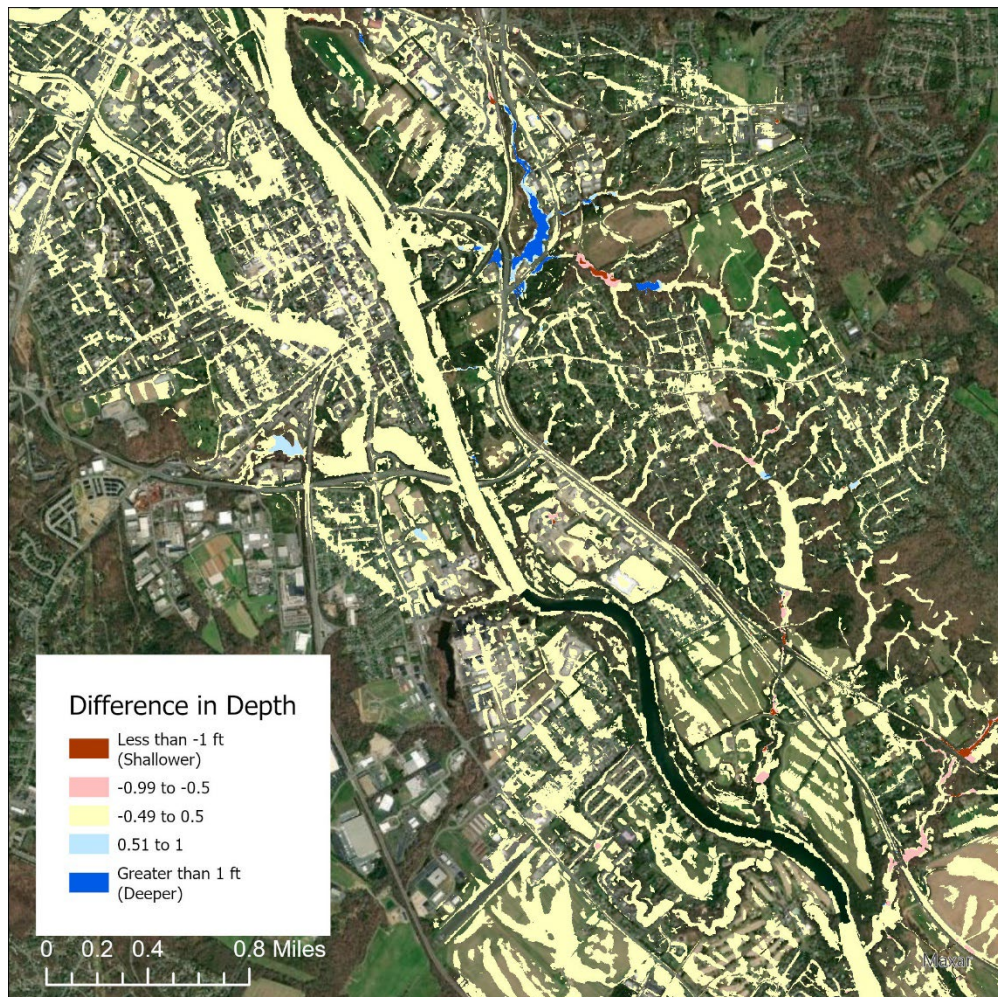


Figure 3. Representative illustration of differences in depth between models using high resolution (1-meter) friction and NLCD-based datasets. The greatest difference in depths is found in stream channels which are not the focus of the pluvial modeling.

A project-wide Manning's Roughness (N) grid was developed from the [National Land Cover Database \(NLCD\) \(2019 Edition\)](#). A simple lookup table (Table 1) was created to convert each land classification code to a roughness value. The HEC-RAS User Manual includes a range of roughness values for each land cover type, and the mean (center) of each range was chosen for this project's roughness lookup.

Table 1. Roughness Lookup Table.

NLCD 2019 Land Use Code	Description	Roughness (Mean of Range from RAS Manual)
11	Open Water	0.038
21	Developed, Open Space	0.04
22	Developed, Low Intensity	0.09
23	Developed, Medium Intensity	0.12
24	Developed, High Intensity	0.16
31	Barren Land (Rock/Sand/Clay)	0.027
41	Deciduous Forest	0.15
42	Evergreen Forest	0.12
43	Mixed Forest	0.14
51	Dwarf Scrub	0.038
52	Shrub/Scrub	0.115
71	Grassland/Herbaceous	0.038
72	Sedge/Herbaceous	0.038
81	Pasture/Hay	0.038
82	Cultivated Crops	0.035
90	Woody Wetlands	0.098
95	Emergent Herbaceous Wetlands	0.068

1.2.2.2 Processing

To develop the grid, the source land cover dataset was reprojected to EPSG:2284 (US feet). Because this data was discretized/classified (not continuous like elevation data), "nearest" resampling was used during the reprojection. Due to the source projection and final projection having different horizontal units (meters versus feet, respectively), the reprojected land cover data has a cell size that was not a round number but was approximately 98 feet, consistent with the source data resolution of 30 meters.

After reprojecting the land cover grid, the land cover class for each NLCD cell cover was mapped to an appropriate Manning's N value using the ranges provided in Table 2-1 of the *HEC-RAS 2D User's Manual*. Execution of this process was performed using a Python script,

which takes as inputs the lookup table and the NLCD raster clipped to the study area and outputs a study-wide raster, which was stored in S3.

1.2.2.3 *Results*

This process results in a COG (mannings.tif) that has the same projection, cell size (approximately 98 ft), and transform as the reprojected NLCD tiff from which it was derived (Figure 4). Each pixel was a floating-point value representing the roughness at that location.

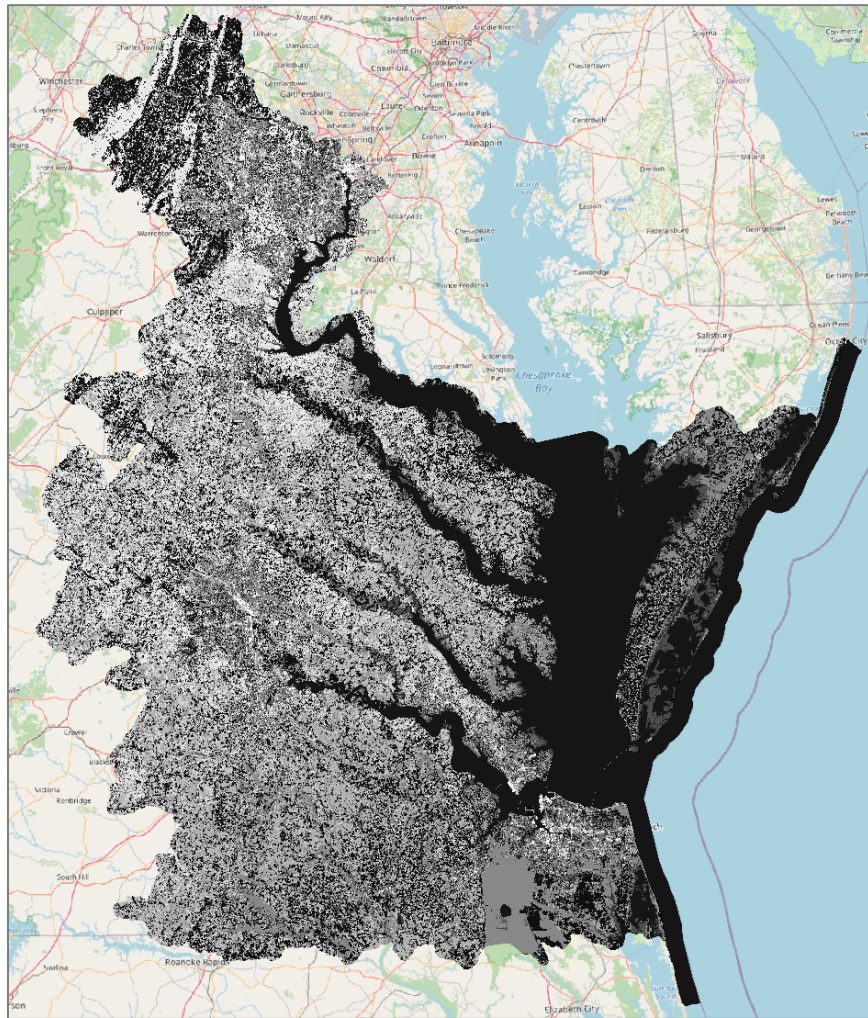


Figure 4. Manning's N grid for the project area is shown here (COG).

1.2.2.4 *QC Process*

A senior engineer reviewed the lookup table relating the NLCD land cover database to Manning's N. The Python script used to apply the lookup value was reviewed by a GIS developer, and the results layer (mannings.tif) was independently spot-checked manually in GIS against the input NLCD tiff to ensure the lookup table was applied correctly.

1.2.3 INFILTRATION GRID

For pluvial modeling, which is often characterized by ponding, low flow velocities, and high surface area, the resolution of infiltration grids can impact the model to a greater degree than traditional riverine-only flood models. Sensitivity analysis performed during pilot modeling confirmed this effect; hence, it was decided that when developing infiltration (CN) grids, additional high-resolution data sources for land cover were leveraged. A project-wide NRCS Curve Number (CN) infiltration grid was developed using land cover datasets shown in Table 2 and [SSURGO soil data](#).

1.2.3.1 Sources

The sources used to develop the infiltration grid are listed in Table 2 below.

In areas of overlap among land cover sources, priority was given (at the pixel level) based on the table below. Some code conflicts were identified (e.g., certain land cover sources used the same index integers as other land cover sources). In these cases, the codes were reassigned such that each land cover source could be fully represented in a composite mosaic of coded values. Then a mosaic land cover dataset was created. Figure 5 shows the coverage area for each of the land cover datasets.

An engineer developed a CN lookup table (i.e., each unique combination of land code and soil type was assigned to a specific CN value. Finally, the land cover mosaic was converted into a CN mosaic using the lookup table.

Table 2. Sources of Land Cover Data for Development of Infiltration Grid.

Priority	Land Cover Dataset	Pixel Size	Source
1	Chesapeake Land Use and Land Cover (LULC) Database 2022 Edition	1 m	https://www.sciencebase.gov/catalog/item/633302d8d34e900e86c61f81
2	Virginia State Land Cover Dataset 2016	1 m	https://vgin.vdem.virginia.gov/apps/virginia-land-cover-dataset/explore
3	NLCD 2021 Land Cover	30 m	https://www.usgs.gov/centers/eros/science/national-land-cover-database

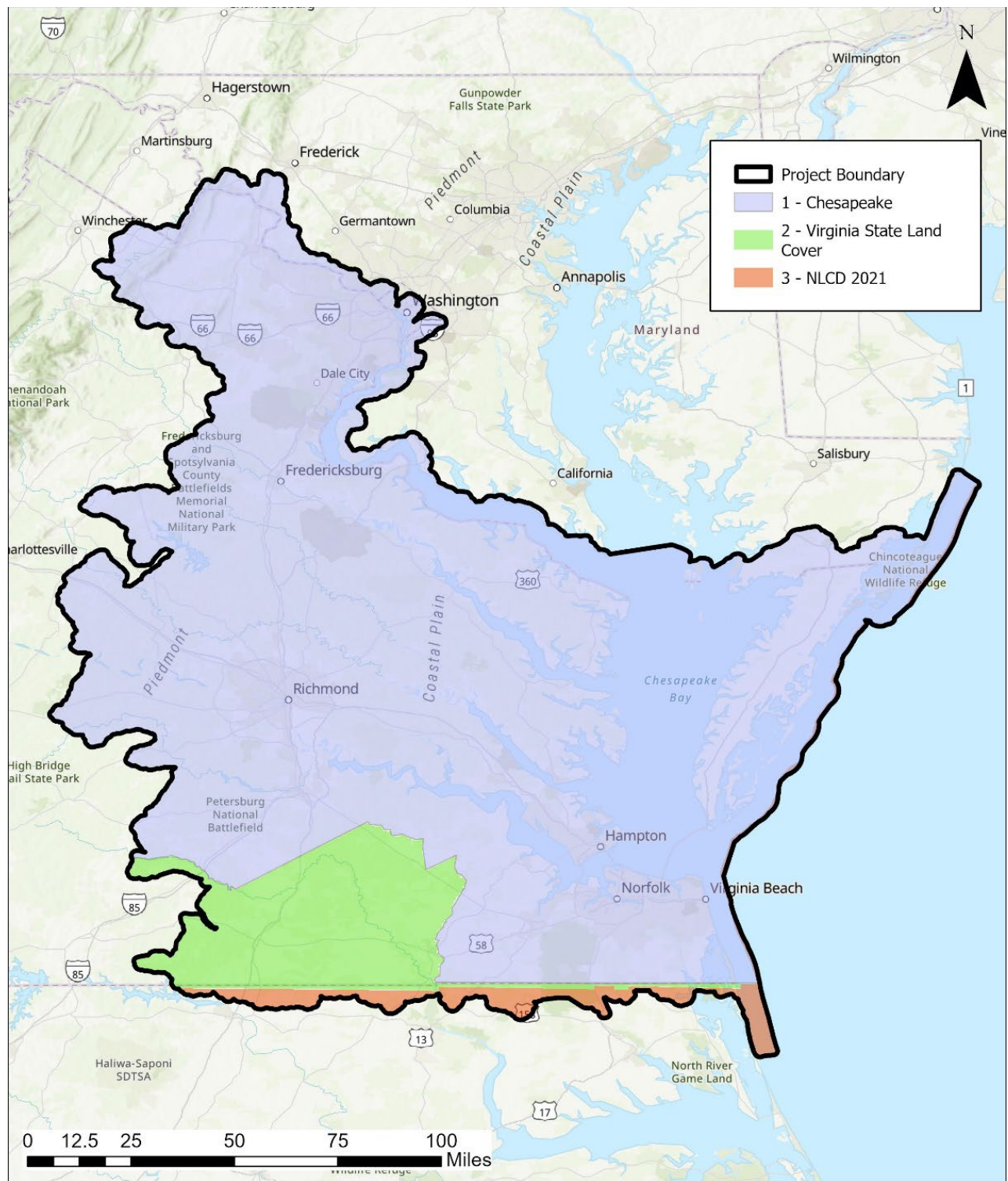


Figure 5. Coverage Area for Land Cover Sources.

1.2.3.2 Processing

The QGIS Plugin 'Curve Number Generator' Tool, Version 2.1.0 was used to create the Curve Number (CN) Grid for this study.³ This tool relates land cover and soil at a particular location to output a curve number value for each distinct combination of land cover and hydrologic soil group (HSG). The Curve Number Generator tool requires an input area of interest boundary polygon and outputs clipped NLCD 2019 Land Cover raster, SSURGO Extended Soil Dataset, and a final curve number layer based on the land cover and HSG values. The lookup table used to relate land cover and HSG with curve number can be found on the tool's GitHub page.⁴ Since the pluvial modeling study area was large, the area was divided into separate input units and executed using the batch processing mode in QGIS.

The tool documentation indicates that the maximum area boundary layer extent for the tool to run was 500,000 acres, but it suggests an area of 100,000 acres to run more accurately. Therefore, the total study boundary was divided into grid cells of just under 100,000 acres each to comply with this suggestion. A fishnet grid of cell sizes of 99,997.37 acres each was created, intersected with the study boundary polygon, and split into separate polygons based on the grid cell numbers. This resulted in the following reference grid in Figure 6, with 160 cells total intersecting the study-wide AOI polygon. The batch processing tool was run for each of the numbered cells.

³ https://plugins.qgis.org/plugins/curve_number_generator/

⁴ https://github.com/ar-siddiqui/curve_number_generator/blob/v2.1.0/curve_number_generator/processing/algorithms/con_us_nlcd_ssurgo/default_lookup.csv

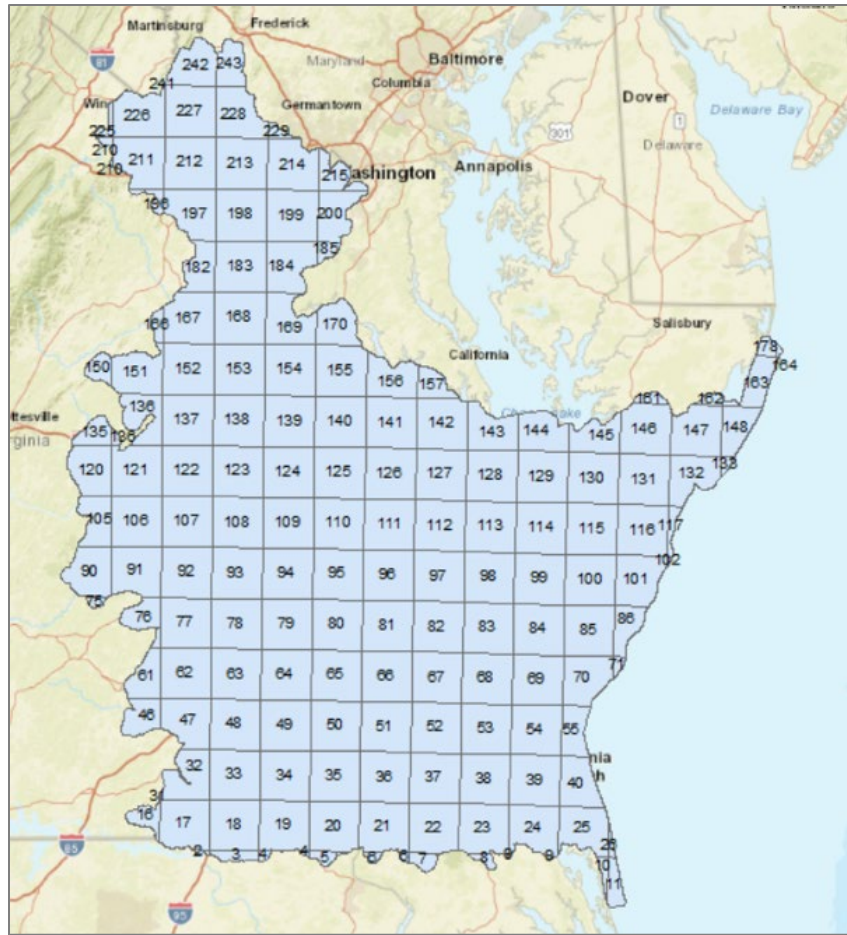


Figure 6. CN Grid coverage area and processing tiles.

A combination of OGR (OpenGIS Simple Features Reference Implementation) and GDAL (Geospatial Data Abstraction Library) command line tools was leveraged to create a single curve number virtual layer (composed of tile tifs) covering the entire AOI.

The raw output of the processing tool was 160 GeoPackages (polygon geometries) containing CN values (Figure 7). Each polygon included attributes naming the soil group or combination of soil groups (A, B, C, and/or D), the NLCD land cover value, the grid code reference, and the final curve number value. The intermediary tiled GeoPackages were rasterized in place to produce 1-meter horizontal resolution CN rasters as COGs (tifs), and a virtual layer .vrt file was created using GDAL to represent the tifs as one layer.

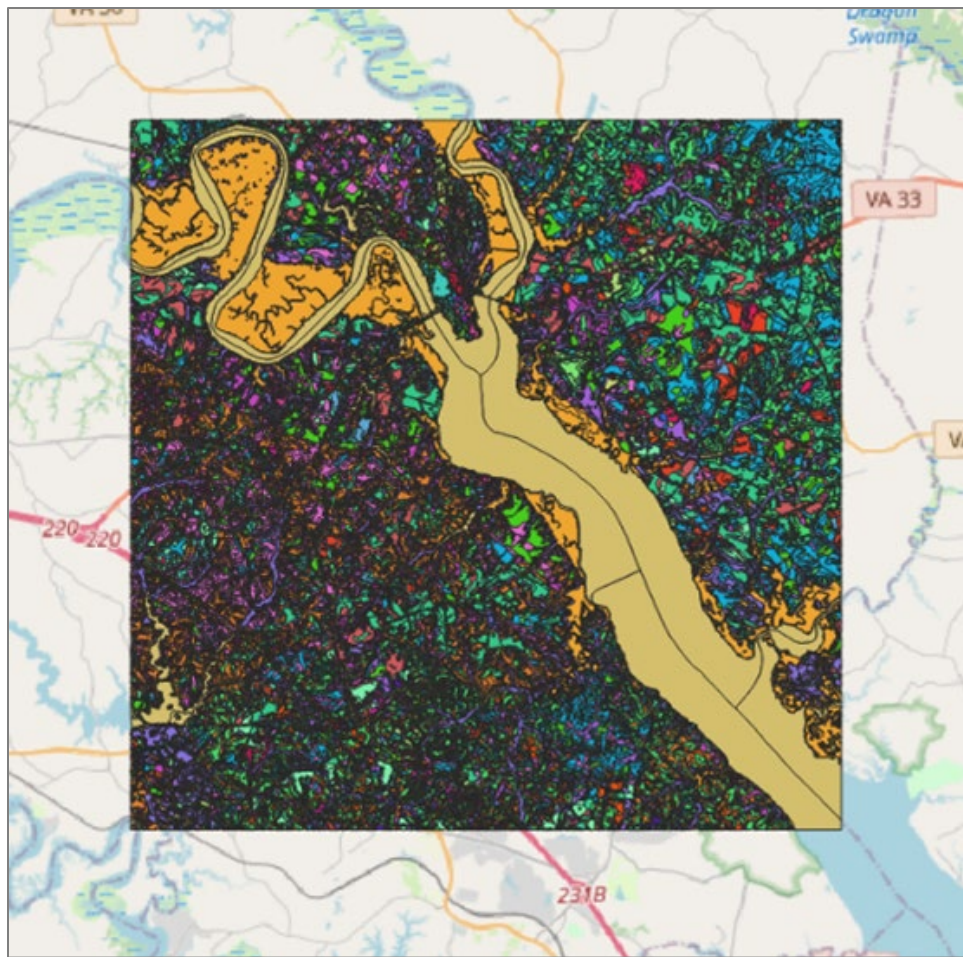


Figure 7. Raw output polygon of the CN tool shown at single tile location.

1.2.3.3 Results

The curve number values range from 30 to 100. Areas with a CN of 100 are all identified as NLCD class 11 (open water) and are correctly identified as such when compared with visual imagery. High CN values (>80) are attributed to areas of urban development and imperviousness. Other areas with high CN values include woody wetlands and emergent herbaceous wetlands. Low CN values (<55) are typically soil type A/B (high infiltration) forested areas. The areas with the next lowest CN value commonly include rural and grassland/herbaceous land classifications. A representation of the infiltration grid is shown in Figure 8.

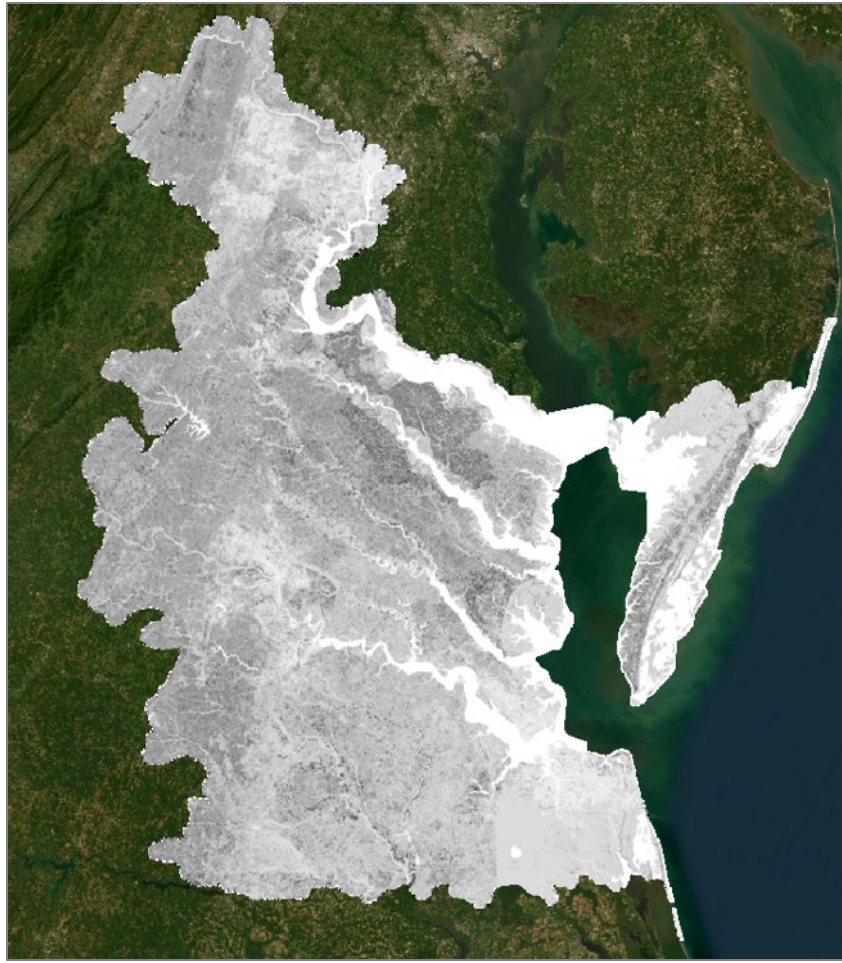


Figure 8. Final CN grid shown as a COG.

1.2.3.4 QC Process

Prior to production use, an engineer performed a review of the raw inputs, intermediate products, and final outputs of the CN production process. The following were reviewed spatially in GIS:

- Each of the three input datasets for land use codes,
- Final land use code re-assignments (avoiding conflicts between source datasets),
- Final land use mosaic (avoiding conflicts between source datasets), and
- Final CN tiles.

The final CN lookup table was reviewed in Excel. The reviewer confirmed that the land code and soil data were correctly attributed, that there were no overlaps in CN

assignments, and that the lookup tables were applied correctly to produce the final CN tiles. A final spot check was performed spatially for approximately 10% of the tiles.

1.2.4 VECTORS

1.2.4.1 *Sources*

The primary vector data sources for model development are:

- USGS Hydrographic datasets:
 - USGS Watershed Boundaries: HUC 12 datasets used for delineating modeling domains, and
 - NHD Flowlines (High Resolution).
- Virginia Geographic Information Network (VGIN) GIS Clearinghouse data:
 - Transportation layers (Road Centerlines) used to develop breaklines in HEC-RAS models and
 - Municipal Boundaries used as reference layers.

1.2.4.2 *Processing*

All vector layers were transformed (reprojected) to NAD83 / Virginia South (EPSG:2284) and loaded into the PostgreSQL database. After uploading, a select-by-location analysis was performed using standard SQL queries to remove all geometries located fully outside of the project AOI.

1.2.4.3 *Results*

The database contains tables representing each layer described in this section. All layers have primary keys and contain original dataset fields and values. Automated processes were used to interact with these datasets as the project progressed. An example of roadway breaklines is shown in Figure 9.

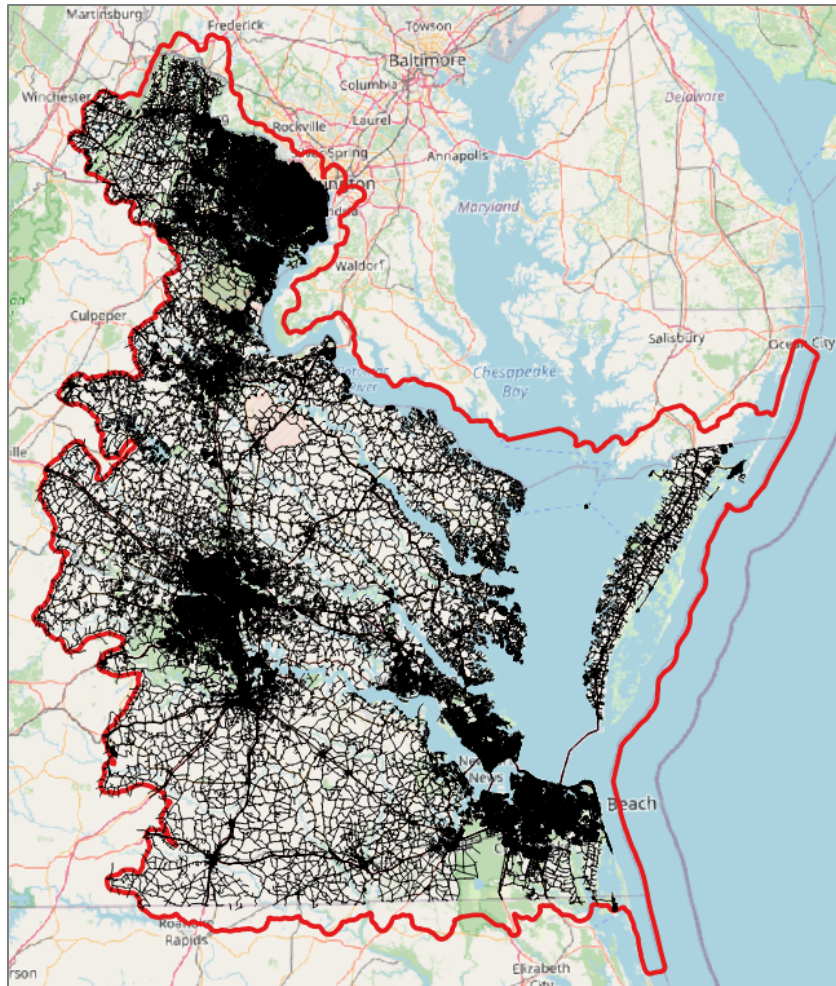


Figure 9. Road centerline data used for HEC-RAS breakline development.

1.2.4.4 QC Process

The QC process involved checking the validity of all geometries, consistency of tabular data with source, as well as visual checks to ensure that the layers provide the necessary coverage over the project AOI.

1.3 MODEL DEVELOPMENT

This section was originally included in TM#1 to describe the development of automated models. This information is now discussed in this report in Section 5.1.

2 TECHNICAL MEMORANDUM 2: MODEL FORCING

This TM provides an overview of the datasets, processes, and foundational inputs required for forcing applied to the pluvial models described in TM #1. Whereas TM #1 focuses on ground surface characteristics (basin boundaries, elevation/topography, friction, and infiltration), TM #2 focuses on the hydrometeorological forcing data (precipitation) across an array of simulation scenarios.

Initially and during the pilot modeling phase, the approach for inputting precipitation data was to choose precipitation depths that align with the latest [NOAA Atlas 14](#) precipitation frequencies for the Ohio River Basin (ORB), which encompasses all of Virginia and bordering states. This methodology is discussed in more detail below.

Following the pilot phase of the CRMP pluvial modeling task, DCR and Dewberry determined that an alternate approach for choosing precipitation depths was warranted. This document refers to this as the “interval-based approach.” This change in approach was meant to increase the long-term applicability of the pluvial modeling relative to future calculations of rainfall frequency in Atlas 15, which is expected to be released later in the 2020s. The initial pilot approach used total precipitation depths chosen from discrete Atlas 14 return periods (e.g., the “100-year storm”). For the production phase of the project, each HEC-RAS plan precipitation depth was instead set to a specific value along a range to cover all reasonably expected depths between the 2-year storm and the 500-year storm, including estimates of future rain amounts informed by climate science.

This section discusses the interval-based approach and how rainfall depths are transformed for use in the pluvial models.

The range of precipitation totals and standard increments used for each storm duration were determined by evaluating NOAA Atlas 14 in the study area in the context of scoped future climate change scenarios. The goal was to choose ranges that fully encapsulate current and future precipitation totals and increments that allow the total RAS plan count to stay within the 99-plan limit.

2.1 INTERVAL-BASED APPROACH

A fixed interval of increasing total precipitation depth has been applied between the plans. For example, if the interval was 1.0 inches and RAS plan “p01” used total precipitation depth of 2.0 inches, then “p02” used 3.0 inches, “p03” used 4.0 inches, and so on.

To achieve this approach, each modeled storm duration (i.e., 2-hour, 6-hour, and 24-hour) needs its own range of lowest and highest precipitation depths considered. Dewberry has estimated conservative limits of this range for each storm duration by

sampling Atlas 14 total precipitation grids and applying MARISA precipitation change factors.

The low end of each duration was taken as the lowest 2-year precipitation at current conditions. The high end was taken as the highest 500-year precipitation at future conditions. Future conditions were estimated by multiplying the current conditions value by a MARISA change factor. This future condition has been defined as the MARISA change factor for the RCP 8.5, epoch 2050-2100, for the 100-year storm. The MARISA dataset does not provide factors for the 500-year storm. A single change factor of 1.79 (79% increase) was selected. This value was the highest MARISA change factor for any county that intersects the watersheds being modeled for the CRMP pluvial study. This value occurs in Fluvanna County, which was not part of the CRMP.

Table 3 below shows, for each storm duration, the relevant Atlas 14 depths for counties within the CRMP study areas, as well as an estimated 500-year depth based on future conditions. The final “Proposed Low” and “Proposed High” ends of the range were rounded down and rounded up, respectively, to the nearest interval to ensure that the final range fully encapsulates reasonably expected values.

Table 3. Proposed ranges of precipitation totals for fixed-interval approach.

Storm Duration	Raw Atlas14 Depth (CRMP Counties Only)		Increased 79% (MARISA highest 100yr 90 th percentile climate factor, RCP 8.5, Epoch 2050-2100)	Proposed Range for CRMP Pluvial Models		Depth Interval Between RAS Plans (inch)	No. RAS Plans*
	2yr Low (inch)	500yr High (inch)		Future 500yr High (inch)	Proposed Low (inch)		
2 hours	1.37	6.55	11.72	1.00	12.00	0.50	23
6 hours	1.82	9.26	16.58	1.00	17.00	1.00	17
24 hours	2.59	13.38	23.95	2.00	24.00	1.00	23
						Total No. RAS Plans*	63

*Number of precipitation plans. Models affected by static tidal boundary condition will then be copied for each scoped future tide scenario.

2.2 TIDAL BOUNDARY CONDITIONS

In the initial approach described by TM #2, tidal boundary conditions could be assigned to future precipitation values based on epoch and recurrence interval. With a change to the interval-based approach, this requires an alternate methodology for assigning tidal boundary conditions such that each modeled precipitation depth must also be modeled in association with all potential tailwater elevations across the CRMP future epochs.

The initial suite of pluvial models has been developed using the present day (2020) CRMP mean high water conditions for any subbasin models that intersect the tidal boundary. For the remaining CRMP scenarios (2040, 2060, 2080, and 2100), Dewberry will create a copy of the subbasin models that intersect the mean high-water boundary for each scenario. The tidal boundary condition will then be adjusted to the appropriate value for each scenario. This exercise will be performed only for subbasin models that intersect the mean high-water boundary (inland models will not be changed). The end result will be a set of pluvial models for 2020 (including all inland and tidal subbasins), 2040 (tidal only), 2060 (tidal only), 2080 (tidal only), and 2100 (tidal only).

2.3 DEVELOPMENT OF BASIN HYETOGRAPHS

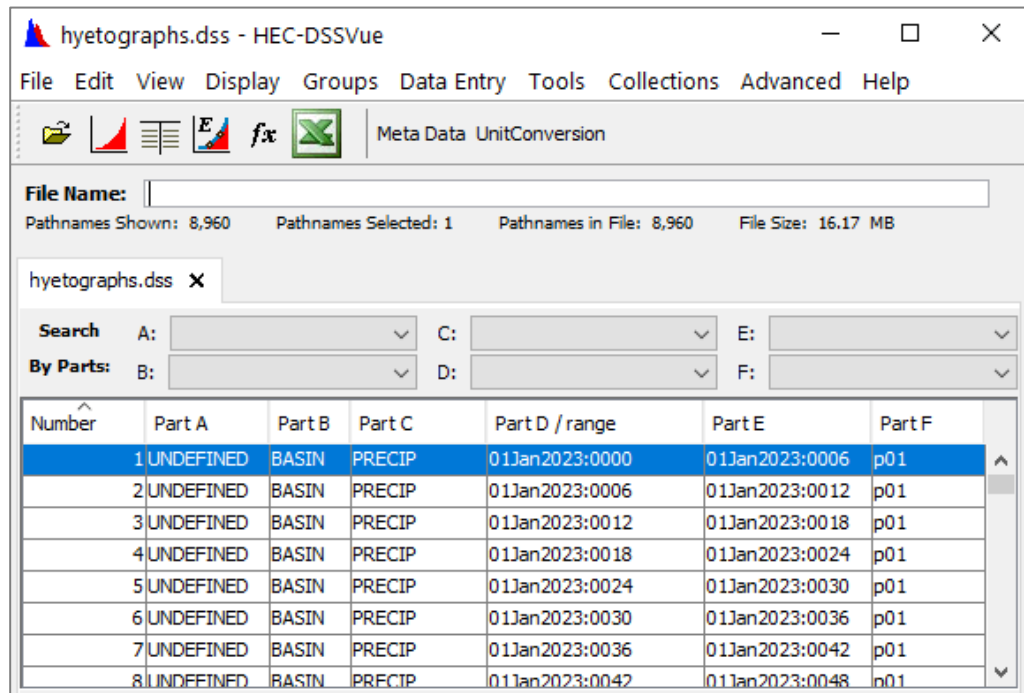
This section describes the development of hyetographs, which show incremental precipitation over time.

For each basin model:

- The basin polygon was intersected with county/municipality polygons.
- The model was associated with the FIPS code having the highest intersected area with its basin.
- The model was associated with the rainfall region associated with the FIPS code.

For each HEC-RAS plan:

- Volume was assigned to the model for each simulation (see Appendix B for rainfall volumes associated with each HEC-RAS plan). The cumulative rainfall distribution was looked up based on the plan's storm duration and the model's rainfall region.
- The cumulative rainfall distribution was converted to an incremental rainfall curve (portion of total falling at each timestep).



Number	Part A	Part B	Part C	Part D / range	Part E	Part F
1	UNDEFINED	BASIN	PRECIP	01Jan2023:0000	01Jan2023:0006	p01
2	UNDEFINED	BASIN	PRECIP	01Jan2023:0006	01Jan2023:0012	p01
3	UNDEFINED	BASIN	PRECIP	01Jan2023:0012	01Jan2023:0018	p01
4	UNDEFINED	BASIN	PRECIP	01Jan2023:0018	01Jan2023:0024	p01
5	UNDEFINED	BASIN	PRECIP	01Jan2023:0024	01Jan2023:0030	p01
6	UNDEFINED	BASIN	PRECIP	01Jan2023:0030	01Jan2023:0036	p01
7	UNDEFINED	BASIN	PRECIP	01Jan2023:0036	01Jan2023:0042	p01
8	UNDEFINED	BASIN	PRECIP	01Jan2023:0042	01Jan2023:0048	p01

Figure 10. Hyetograph records in DSS format.

2.3.1 QC PROCESS

The hyetograph-building process was a routine written in Python and SQL. A GIS developer reviewed the code, the inputs, intermediary outputs, and the final outputs were reviewed by an engineer. A spreadsheet was prepared by the reviewing engineer, comparing expected values (sampled/calculated by hand) with the outputs of the routine.

2.4 PIPELINE AND OUTPUTS

2.4.1 HEC-DSS FILES WITH HYETOGRAPHS

For each basin model, a single precipitation DSS file (hyetographs.dss) was created to contain hyetographs for all HEC-RAS plans. Each record in hyetographs.dss represents the depth of rain falling in a 0.1-hour (6-minute) timestep.

Since records for all hyetographs are in the same table, the HEC-RAS program can group the records into discrete hyetographs using the final component of the records' "pathname" (i.e., component "F" in DSS terminology). For example, all records associated with plan "p01" have a pathname like "/A/B/C/D/E/p01/".

Note that while each record in hyetographs.dss does have a geospatial grid, for this project there was spatial uniformity among the pixels of each record (see the Interval-Based Approach in Section 2.1 that describes how Atlas 14 was masked by each basin's polygon and reduced to a mean value of pixels within that basin). The application of uniform spatial precipitation was deemed sufficient for this project because model domains contain an area of 10 square miles or less, which is within the limit of requiring the application of an areal reduction factor.

2.4.2 UNITS

The final incremental hyetographs use vertical units of inches and have a timestep of 0.1 hours (6 minutes).

3 TECHNICAL MEMORANDUM 3: MODEL PIPELINE

This TM describes the steps of the semi-automated workflow used to develop the HEC-RAS models. The input data sources, modeling assumptions and defaults, simulation scenarios, data storage infrastructure, and other considerations are described in TM #1 and TM #2.

3.1 HUC-12 REFERENCE MODEL DEVELOPMENT

The first step in model development was the creation of a fully automated pluvial HEC-RAS model covering a raw HUC-12 basin. As described in TM #0 and TM #2, the automated model performs the following steps during setup:

1. Adds breaklines along VGIN's Virginia Road Centerlines major roads (all roads, not including local neighborhood and rural roads, MTFCC S1400 classification) and some streams (NHD high resolution features whose drainage area > 1 sq mi).
2. Modifies terrain to incorporate "burn lines" at major stream-road crossings.
3. Creates a default outflow boundary condition along its entire perimeter
4. Applies gridded timeseries precipitation as its sole source of hydrometeorological forcing data (no riverine inflows).

This HUC-12 model was then used to provide context and watershed response for engineers to use as a reference when partitioning the HUC-12 into individual model domains in the next step.

3.2 MODEL DOMAIN DELINEATION

The domain model development process started with an engineer splitting a HUC-12 into individual model domains. The primary goal of this step was to produce a set of small domains (typically less than approximately 10 square miles, consistent with the recommended limit for requiring areal reduction factor) with boundaries defined to capture the response of the area of interest due to an intense rainfall event, with normal depth or tidal HEC-RAS outflow boundary conditions (OBCs) controlling flow outside of the domain.

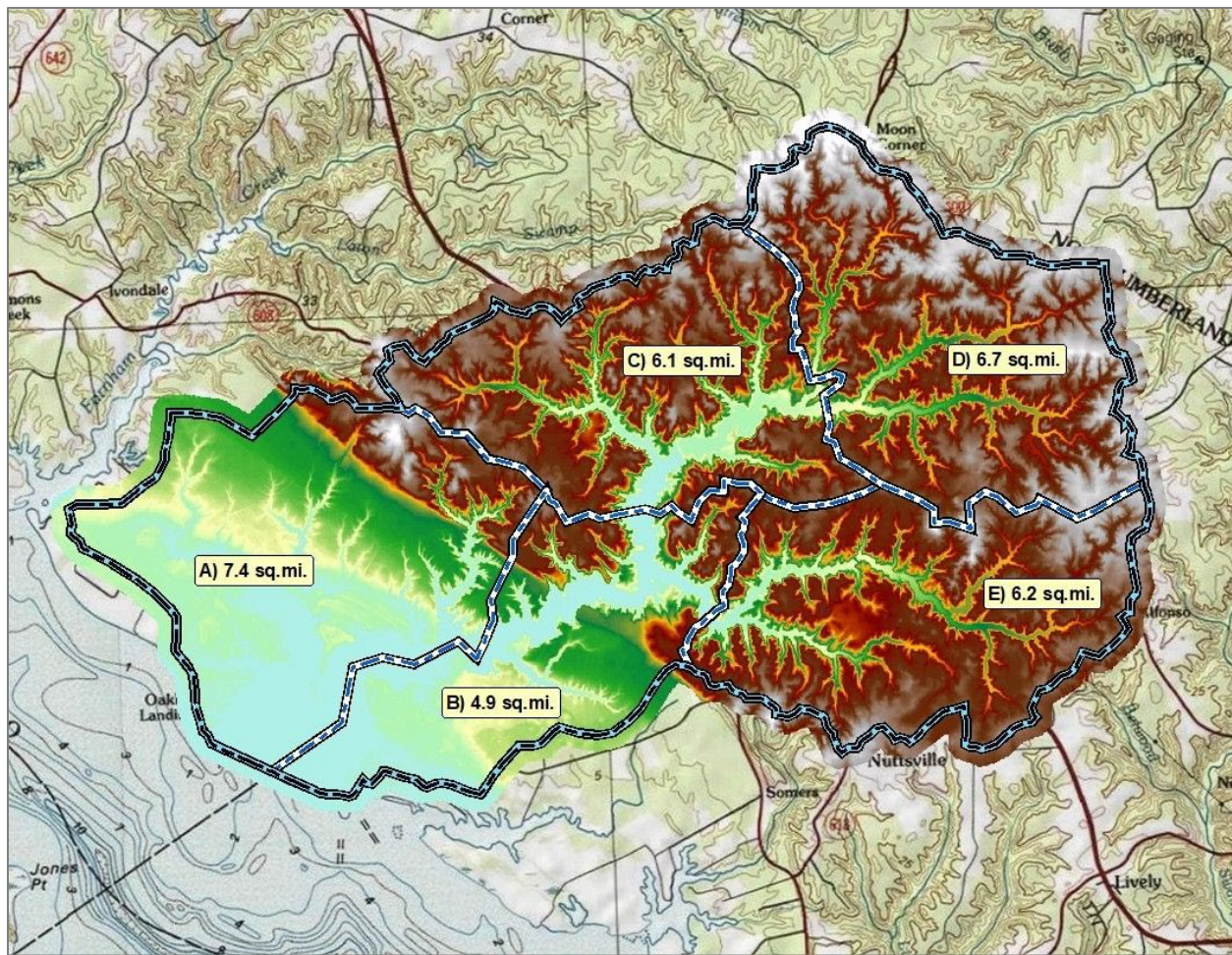


Figure 11. An example HUC-12 basin split into five domains.

Figure 11 above illustrates HUC 020801040601 and the five smaller domains that it was split into by an engineer during the initial phases of the pilot. The domains are labeled A through E along with their individual area in square miles.

For each HUC-12, after an engineer has divided the area into model domains, boundaries are applied and reviewed. Once approved, the engineer uploads a shapefile of the boundaries of the domains into the model management system. The contents of the shapefile are inserted into the database, which serves as the canonical source of model data for later stages.

3.3 MODEL CREATION

The model management system then executes an automated procedure to create an HEC-RAS model for all the model domains created per HUC-12. The automated model was generated following the same default parameters as the larger HUC-12 model.

3.4 MODEL REFINEMENT

Following the automated creation of the discrete models, engineers reviewed the model output and made manual changes in a model refinement process. The refinement process was undertaken for each model independently by engineers.

3.4.1 MESH

The default 2D mesh spacing was set to 100 feet.

Parameters of previously generated breaklines were adjusted as necessary, and in some rare cases, new breaklines were drawn. Examples where new breaklines were drawn include along dam crests and roads that act as significant pluvial obstructions.

Breakline center alignments were automatically defined along Road Centerlines using transportation data from the Virginia Road Centerlines (RCL) layer, accessed 2/14/2023 from the Virginia Geographic Information Network (VGIN) GIS Clearinghouse. The mesh spacing around breaklines was set to 50 feet. The total number of "near repeats" (see HEC-RAS [documentation](#)) was set as zero. An example of this is shown in Figure 12.

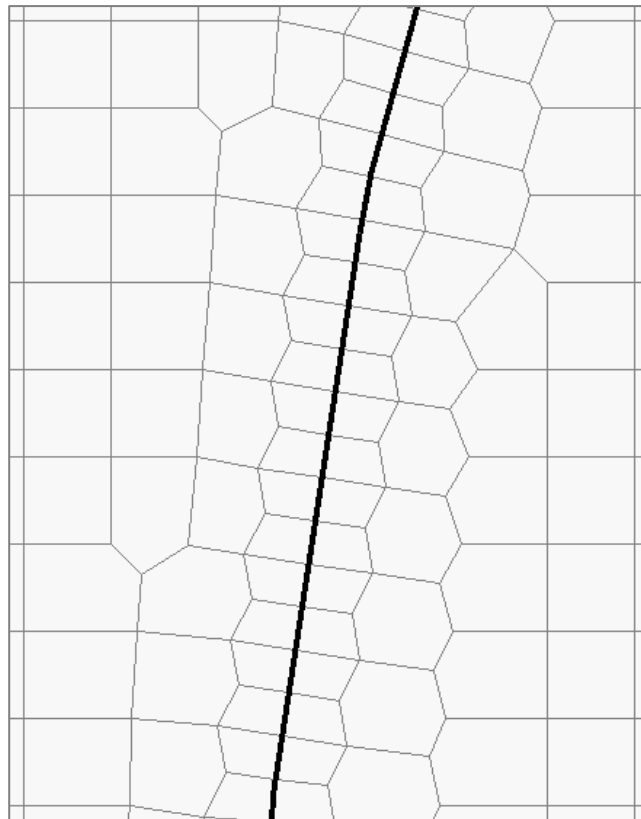


Figure 12. Breakline effect on 2D model mesh, with zero "near repeat" lines.

3.4.2 TERRAIN

In the automated initial model, terrain modification channel lines (i.e., burn lines) were included in the topography dataset for some major stream-road crossings. Engineers adjusted and/or drew new burn lines as needed.

Terrain modification lines, in this case “channel” or “burn” lines, were automatically defined along National Hydrography Dataset (NHD) high-resolution flowlines, within 200 feet of where flowlines intersect road lines. The default size and shape of these automated burn lines were set as shown in Figure 13 below:

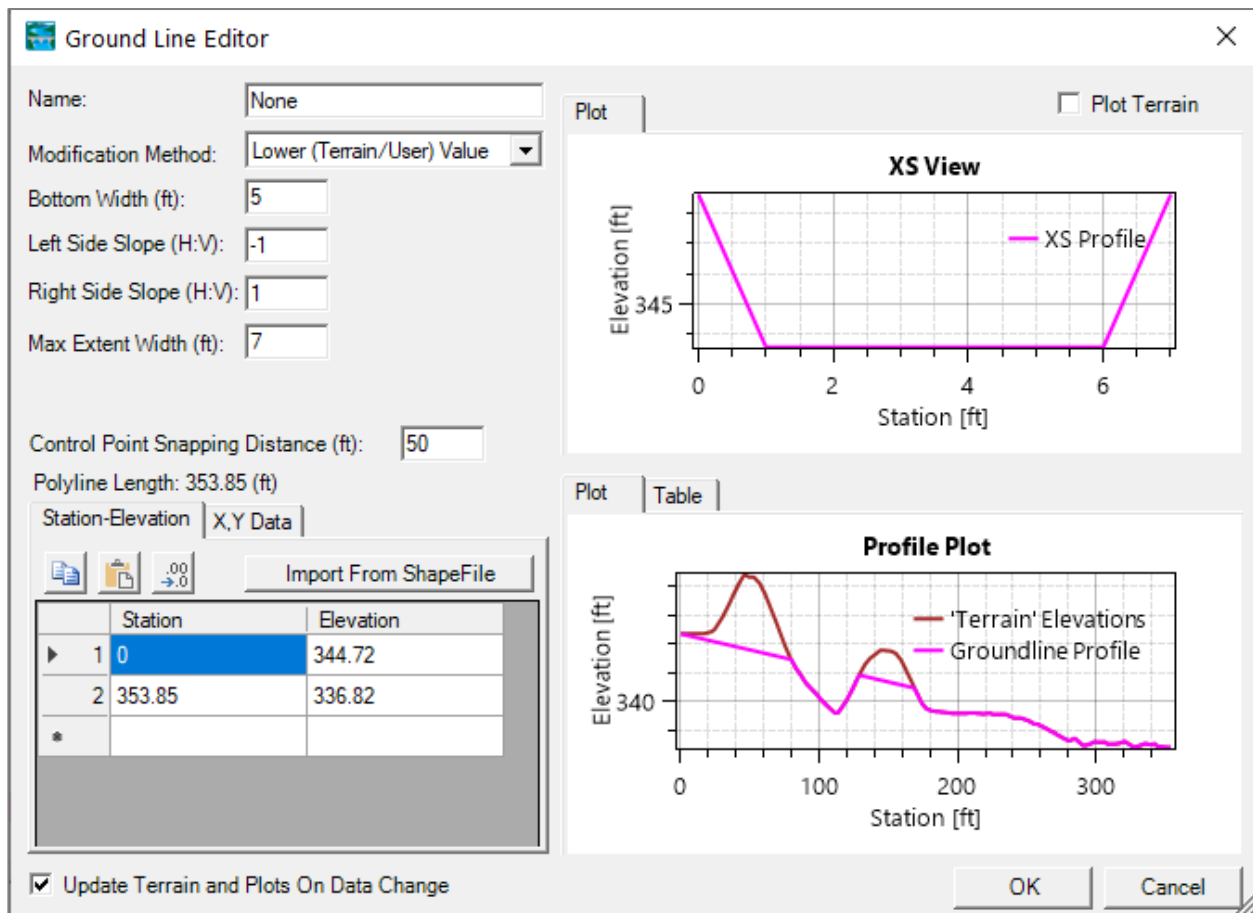


Figure 13. HEC-RAS screenshot: burn line parameters and effect on stream profile.

If warranted, engineers used engineering judgment to revise the automated burn lines. For example, burn lines were removed in some areas where the channel was already represented by the base DEM, which can occur for bridges but rarely occurs for culverts. The final terrain used by the HEC-RAS model includes these adjustments in an HDF file that accompanies the original topography file.

3.4.3 OUTFLOW BOUNDARY CONDITIONS (OBCS)

To allow water to freely exit the model anywhere along its perimeter, a default normal depth boundary condition was applied to the perimeter of every model, with a normal depth slope of 0.01 (1%).

For basins affected by tide (present or future), engineers assigned a static water surface elevation to represent high tide at the relevant scoped climate scenarios. These static boundary conditions were included as additional boundary condition lines in HEC-RAS, and the geometry of the default full-perimeter normal depth boundary condition was edited to allow for the static elevation lines where appropriate.

3.5 PARALLEL MODEL EXECUTION AND POSTPROCESSING

When a model's geometry and boundary conditions have been through QA/QC stages and finalized, the project's modeling system executes each plan in parallel using the Linux "RAS Unsteady" executable. Then the system sends the raw results to a Windows machine for postprocessing. The Windows machine runs the HEC-RAS postprocessing routine to produce a flood depth raster for each plan, then transforms those rasters into cloud-optimized GeoTIFFs (COGs) in the Web Mercator coordinate system for high-performance, interoperable serving. No changes are made to the output from the HEC-RAS mapper (i.e., depths are not adjusted).

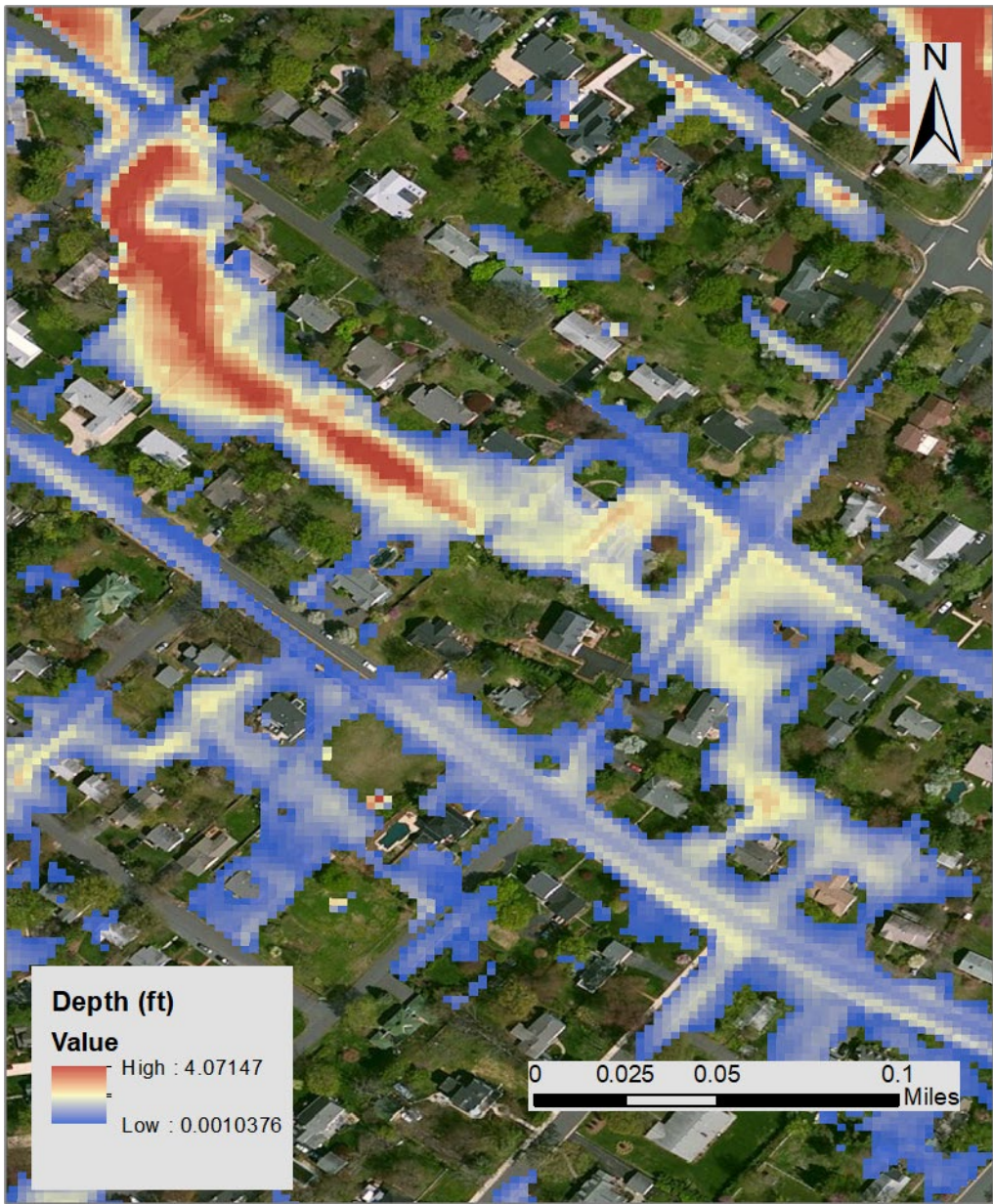


Figure 14. Sample preliminary results for an area demonstrating a 24-hour duration storm. Note that the model identifies flood hazards outside of stream channels in residential areas.

The figure above (Figure 14) shows preliminary pilot depth grid results for HEC-RAS plan p84 (in the RAS plan schema from the pilot phase, which is different from the production schema). This simulation represents the 24-hour, 500-year storm at the climate scenario defined by the 2050-2100 epoch, with representative concentration pathway (RCP) of 8.5. The total precipitation of this simulation was approximately 13 inches at this location. A similar 13-inch interval-based precipitation depth will be represented in the production modeling. In this figure, flood depth values range from approximately 0 to 10 feet.

3.6 QA/QC STAGES

At various stages in the model pipeline, quality assurance and quality control checks were performed. Some checks were manual, and some were automated. Please refer to the project's quality plan for details. Key elements of quality assurance and control in the production process included:

- Frequent discussion of sources of quality issues in model development
- Front-end quality risk mitigation ensured by means of:
 - Documentation of data sources
 - Establishment and documentation of production team standard operating procedures
 - Scripting key production steps to ensure consistent application of production processes for all input data.
 - Establishing a central data repository for final products for the production process, validating final status of products before production
- Performed internal quality reviews in model development, which included:
 - Review, conducted by a senior engineer, of model delineation according to established SOP
 - Ensuring all input data provided full coverage of the study area
 - Review of automated outputs by the production team to ensure that they were in accordance with the established parameters

4 TECHNICAL MEMORANDUM 4: PILOT MODELING

This TM describes the activities and outcomes of the pilot study designed to explore and refine best practices to be used for the technical approach of the production of the pluvial models in the coastal areas of the Commonwealth of Virginia. The coastal areas incorporate the 57 counties under the Coastal Resilience Master Plan. The pilot effort identified best practices for implementing existing/future condition rainfall scenarios, model setup, and simulation across simple to complex areas within the study area. HEC-RAS models and depth grids from simulations accompanied the delivery of the documentation and were shared via download links. Lessons learned from the pilot modeling were identified and implemented as needed for full-scale production.

Process Highlight: This section of the report details the outcomes of the pilot modeling study. As a result, this section may refer to data or procedures that were not used in the final production of pluvial modeling for the CRMP study area. Any updates to the methodology provided in this section can be found in Section 5 of this document. The information presented here is for documentation purposes only.

4.1 SELECTED PILOT BASINS

Nine hydrologic unit codes (HUC) were selected from a provisional list of HUCs provided for the pilot study by the Commonwealth and divided into a total of 57 subbasins. The pilot HUCs were selected to represent a wide range and combination of terrain conditions, population density, tidal influence, and other physiographic considerations. The HUC locations are shown in Figure 15 and details of the HUC characteristics are provided in Table 4.

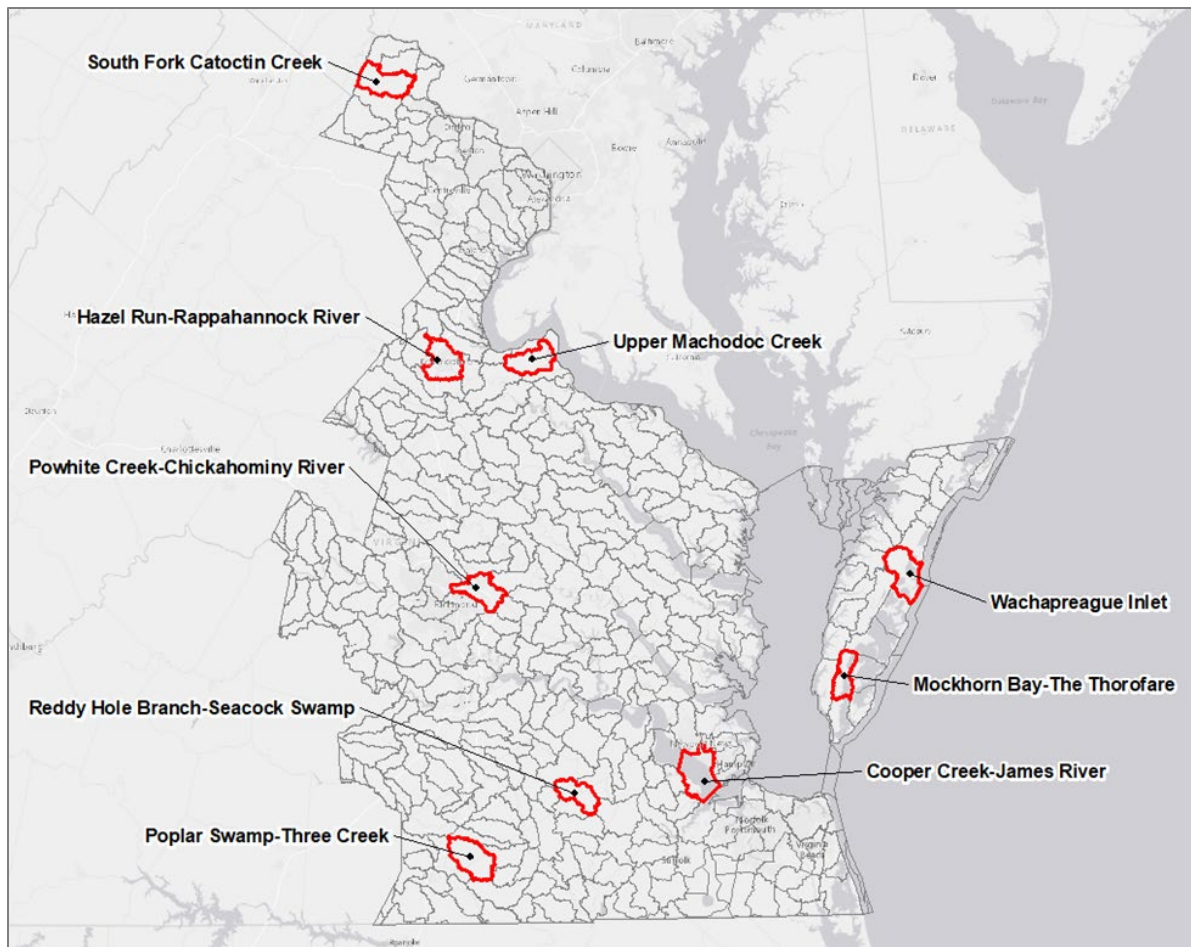


Figure 15. A map of the HUC-12s in the study area with locations modeled in the pilot study shown in red.

Table 4. Summary of HUC-12s and relevant data used for selection in the pilot.

HUC	Name	Terrain	Population Density Type	Tidal Conditions
020403040104	Wachapreague Inlet	Shoreline/tidal flats	Rural	Yes
020403040301	Mockhorn Bay-The Thorofare	Moderate ridge/shelf above tidal flats	Rural	Yes
020700080301	South Fork Catoctin Creek	High relief with stream network	Dispersed rural suburban and farmsteads	No
020700110601	Upper Machodoc Creek	High relief with stream network, steep ridge/shelf, outlet directly to the Potomac River	Rural	Tidal River
020801040102	Hazel Run-Rappahannock River	Moderate relief with major river	Urban	Tidal River
020802060501	Powhite Creek-Chickahominy River	Moderate relief with swamp	Urban	No
020802060906	Cooper Creek-James River	Shoreline	Urban	Yes
030102011004	Poplar Swamp-Three Creek	Moderate relief with swamp	Rural	No
030102020401	Reddy Hole Branch-Seacock Swamp	Moderate relief with swamp	Rural with small urban area	No

4.2 MODELING PROCESS

The information in this section builds upon the information in the above technical memos. TM #1, TM #2, and TM #3 provide important context for the pilot modeling process described below.

4.2.1 BASIN MODEL CREATION

Raw input datasets - including the digital elevation model (DEM), Manning's N grid, SCS Curve Number (infiltration) grid, NOAA Atlas 14 Precipitation grids, NHD streamlines, Virginia roads, precipitation distribution tables (temporal), and climate change factors - were developed in advance of the pilot for the entire study area. The model setup process was outlined as follows:

- HUC-12s were divided into smaller subbasins suitable for pluvial modeling. This step was performed manually by engineers selecting a HUC-12, reviewing natural and hydraulic features, and splitting the HUC-12 into subbasins.
- These subbasins were then buffered by about 500 feet to achieve adequate overlap and to ensure no gaps in model coverage results for the HUC-12 watershed.
- A senior engineer reviewed the watershed division and resulting subbasin polygons.

After approval, the subbasin polygons were uploaded into the modeling system. For each subbasin developed in this step, an ID was assigned composed of its parent HUC-12 as a prefix and an arbitrary increment as its suffix (e.g., 020403040104_0, 020403040104_1). The suffix has no hydrologic or hydraulic significance.

4.2.2 INITIAL AUTOMATION

Following the development of the modeling basins for each HUC-12, a series of automation steps were triggered. The processes described here were part of a cloud-based system, and each modeling basin was inserted into a pipeline consisting of the following steps:

- The project-wide raw inputs were masked/clipped and converted into layers compatible with HEC-RAS.
- Hyetographs for all HEC-RAS plans (rainfall scenarios run on each model) were generated from NOAA total precipitation grids and written into a .dss file for that model.
- A HEC-RAS mesh (with breaklines) was generated.
- HEC-RAS Terrain Modification Lines (burnlines) were incorporated into the mesh.
- Standard HEC-RAS model files (.prj, .g01, .g01.hdf, .pNN, .uNN, .rasmap, etc.)

were generated.

A default mesh of 100-ft was used, and breaklines were assigned 50-ft mesh spacing. The diffusion wave equation was the selected solver, and the computational interval (timestep) was set to 10 seconds.

4.2.3 MODEL DEVELOPMENT

Model development involves the refinement of the model by the engineer to create the final geometry. The automated models from the previous step were reviewed and modified for consistency and accuracy that was unable to be incorporated at the automation stage. Engineers ensured that the projection, geometry associations, mesh spacing, breakline spacing, boundary conditions, and plan run times were appropriate and made changes as needed.

For models that do not include a tidal boundary, a default normal depth slope (0.01 ft/ft) was retained (from the automated process) for the entire lasso around the mesh domain. The ends of the lasso boundary were checked to ensure that they do not overlap on the same cell face, which can result in errors. Where the boundary ends may overlap at the same face, the engineer made a correction to ensure proper model behavior and that flow exits the model at the boundaries.

For tidal boundary locations, a new boundary line was placed along the tidal boundary. In these cases, the default lasso boundary was shortened to avoid overlapping the same cell face with the tidal boundary. This approach was applied to both open shoreline and boundaries at tidal rivers.

The tidal boundaries were assigned a constant stage hydrograph for the duration of the model run, with elevations selected from the mean high water stillwater elevation rasters from the Virginia Department of Conservation and Recreation Coastal Resilience Master Plan. The stillwater elevations cover different epochs from 2020 to 2100 and are shown in Table 5. These elevations apply to the pilot models only.

Table 5. Static tide heights for applicable models (all units are feet NAVD88).

Model ID	2020 applied to "Present"	2060 applied to MARISA "2020-2070"	2080 applied to MARISA "2050-2100"
020403040104_0	2.050	4.890	6.610
020403040104_1	2.000	4.870	6.600
020403040104_2	1.980	4.800	6.520
020403040104_3	2.050	4.890	6.610
020403040301_1	2.160	5.050	6.760

Model ID	2020 applied to "Present"	2060 applied to MARISA "2020-2070"	2080 applied to MARISA "2050-2100"
020403040301_2	2.300	5.270	6.990
020403040301_3	2.210	5.160	6.890
020403040301_4	2.120	5.020	6.740
020403040301_5	2.220	5.200	6.950
020700110601_1	1.280	3.840	5.480
020700110601_2	1.280	3.840	5.480
020700110601_3	1.280	3.840	5.490
020700110601_6	1.280	3.840	5.480
020801040102_0	1.310	4.110	5.840
020801040102_7	1.530	4.210	5.890
020801040102_8	1.530	4.210	5.890
020802060906_0	1.490	4.295	6.000
020802060906_1	1.525	4.280	5.975
020802060906_2	1.525	4.325	6.040
020802060906_3	1.480	4.245	5.935

Breaklines were incorporated into the mesh during the automation processes for major waterways and roadways. Based on engineering judgment, engineers added breaklines for important features such as roadways or waterways that were not part of the automation process. In some cases, breaklines that were significantly misaligned with their respective features were adjusted to better match the underlying terrain. Breaklines that have no significance to the pluvial modeling may have been removed (e.g., minor waterways outside of developed areas or short segments with no relevance). Breaklines were then enforced, and any resulting mesh errors were resolved. Near repeats and cell protection radius were incorporated in some locations based on engineering judgment and modeling factors.

Burnlines were also incorporated during the automation processes to allow for flow at locations that lack hydro-reinforcement (culverts and bridges not represented in the DEM). These parameters were reviewed, modified, or added as necessary by the engineer developing the model. Common issues that may have been corrected were misaligned burnlines, burnlines not long enough to cut through the feature, or missing burnlines. In general, where unreasonable ponding occurred or conveyance was significantly restricted, burnlines were added.

4.2.4 MODEL REVIEW

Model review in the early phases was largely directed at identifying appropriate assumptions for uniform parametrization, common issues, and best practices for developing models that were consistent and effective across the variable study area. More details about these activities are described in the Sensitivity Analysis section below.

Boundary conditions were reviewed for all models to ensure boundary lines were applied correctly and the data set for tidal boundary still water elevations were extracted appropriately. Reviews also included checks to ensure there was sufficient conveyance through the model without significant or widespread ponding. Where significant ponding or insufficient conveyance occurred, additional burnlines were recommended.

Velocity results were reviewed based on a threshold of 25 feet per second (fps). Approximately 15% of the models exhibited high velocities exceeding 25 fps. Unrealistic velocity values may indicate inaccurate results at these locations and require modeling refinements to resolve. However, when present, high velocities occurred primarily in channels or at the upstream end of tidal river boundaries where the downstream boundary was forcing the upstream elevation. These areas are associated with the fluvial process and are not considered significant to the pluvial process results.

All the model runs included in the pilot were free of water surface elevation errors using the assigned plan settings. The maximum volume percent error was less than 0.5%. The volume percent error was less than 0.2% for plans incorporating lesser frequency storm events, with two exceptions. The volume percent error for the more frequent storm event was generally between 0.2% and 0.5% for all non-tidal domains. The volume percent error for tidal domains was less than 0.2%.

As the automation process was refined, subsequent reviews focused on ensuring the mesh and breakline spacing were correct, boundary conditions, plan run times, and the ponding and conveyance results for each model.

4.2.5 MODEL SIMULATIONS

Following model development and review, an automated process was executed in the cloud to prepare files and execute simulations for all of the combinations of frequency, epoch, and duration included in the pilot. This process included the following steps:

- An unsteady flow file was created using the appropriate forcing from the precipitation .dss file for each model.
- Where tidal boundaries exist, known water surface elevations were applied directly to the unsteady flow file.
- Each plan was then run in the cloud using a Linux-based version of the HEC-RAS unsteady compute.

- Each plan was post-processed (i.e., written to a results .tif file) and written to an output location within the model directory.

4.3 SENSITIVITY ANALYSIS

A sensitivity analysis was conducted during the pilot model period to identify appropriate parameters for applying to models during the automated and manual model development steps. Results from the sensitivity test were then used to modify steps in the production workflow (see Section 5.2). This section describes the process undertaken and the results applied to the modeling framework.

4.3.1 SIMULATION TIME WINDOW

To determine the necessary simulation time window for each storm duration, pilot basin 020700080301_2 shown in Figure 16 below was selected for testing because of its long flow paths. The reach of North Fork Catoctin Creek that is contained within this basin has a longitudinal profile of approximately 8 miles.

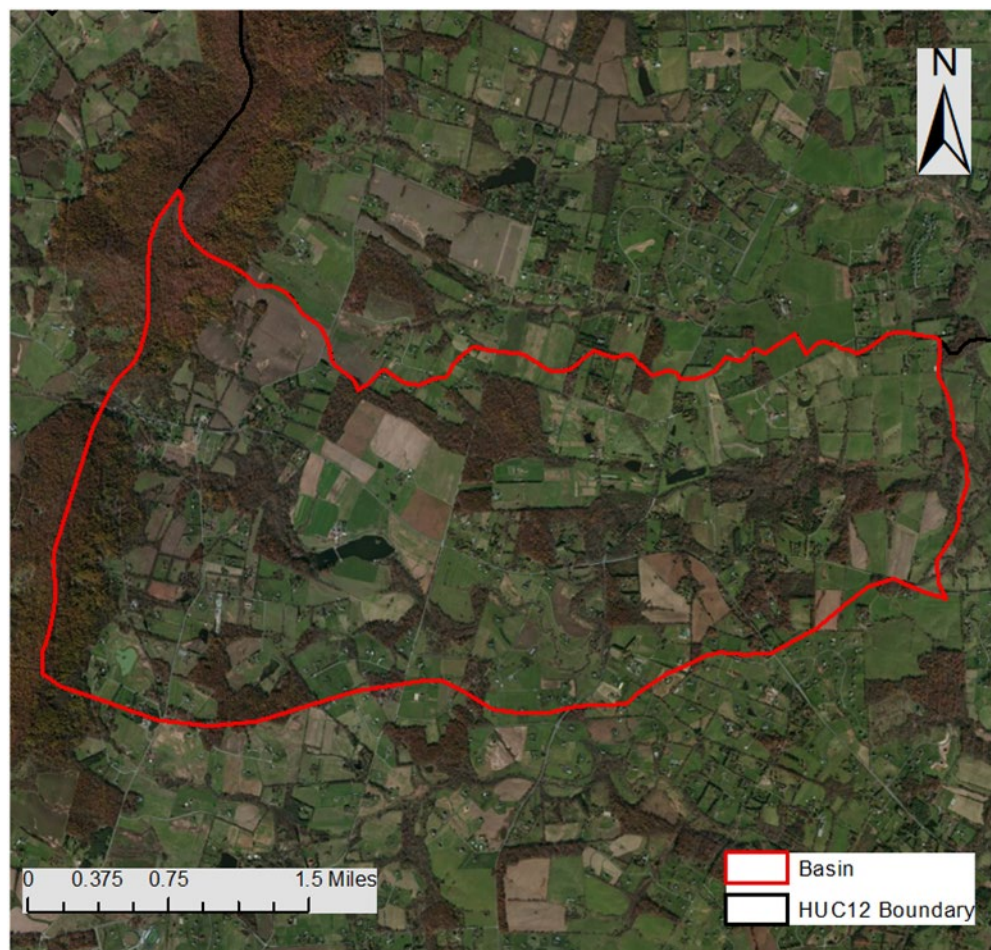


Figure 16. Basin 020700080301_2 includes rural areas with farmsteads dispersed throughout.

4.3.2 SENSITIVITY TEST

This basin was utilized to determine the appropriate simulation time window for the 2-hour, 6-hour, and 24-hour storm durations. Each storm duration was run with three different simulation times. The 2-hour pilot plan (p01) was run simulation times of 2, 12, and 36 hours. The 6-hour pilot plan (p13) was run for 6, 12, and 24 hours. Lastly, the 24-hour pilot plan (p84) was run for 24, 36, and 48 hours. The outlet hydrograph for each run was used to determine the validity of the simulation duration are provided in Section 4.3.2.1.

4.3.2.1 *Sensitivity Results*

Results of the simulation duration testing are shown below in Figure 17, Figure 18, Figure 19. Each chart includes the simulated hydrograph at the downstream outlet of the basin for each model simulation time tested. These charts were used to evaluate the time necessary to capture peak discharges from the basin.

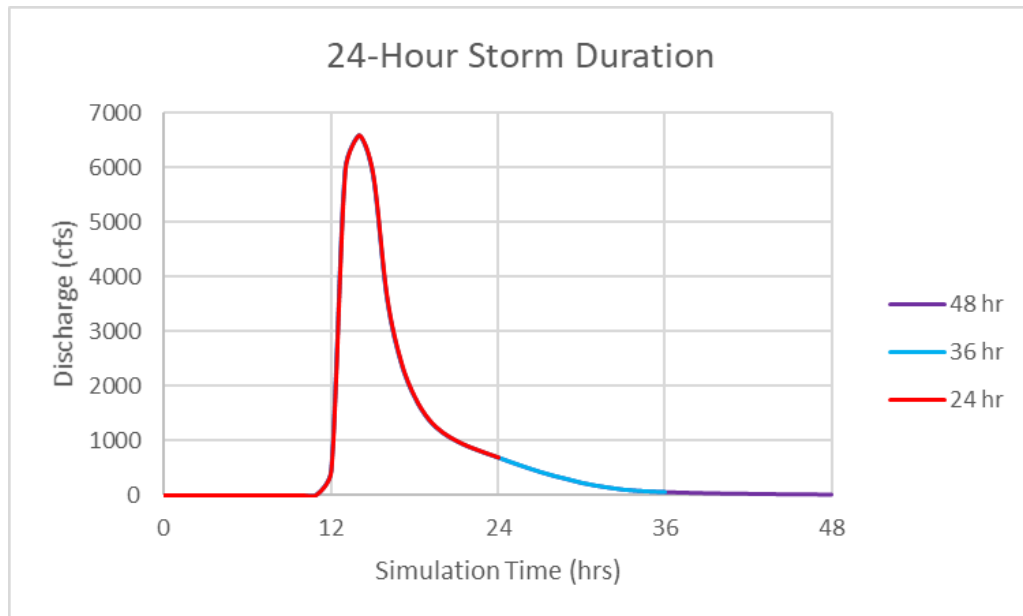


Figure 17. 24-hour event simulation hydrographs. The event was run with simulation times of 24, 36, and 48 hours.

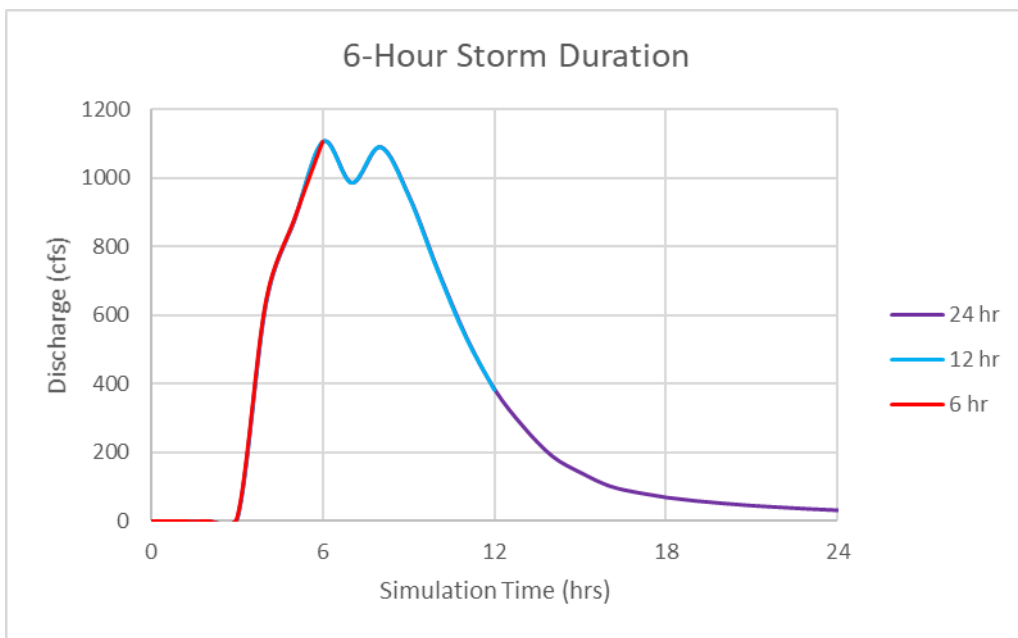


Figure 18. 6-hour event simulation hydrographs. The event was run with simulation times of 6, 12, and 24 hours.

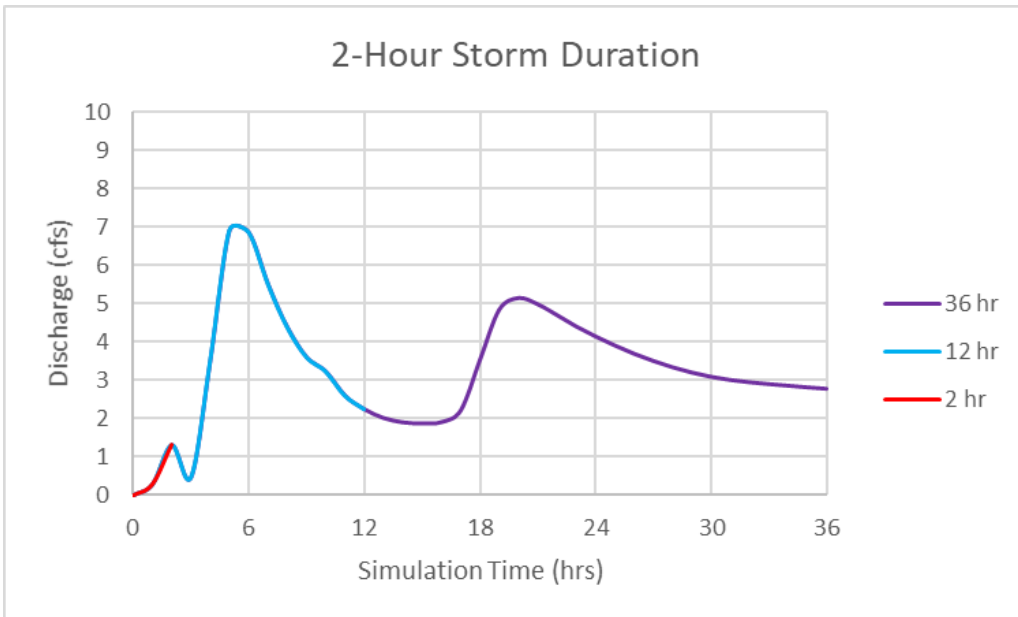


Figure 19. 2-hour event simulation hydrographs. The event was run with simulation times of 2, 12, and 36 hours.

4.3.2.2 *Recommendations*

Based on the results of the tested scenarios, the simulation durations specified in Table 6 below were recommended and implemented in modeling. Note that for the 2-hour event, a 12-hour simulation time was recommended and implemented. This was due to the fact

that at the outlet, minimal discharge was observed throughout the simulation. The relatively minimal precipitation volumes result in low flows in the channels for the 2-hour events, leading to slow travel times due to limited mass and energy in the system. The peak for the 2-hour event was approximately 7 cubic feet per second (cfs) versus about 7,000 cfs in the 24-hour event. As such, the 12-hour simulation time was sufficient because the primary flooding of concern in this study (pluvial) peaks within the 12-hour simulation timeframe, as shown in Figure 20 below.

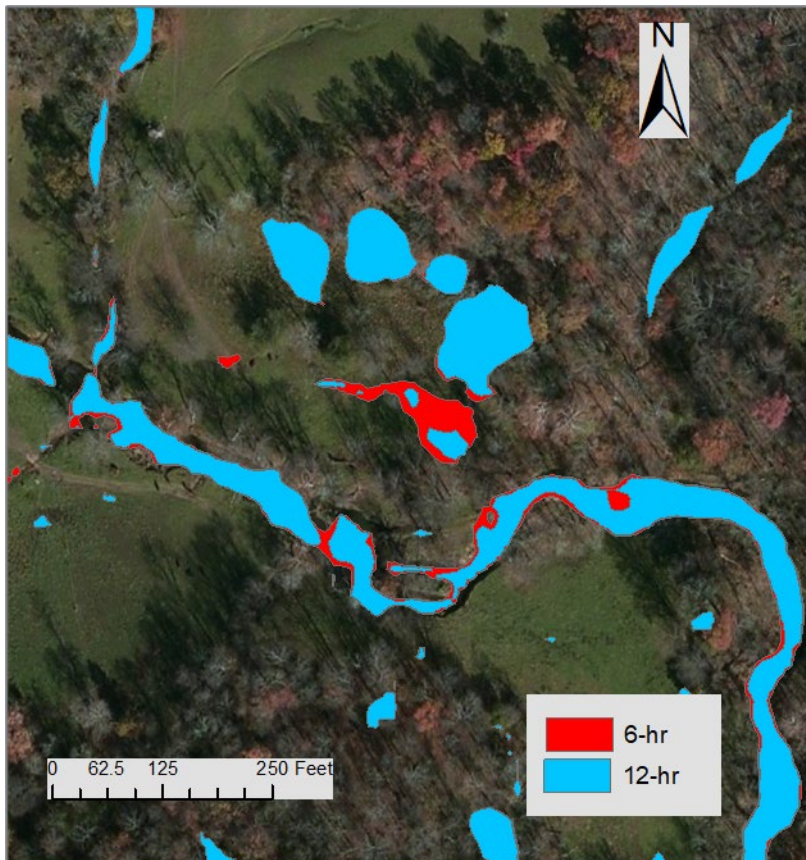


Figure 20. 2-hour event simulation at simulation times 6 and 12 hours. Pluvial flooding can be seen to peak at around 6 hours.

Table 6. Results from simulation time window sensitivity analysis.

Duration	Plan	Simulation Time (Hours)
2-hr	p01	12
6-hr	p13	12
24-hr	p84	24

4.3.3 BURNLINE TESTING

To test the most effective sizing of burnlines for this study, basin 030102011004_6 (shown below in Figure 21) was selected. This basin was selected as there were several instances of the terrain not including a cut to convey water underneath a roadway or structure. A cut in the terrain was necessary to model proper hydraulic connectivity.

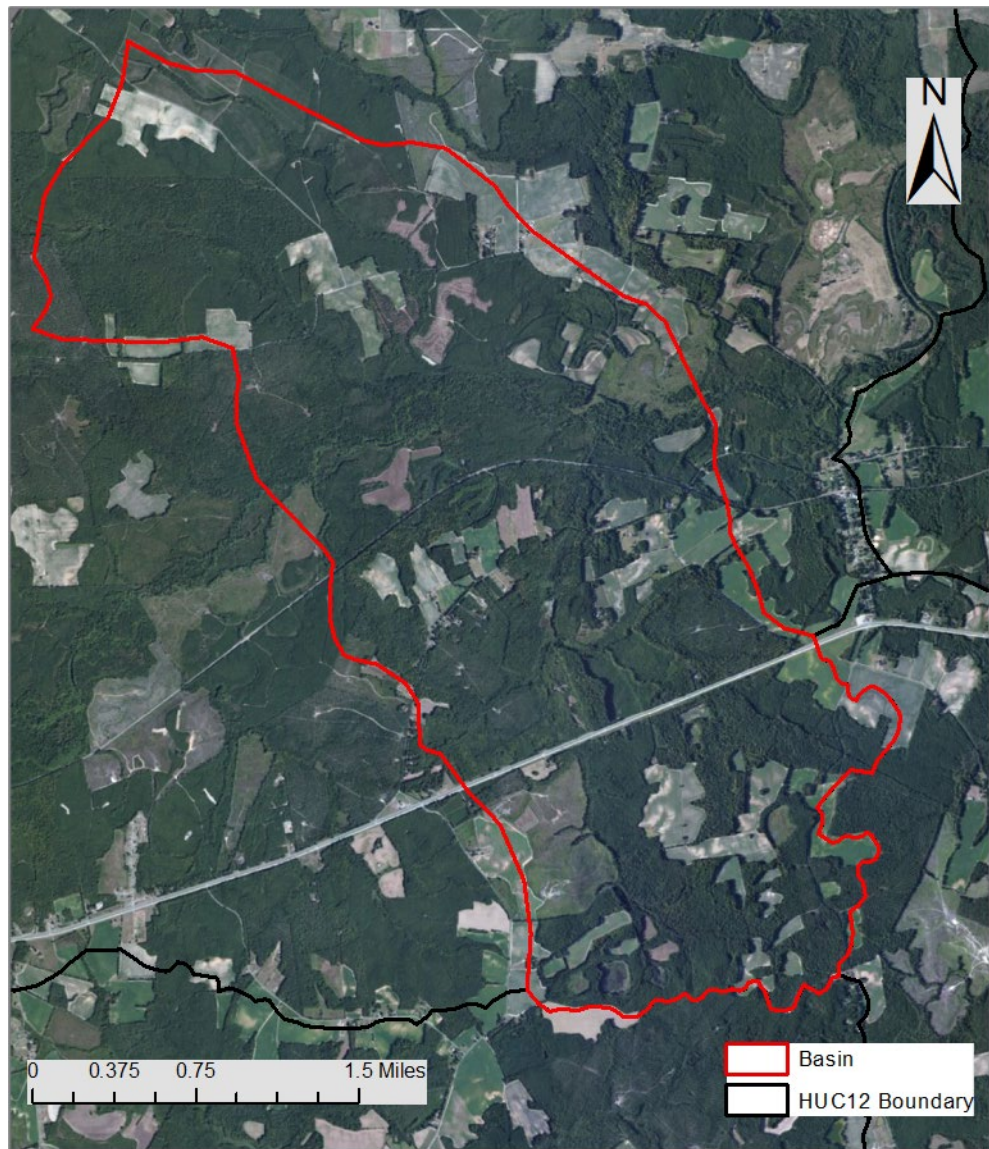


Figure 21. Basin 030102011004_6 includes rural areas with swamp and marshland running throughout.

4.3.3.1 Sensitivity Test

Burnline shape was determined by adjusting the dimensions of the channel to ensure hydraulic connectivity was within reason (not conveying excess water or unreasonable ponding behind structure, see Figure 22).

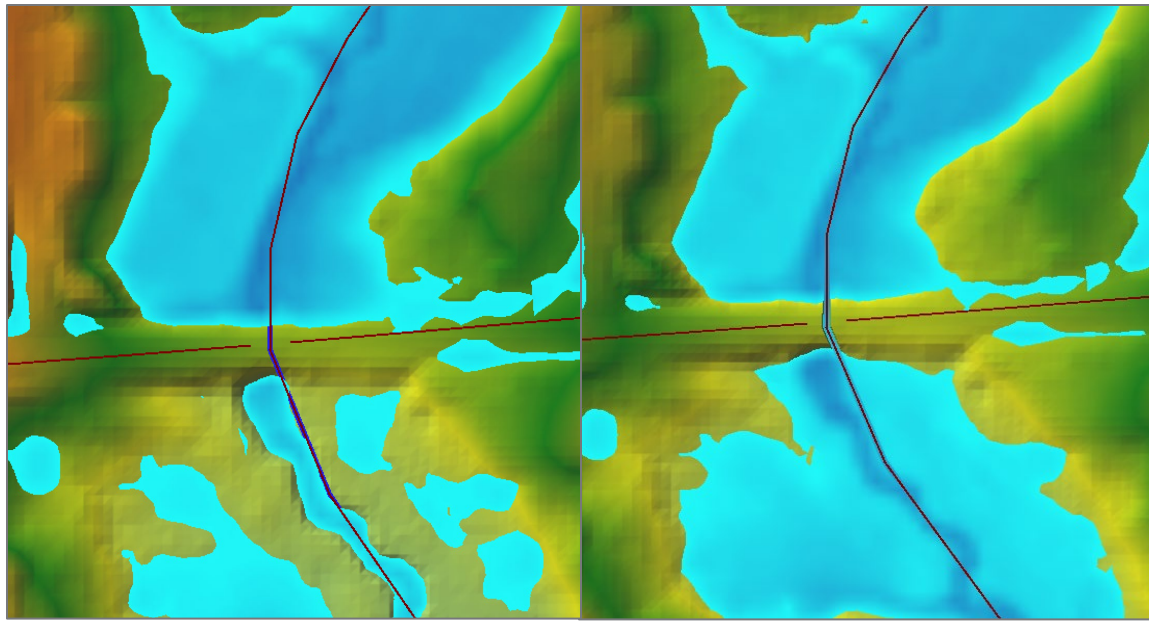


Figure 22. Example of ponding behind structure (left) vs. increased burn width using engineering judgment (right), where flow direction is top to bottom.

Hydraulic connectivity was analyzed by measuring the maximum flow of water through the cut channel and by visually checking for ponding upstream. To measure flow through the channel, a profile line was drawn in RAS across the roadway, which produces a hydrograph for the conveyed water, as shown in Figure 23 below.

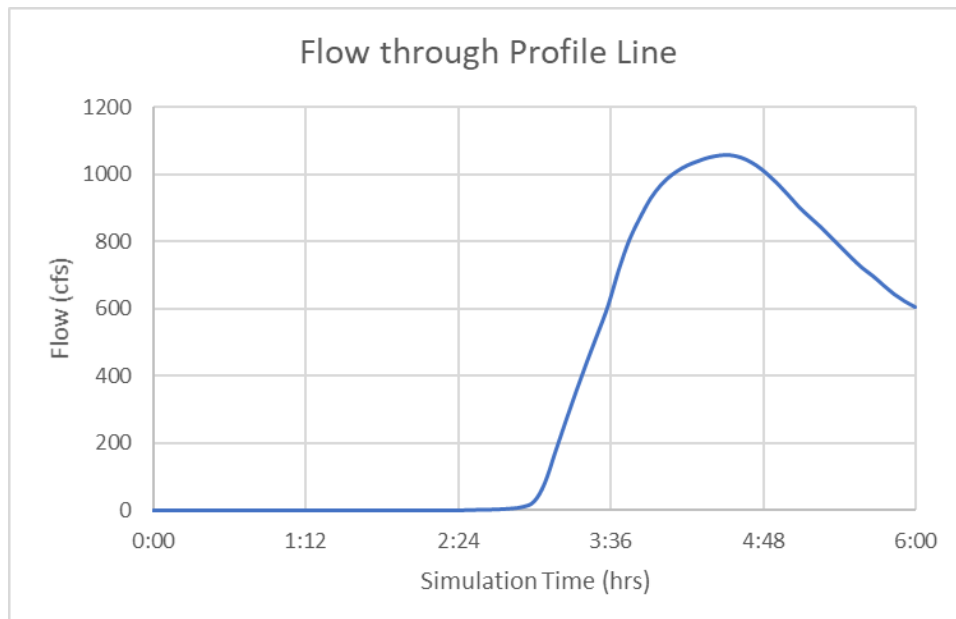


Figure 23. RAS-generated hydrograph using cut profile line.

4.3.3.2 Sensitivity Results

The burnline dimensions tested had relatively similar results with the smaller-sized cuts conveying less water as expected (see Table 7). Doubling the top and max reach between trials A and B gave minimally different results. Doubling once more between trials B and C and steepening the side slope resulted in an approximately 11% increase in conveyed flow. Values in the max conveyance columns are from the peak of the respective hydrographs.

Table 7. Burnline Sensitivity Analysis (100 ft grid, 50 ft breakline spacing).

Trial	Top Width (ft)	Left Slope (H:L)	Right Slope (H:L)	Max Reach (ft)	Max Conveyance Across Profile Line (cfs)	
					Location 1	Location 2
A	2.5	1	1	3.5	1039	837
B	5	1	1	7	1056	842
C	10	2	2	15	1178	931

4.3.3.3 Recommendations

For this analysis, two burnline locations were chosen in this basin to determine effective channel burn sizing. Burnline dimensions with a top width of 5 ft, a side slope ratio of 1:1, and a maximum width of 7 ft were selected. This size was selected as it was a reasonable approximation of the average channel size and does not increase or decrease flow through the reach significantly. As more models were vetted in the pilot process, an expanded set of recommendations was established for considerations such as drainage area, road width, and culvert/bridge assumptions. Ultimately, the recommended burnline dimensions were applied as an initial assumption for burnline sizing. However, in production, burnline dimensions were modified based on the aforementioned considerations using engineering judgment.

4.3.4 MODEL WARM-UP PERIODS

To understand the challenges and identify parameters suitable for modeling tidal shorelines, Basin 020403040301_1, shown in Figure 24, was selected. This basin was selected due to the presence of a large estuary as well as a network of tidally-influenced streams that are likely to be found across the Virginia coast.



Figure 24. Basin 020403040301_1 includes tidal shoreline with tidal streams and estuaries.

4.3.4.1 Sensitivity Test

The modeling scenarios specified in Section 4.3.4.2 were used to help determine the necessity of warm-up periods in tidally-influenced coastal regions. As a baseline, the modeling approach included a dry start and two external boundary conditions, one being a normal depth with a slope of 0.01 for the inland portion of the basin and a fixed stage hydrograph where the 2100 mean high water elevation was applied. The subsequent scenarios tested implement model warm-up periods ranging from 1 to 20 hours in addition to the baseline approach.

4.3.4.2 Sensitivity Results

As seen in Table 8 below, the addition of a warm-up period in coastal basin modeling did not result in any variation in inundation. It only resulted in additional computation time as the warm-up period reaches the 10-hour mark.

Table 8. Results from model warm-up period sensitivity analysis.

Scenario	Description	Inundated Area (mi ²)	Computation Time (mm:ss)
A	Normal Depth (s=0.01) for inland area + known water surface elevation in tidal/coastal region using 2100 mean high water elevation.	4.59	01:16
B	A + 1 hr warm-up period	4.59	01:16
C	A + 5 hr warm-up period	4.59	01:16
D	A + 10 hr warm-up period	4.59	01:21
E	A + 20 hr warm-up period	4.59	01:29

4.3.4.3 Recommendations

Based on the results of the tested scenarios, it was determined that a warm-up period for coastal models was not necessary. This recommendation was implemented in production.

4.3.5 CLIPPED COASTAL MODEL DOMAINS

To test the need for model domains that cover offshore regions, basin 020403040301_2, shown in Figure 25, was selected. This basin was appropriate for this testing due to the significant offshore area found in the model domain.

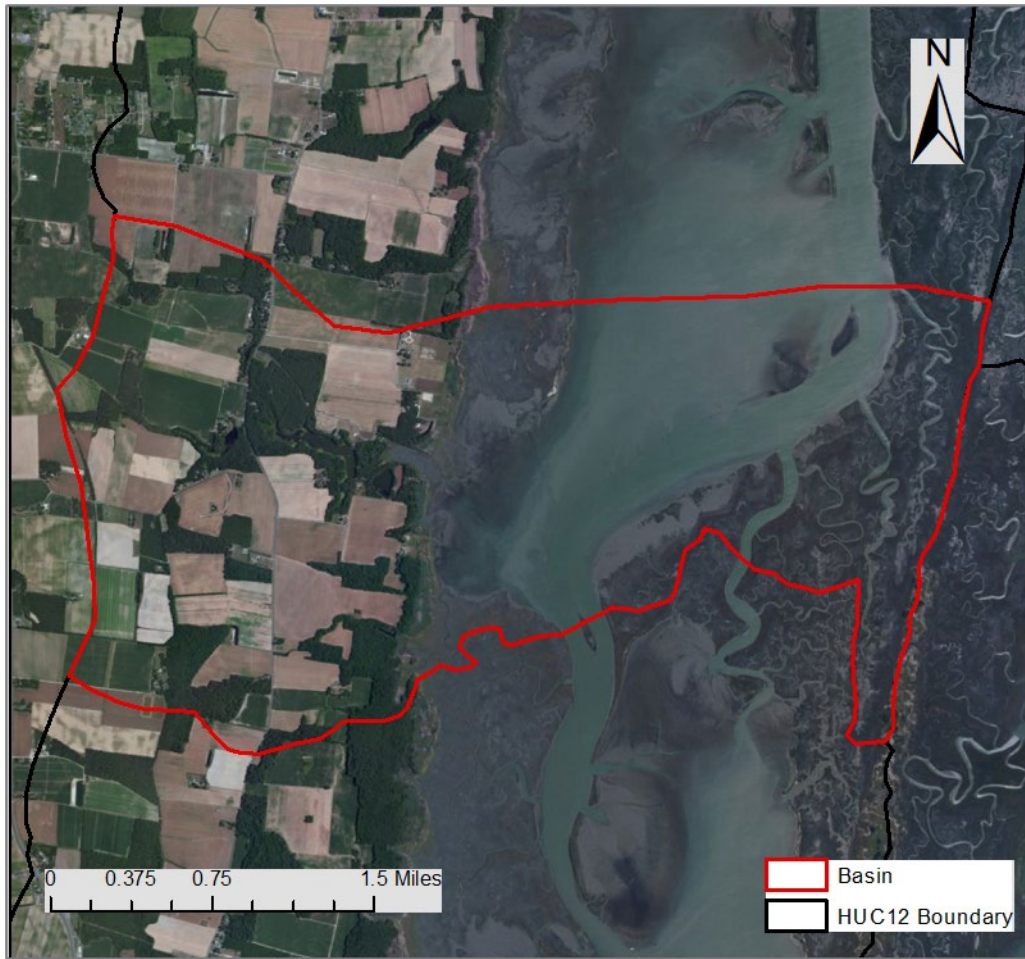


Figure 25. Basin 020403040301_2 includes tidal shoreline with tidal streams and estuaries.

4.3.5.1 Sensitivity Tests

Simulations for this basin were run with:

- The complete subbasin, which conforms to the HUC-12 boundary and
- A clipped subbasin where the downstream boundary was clipped to an approximate 1000-foot offset to the location where the mean high-water elevation breaks along the shoreline.

The clipped basin is pictured below in Figure 26.

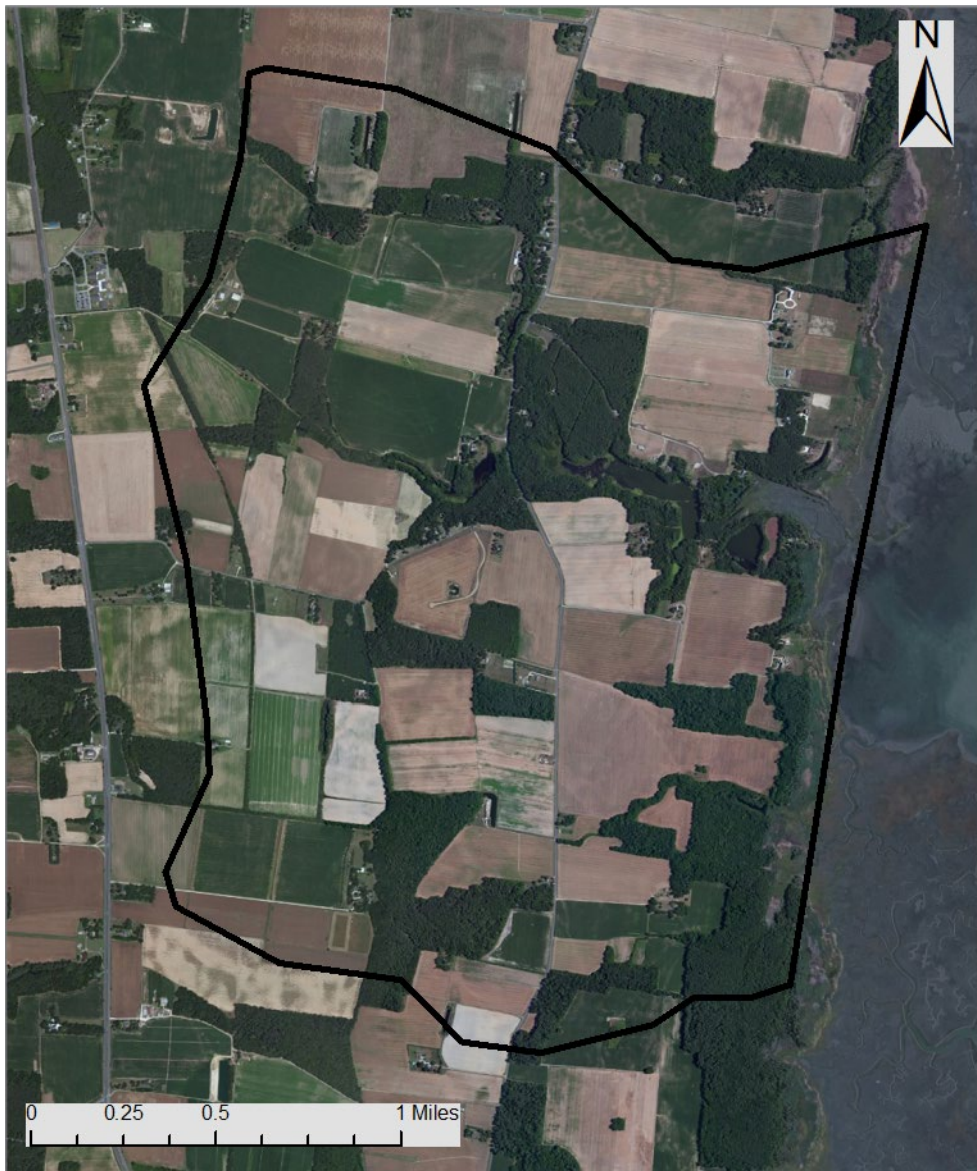


Figure 26. Clipped boundary of Basin 020403040301_2.

4.3.5.2 Sensitivity Results

As seen in Table 9, the difference in inundated area between the two scenarios was minimal ($< 0.1 \text{ mi}^2$). The mapped output of the clipped and original basin models can be found in Figure 27. The main difference illustrated in this testing was reduction of computational run time.

Table 9. Results from clipped basin boundary sensitivity analysis.

Scenario	Description	Tidal Boundary Condition	Inundated Area (mi ²)	Computation Time (mm:ss)
A	Complete basin boundary	Fixed stage hydrograph (2100 mhw)	1.61	00:30
B	Basin boundary clipped so that the downstream boundary condition was approximately 1000 ft offset from shoreline	Fixed stage hydrograph (2100 mhw)	1.69	00:17

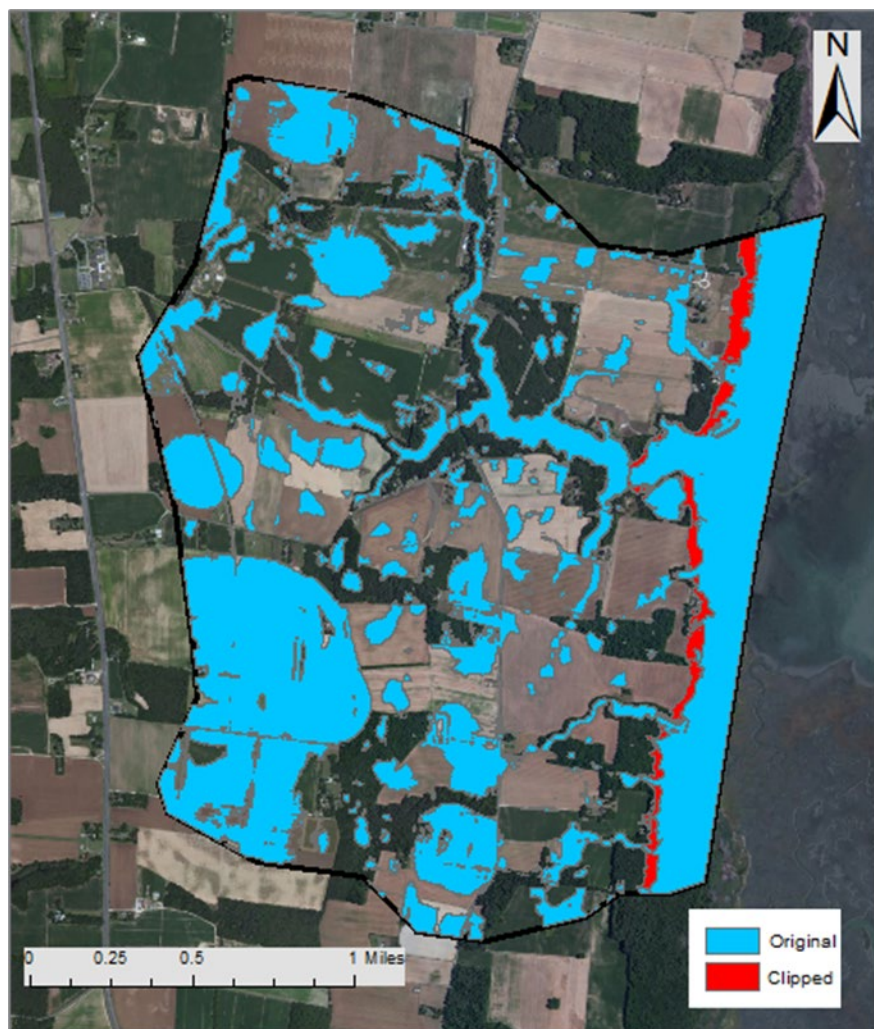


Figure 27. Comparative inundation between clipped and non-clipped coastal basin boundaries.

4.3.5.3 *Recommendations*

As demonstrated in Figure 27, the clipped basin boundary results in higher coastal inundation when compared to the original basin boundary. The inland inundation extent was comparable in both scenarios. It was recommended that clipped basin boundaries be applied in this study because the impact clipped basin boundaries have on overall flood inundation was minimal. In production, clipped domains were utilized in tidal models with no existing infrastructure. Further discussion on this topic can be found in Section 5.2.1.3.

4.3.6 TIDAL BOUNDARY CONDITIONS

To understand the challenges and identify the parameters suitable for modeling along coastal shores with varying mean high water elevations, basin 020403040104_2, shown in Figure 28 below was selected. This basin's lengthy coastal boundary, which spans approximately 2 miles, makes this basin appropriate for testing the effect that variable mean high-water elevations have on the modeling approach in such scenarios.

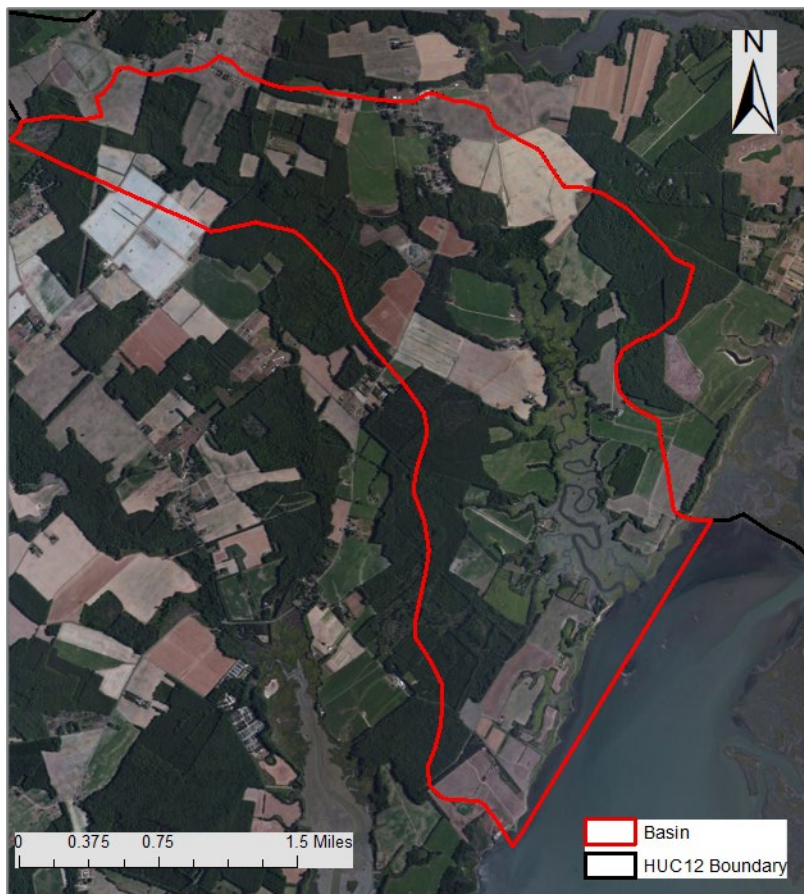


Figure 28. Basin 020403040104_2 includes rural tidal shoreline along with tidally-influenced streams. Note that the open boundary spans approximately 2 miles.

4.3.6.1 Sensitivity Tests

To test the viability of the assumptions made in the case of basins with non-constant water surface elevations along the downstream coastal boundary, three modeling approaches were tested. Known water surface elevations were applied as the tidal boundary condition using the minimum (A), maximum (B), and average (C) 2100 mean high water elevations.

4.3.6.2 Sensitivity Results

As seen in Table 10, the inundated area across the three test scenarios doesn't vary significantly ($< 0.1 \text{ mi}^2$). It can be concluded that all the options below are viable modeling approaches.

Table 10. Results from variable mean high water elevation sensitivity analysis.

Scenario	Tidal Boundary Condition	Inundated Area (mi^2)
A	Minimum 2100 mean high water elevation	3.34
B	Maximum 2100 mean high water elevation	3.40
C	Average (min-max) 2100 mean high water elevation	3.37

4.3.6.3 Recommendations

Based on the results presented in Table 10 above, it was recommended that in the case of non-constant water surface elevations along coastal boundaries, the average mean high water elevation should be applied as the downstream boundary condition. In production, a point shapefile was used to extract mean high water elevation values for each epoch to be applied in modeling. In areas of the project where this shapefile did not provide coverage, the recommended approach was utilized.

4.3.7 HYDRAULIC AND COMPUTATIONAL PARAMETERS

To understand the effects of mesh resolution, boundary conditions, and computational interval, multiple basins are selected to compare the results from topographically different study areas. The basins selected, 020700080301_0, 020802060501_3, and 020700110601_4, consist of steep rural, urban, and tidal rural areas respectively (see Figure 29).



Figure 29. Basins 020700080301_0 (A, steep rural), 020802060501_3 (B, urban), and 020700110601_4 (C, tidal rural).

4.3.7.1 Sensitivity Tests

To test the effects of different mesh and breakline resolutions on computational time and inundation area, model runs for each basin with grid resolutions of 200x200 ft, 100x100 ft, and 50x50 ft were compared with a baseline 150x150 ft mesh. Each simulation was also run with and without 50 ft breaklines to determine efficient and accurate mesh settings. Results for each of the study areas and simulations are summarized in the table below.

4.3.7.2 Sensitivity Results

As seen in Table 11, computation time increases as the mesh and breakline resolution increases. Compared to the 200x200 ft resolution, the 100x100 ft mesh size results in an acceptable increase in compute time, while the 50x50 ft mesh size returns an increase up to 20 minutes for one profile run. Enforcing 50 ft breaklines with each of the mesh resolutions has relatively little impact on computational time, except in scenarios where the mesh resolution was much coarser than the breakline resolution.

Table 11. Results from mesh resolution sensitivity test. Please note that A, B, and C refer to specific subbasins and are color coded in the table below.

		Compute Time (mm:ss)			Inundated Area (mi ²)		
Mesh Resolution (ft ²)	Breakline Resolution (ft ²)	A	B	C	A	B	C
200	-	00:39	00:42	00:32	1.33	3.24	0.86
100	-	02:49	02:52	01:50	1.27	3.31	0.92
50	-	20:54	19:45	13:19	1.31	3.3	0.89
200	50	01:06	01:20	00:53	1.33	3.32	0.91
100	50	03:04	03:00	02:23	1.27	3.35	0.94
50	50	19:45	19:08	13:04	1.31	3.29	0.9
150	75	01:03	01:09	00:50	1.32	3.34	0.93

A: 020700080301_0

B: 020802060501_3

C: 020700110601_4

4.3.7.3 Recommendations

An overall mesh resolution of 100x100 ft cells with 50 ft near spacing at breaklines was recommended and implemented in production. These parameters were chosen to produce consistent models throughout the study area, providing high-resolution coverage where needed while reducing unnecessarily long runtimes and complex mesh build issues that result during model development and iteration.

4.3.8 COMPUTATION INTERVAL SENSITIVITY ANALYSIS

This analysis compared the effect of computational interval or timestep setting in the HEC-RAS unsteady solver on total compute time and maximum inundation area. This test was conducted to establish as rapid a simulation execution as possible (i.e., minimize the time needed for each model to run) while also achieving an appropriate level of detail without the loss of accuracy or otherwise impacting the quality of the results.

4.3.8.1 *Sensitivity Tests*

Three time intervals were selected for this test: 1 second, 10 seconds, and 20 seconds. Each model was run using the three time intervals.

4.3.8.2 *Sensitivity Results*

As shown in Table 12, total computational time varies greatly depending on the chosen time interval. A time step of 1-second increases compute time for a given basin while maintaining a similar area of inundation as a 10-second time step. Further increasing the interval to 20 seconds decreases compute time, though the area of inundation begins to vary as computational resolution decreases.

Table 12. Time interval sensitivity analysis results.

Time Interval (s)	Compute Time (mm:ss)			Area (mi ²)		
	A	B	C	A	B	C
1	20:03	24:12	16:33	1.16	2.86	0.94
10	03:15	02:55	02:26	1.17	2.86	0.94
20	02:00	02:06	01:29	1.26	2.88	0.95

A: 20700080301 B: 20802060501 C: 20700110601

4.3.8.3 *Recommendations*

To maintain a balance of total computation time and modeling accuracy, it was determined that a 10-second time step was sufficient for production. This assumption reduces the run time for each model when compared with the 1-second interval while still providing a reasonable level of accuracy.

4.3.9 BOUNDARY CONDITION SENSITIVITY ANALYSIS

This analysis compared a generalized normal depth boundary condition (0.01 across all models) to independent normal depths measured from each model. This analysis uses the same basins from Section 4.3.6.

4.3.9.1 *Sensitivity Tests*

Using the suggested 100x100 ft mesh size with 50 ft breaklines, each model was run with a normal depth of 0.01 and a calculated value measuring the slope from the last 1000 ft of the downstream portion of the model.

4.3.9.2 *Sensitivity Results*

As shown in Table 13, boundary condition setting has a minimal impact on the computational time needed for each model. Maximum inundation area changes are minimal at each basin's main outflow location as shown in Figure 30.

Table 13. Boundary condition sensitivity analysis results.

	Compute Time (mm:ss)			Area (mi ²)		
	A	B	C	A	B	C
Normal Depth	03:04	03:00	02:23	1.27	2.89	0.94
Calculated	03:15	02:55	02:26	1.27	2.84	0.93

A: 20700080301 B: 20802060501 C: 20700110601

4.3.9.3 *Recommendations*

Given the minor difference in flood extent between the measured and default normal depth value, it was determined that a normal depth of 0.01 was reasonable across all models for production. An example of the difference in flood extent can be seen below in Figure 30. This assumption streamlines the model generation process while still providing reasonable results at model boundaries.

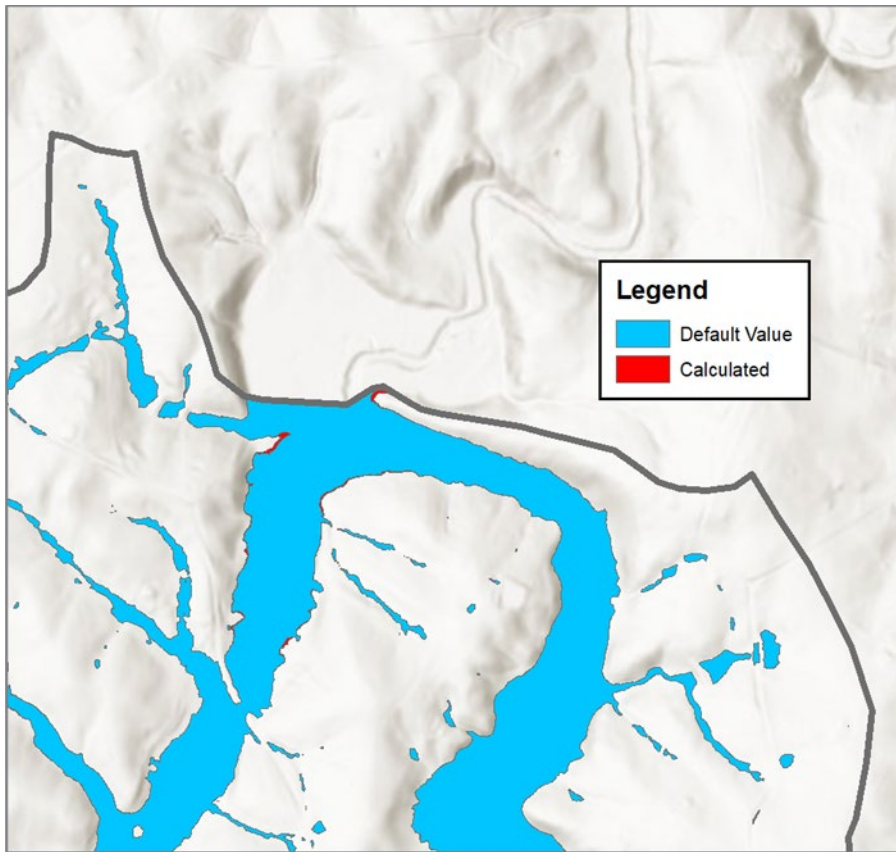


Figure 30. Difference in inundation at boundary between default and measured normal depth.

4.4 PILOT DATA DELIVERABLES

4.4.1 HEC-RAS MODELS AND DEPTH GRIDS

To access the deliverables from the pilot studies, the user downloaded 1) a .tar.gz file and 2) the batch file titled “model-unpack.bat”. The .tar.gz file included the individual basin models along with the resulting depth grids for a given HUC-12. Files from the .tar.gz file that could be extracted using a provided “model-unpack.bat” utility. Directions provided were:

- Download the .tar.gz file for the HUC-12 of interest using the provided link.
 - .zip was inadequate since it does not store file timestamps to 1-second precision causing HEC-RAS to think inputs have been updated, unnecessarily re-preprocessing geometry.
- Download “model-unpack.bat” and ensure it was placed within the same folder location of the HUC’s .tar.gz file.
 - Need Windows 10 with “C:\Windows\System32\tar.exe” (if not available, use 7zip program to unarchive).

- Double-click “model-unpack.bat.” Doing so will begin file extraction.
- HEC-RAS models will be unarchived into the user’s home folder (on C: drive) under a subfolder named “pilot.”

Once extraction from the .tar.gz file had been completed, the user was able to find individual basin models and depth grids for a given HUC-12 in the form of .vrt files for each simulated plan. Figure 31 illustrates the folder structure of the deliverable.

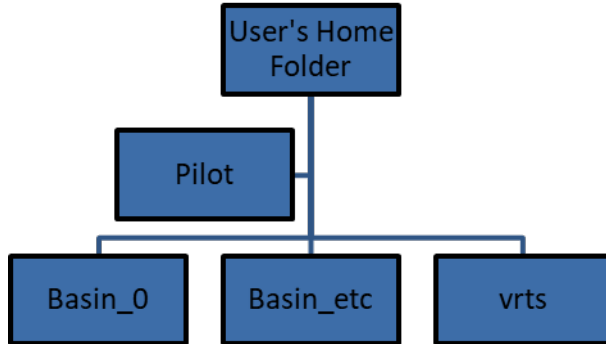


Figure 31. Deliverable folder structure once file extraction was complete.

- Each .vrt file referenced all depth rasters (.tif files) across all basins for a given plan. Each .vrt was treated like a single raster mosaic layer – able to drag-and-drop it into QGIS, ArcMap, or ArcGIS Pro. The reference paths inside the .vrt were relative.
- Note that results of pluvial models were not applicable at locations with considerable drainage area, which fall under the domain of riverine or “fluvial” models.

5 TECHNICAL MEMORANDUM 5: PRODUCTION MODELING

This TM describes the production processes and outcomes for the pluvial models for the Virginia Coastal Resilience Master Plan. The study area encompasses the 57 coastal counties in the Commonwealth of Virginia.

The production effort involved the execution of a semi-automated workflow using tools and processes developed and described in TM #1-4. Any deviation from information found within the aforementioned TMs will be detailed subsequently in Section 5.2. This TM describes the final production for all relevant subbasins in the coastal counties, adds details on the final methodology and modeling team approach, includes methods used for the review of outputs including quality control processes, and provides a summary of post-processing steps and a comprehensive list of final products.

5.1 PRODUCTION MODELING

As described in TM #4, the first step in the model development process was to create subbasins from HUC-12s in the study area. As shown in Figure 32, this process resulted in the creation of 1,830 models generated from 419 HUC-12s. Each of these model basins was developed and reviewed by engineers prior to the automated creation of a HEC-RAS model.

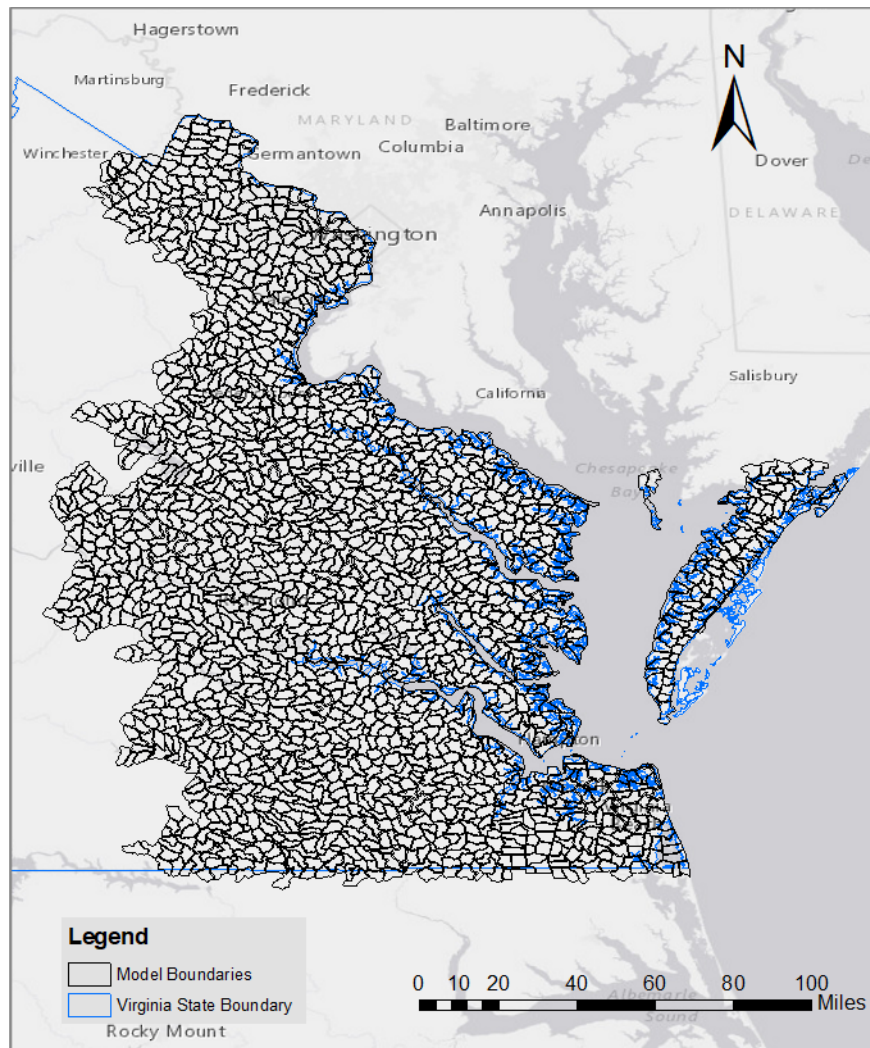


Figure 32. Map of the 1,830 modeled basins developed from the 419 coastal HUC 12s in the study area.

For a detailed description of the methods followed during model production for basin delineation, please refer to Section 4.2 and Section 4.3 of TM #4.

5.2 MODELING PROCESS

5.2.1 MODEL MANAGEMENT

Due to the large number of models developed and refined in the production process, a modeling database was used by all engineers on the project to ensure quality and consistency and to enable tracking of progress and issues encountered. The autogenerated models (see Section 3.4 of TM #3 for details and parameters) were transferred from the cloud to a shared network drive to allow easy access for all engineers working on the project.

In order to track the changes and refinements to the autogenerated models, engineers created a copy of the model and performed the necessary revisions and quality checks on what was referred to during production as the “engineered” model.

A team of approximately ten engineers participated in the development of the production models. An engineering lead was assigned to the study to manage modeling and quality control assignments. The model assignments as well as the notes, issues, and comments made by the modeler or QC reviewer were tracked in a spreadsheet and in the modeling database.

To ensure a consistent approach in refinement and modeling, a weekly meeting was held throughout the production period. These meetings were attended by all of the engineers involved in the modeling as well as the technical, engineering, and quality lead for the project. Each engineer was assigned a set of models to complete for the upcoming week or as dictated by each individual’s pace. Issues that arose during production were discussed in the meetings and in an online forum created for this project. The online forum provided the engineers with a centralized platform to raise issues discovered outside of the weekly meetings and the opportunity to discuss technical issues. A resolution to the issues raised on the forum was provided as soon as possible and brought to the group’s attention in the following weekly meeting. Examples of issues encountered are detailed in the following subsections.

5.2.1.1 Sizing & Review of Channel Burnlines

The first step in model review involved the identification of areas with excessive ponding behind roads and crossings. The automated process used to develop the models included channel burnlines; however, engineering judgment was used to add, remove, or update burnlines as needed. For consistency, a rule was established for determining if ponding was excessive: in locations where the observed depth of the automated model was 10 feet or higher on either side of a road or embankment, a burnline was created or adjusted to reproduce the hydraulic connectivity provided by a bridge or culvert not incorporated in the terrain. These modifications resulted in reduced ponding consistent with what is expected to happen in the physical environment. An example of a location requiring a channel burnline creation is provided in Figure 33.

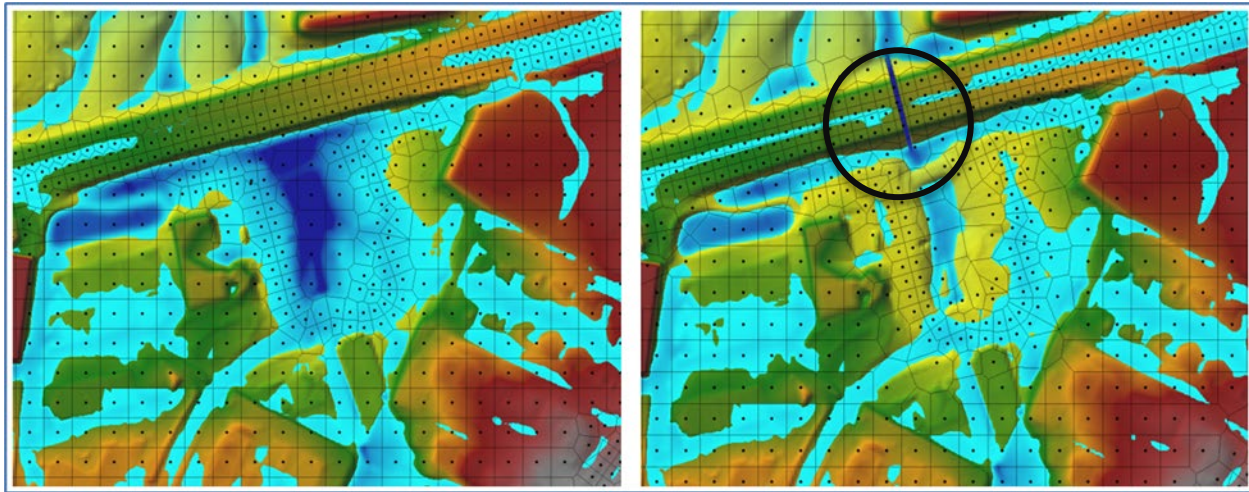


Figure 33. Location requiring channel burnline before (left) and after (right) the burnline inclusion. Note the reduction in ponding to the hydraulic connectivity created by the burnline.

As noted in TM #3, the technical implementation of terrain modifications was performed by cutting a channel through roads/embankments. Default channel dimensions were set with a bottom width of 5 feet, a slope ratio of -1 on the left side, 1 on the right side, and a width of 7 feet, as shown in Figure 34 below. However, the sizing of these channel burns was ultimately left to the professional judgment of engineers based on aerial imagery and the severity of ponding.

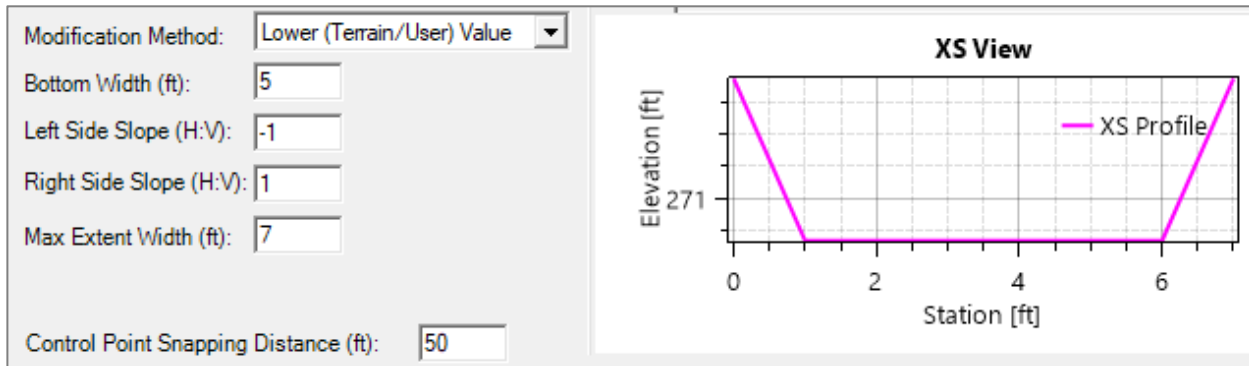


Figure 34. Default dimensions for channel burnlines used throughout the study.

Engineers removed or corrected cases where the automated model development process created burnlines in locations where they were not needed. Examples include locations where the burnlines were unnecessarily long, did not completely cross the road/embankment, were misaligned, or where an existing cut in the terrain was present. An example of a burnline removed due to a preexisting cut in the terrain is shown in Figure 35 below. Quality reviews of burnlines included checks to ensure that placement, dimensions, and consistency of burnline usage were appropriate.

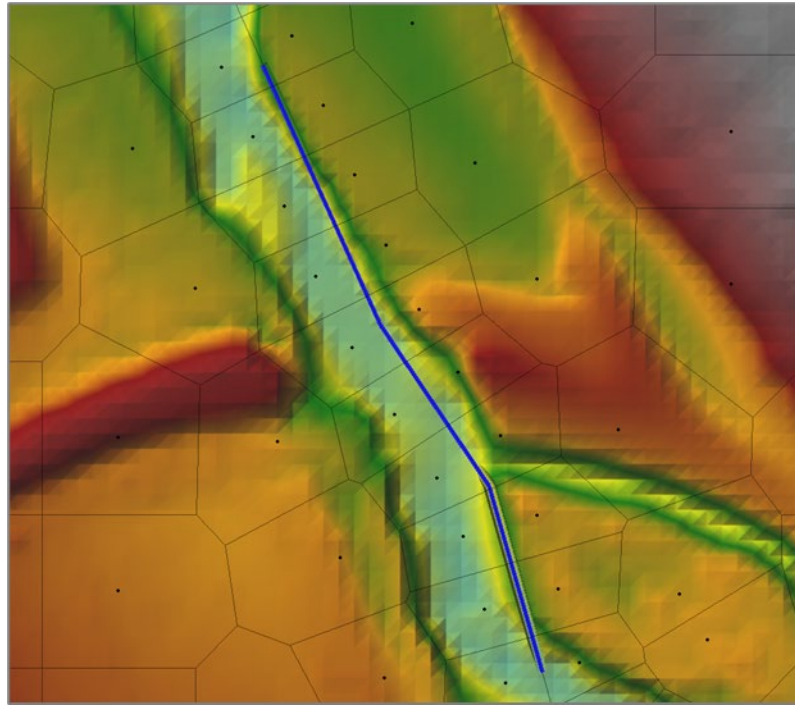


Figure 35. Example of a burnline removed due to a preexisting cut in the terrain. The automated routine included a small burnline in this large channel that was not needed and was removed from the engineered model.

5.2.1.2 Dam and Reservoir Modeling

Small dams (i.e., lakes and ponds) were a common feature found in many of the models across the study area. Although modeling of dams and reservoirs was not included in the production study, approaches for incorporating storage areas and hydraulic structures were required. As shown in Figure 36, a breakline was added at the outlet of dams and reservoirs, with spacing and near repeats (consistent with those listed in Section 3.4 of TM #3). Due to the focus on pluvial flood hazards, no conveyance structure or parameters were applied at the outlet. The behavior in these locations was controlled by the surface level of the storage area and outlet features included in the topography. In simulations where significant volume accumulated in storage areas, flow out of storage areas was computed across cell faces, consistent with all other areas in the model.

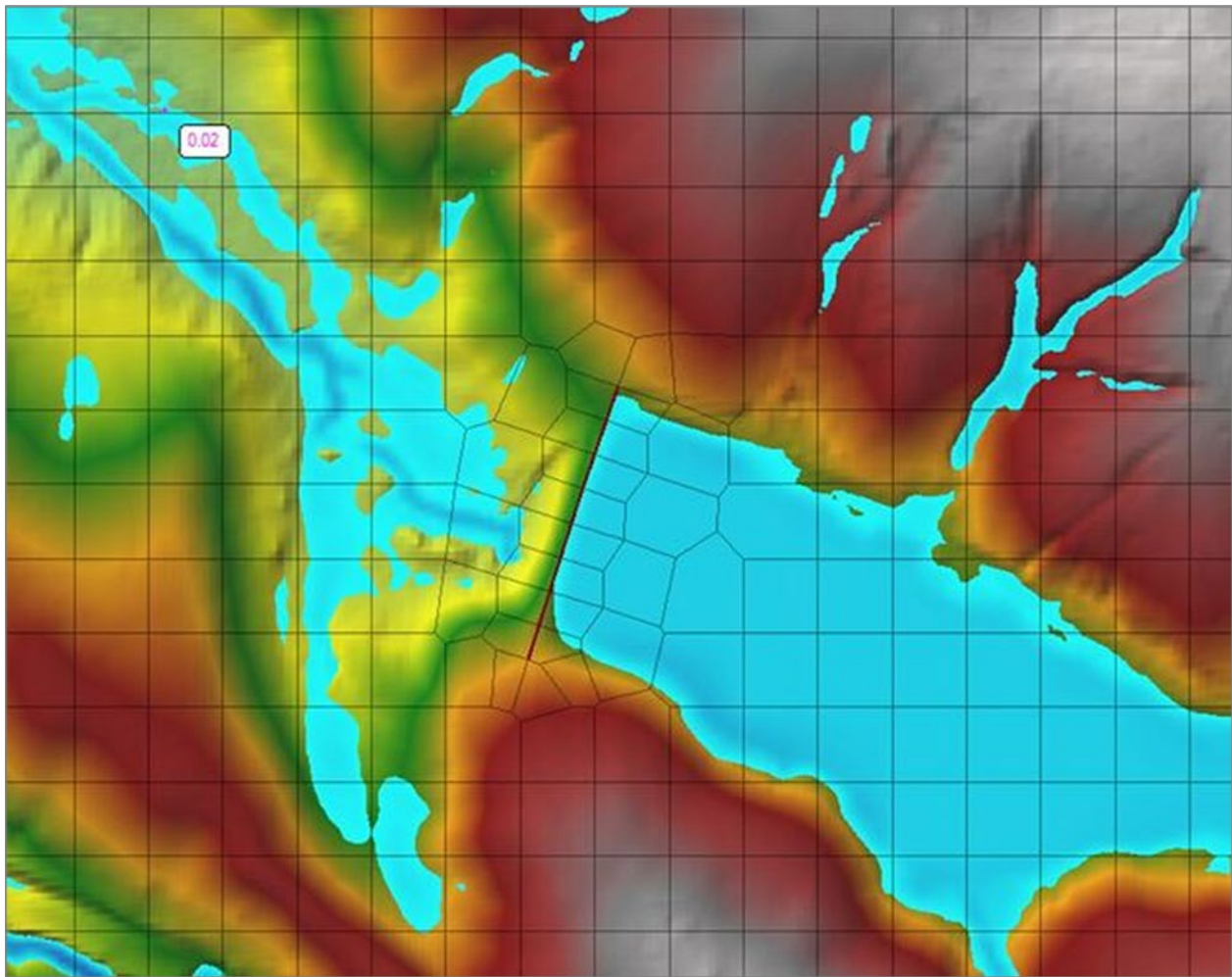


Figure 36. Breakline along the crest of a small reservoir. Note that no conveyance structure or mechanism was added to the model.

5.2.1.3 Tidal Modeling

Application of tidal water surface elevations for production modeling used the methods described in Section 4.3.6 of TM #4. The determination of which models included a tidal boundary and the identification of the mean high water (MHW) surface elevation for each of the model boundaries required for the modeled epochs (i.e., 2020, 2040, 2060, 2080, and 2100) was managed using the following semi-automated approach:

1. An engineer intersected the 1,830 model basins with the 2100 MHW surface elevation data created for the Virginia Coastal Resilience Master Plan. This identified which basins would require a tidal boundary condition.
2. An engineer then manually added points at the approximate midpoint of each model boundary's downstream outlet using GIS software and attributed the points with water surface elevations from each of the modeled epoch grids.

3. A senior engineer then performed a quality review of the data, including evaluation of placement per model and appropriate attribution from the data extraction process.
4. A shapefile containing this data was provided to the engineers and added to each model during the review/refinement process. This allowed the engineer to perform a quality control of the point placement and associated tidal values.

In the model, tidal boundaries were assigned a constant stage hydrograph for the duration of each simulation, with elevations recorded from the aforementioned tidal values point shapefile or from the still water elevation rasters, as needed. Figure 37 below illustrates the locations of points used in production to help record tidal values used in modeling.

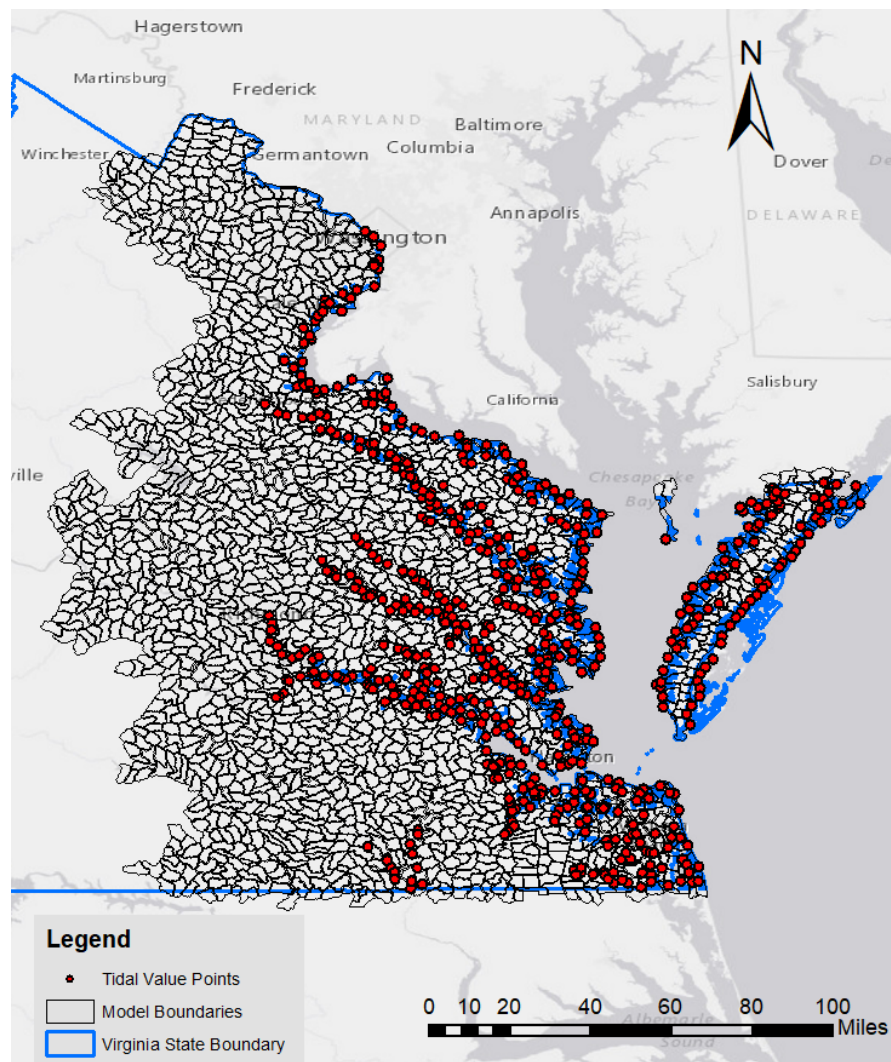


Figure 37. Water surface elevation points used to apply tidal values as boundary conditions for production models in the study.

The tidal model clipping procedure, originally discussed in Section 4.3.5, was reviewed using the methodology followed by engineers in production. The established process was to construct tidally influenced models by applying two external boundary conditions - stage hydrograph and normal depth. However, in the pilot modeling phase, a single external boundary condition, stage hydrograph, was utilized. Review of the outputs of this modeling approach indicated that inundation increased along the shoreline in clipped model domains. Figure 38 and Figure 39 below show the difference in computed flood depths for the clipped and unclipped versions of the 020403040301_2 basin. Figure 38 shows depth differences calculated for the model produced using the pilot modeling approach, while Figure 39 shows depth differences calculated for the model produced using the production modeling approach.

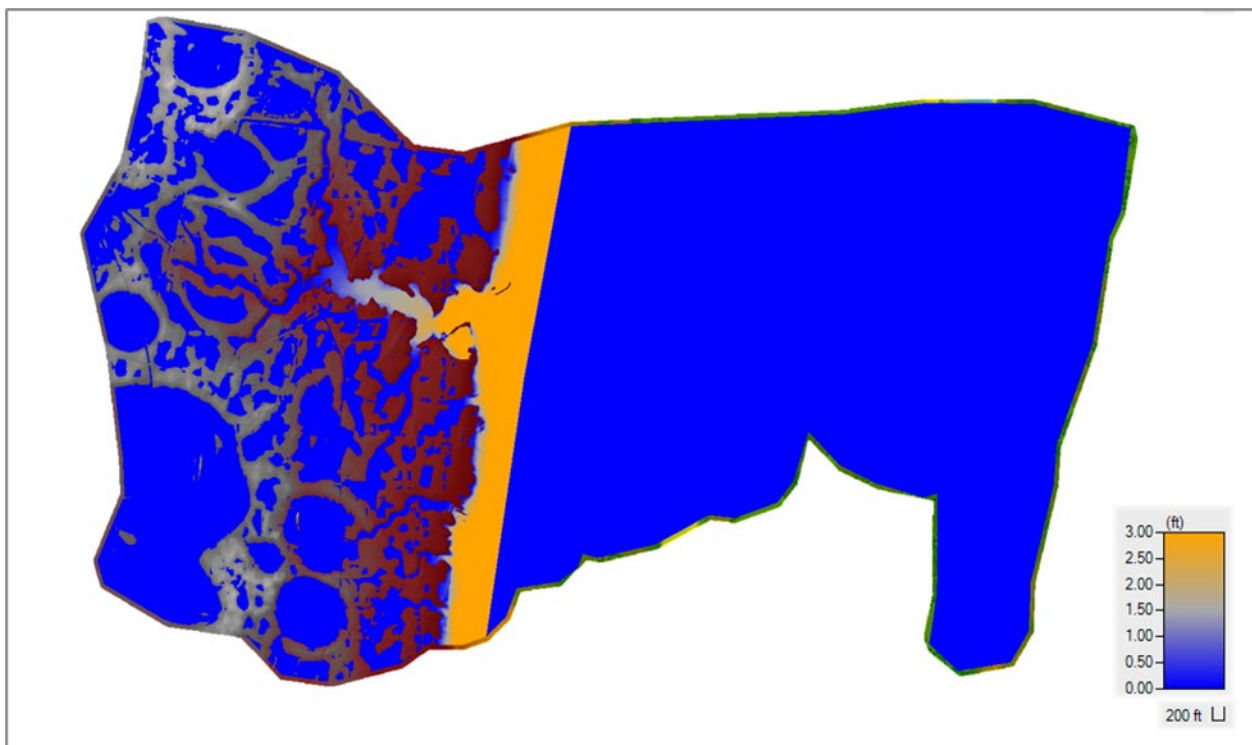


Figure 38. Flood depth difference for basin 020403040301_2 using the pilot single stage hydrograph approach.

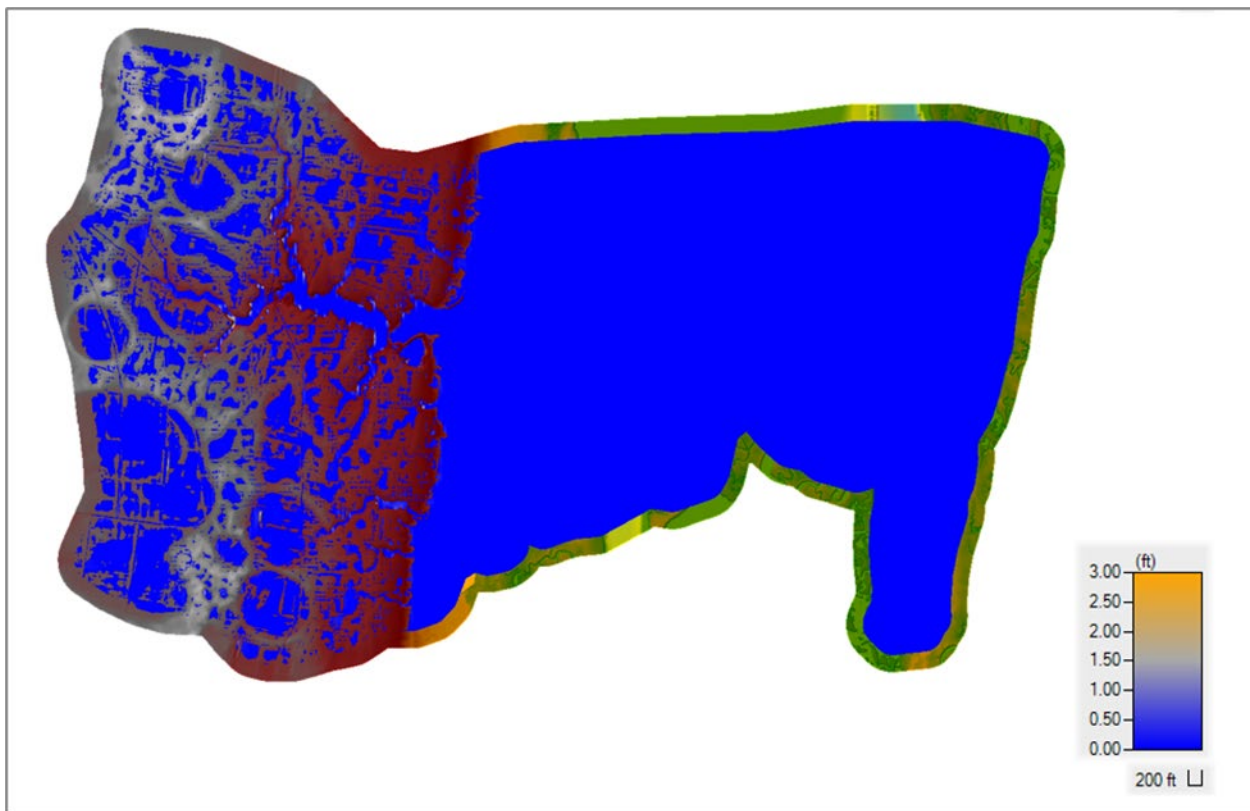


Figure 39. Flood depth difference for basin 020403040301_2 using the production (stage hydrograph and normal depth) modeling approach.

It was determined through the comparison of simulation results of the clipped and unclipped model domains that the pilot modeling approach resulted in a 3-foot increase in flood depths along the shoreline. On the contrary, the modeling approach followed in production resulted in no increase in flood depths along the shoreline. Therefore, it was concluded that the recommendation of clipping model domains along the coast is valid. Tidal domains were clipped so that the tidal boundary was approximately 1,000 ft offset from the coastal shoreline. Additional offshore area was included in tidal models where houses, roads, trails, or any other form of infrastructure existed. Engineers verified this through the use of the 2100 mean high water depth grid as well as available aerial imagery.

5.3 MODEL REVIEW

5.3.1 QUALITY CONTROL

Quality control checks were identified and implemented throughout the production process. Model review in the early phases of production included a review of approximately 10% of models within the study area by a senior engineer. Issues found during these reviews were documented as comments in the project's progress tracking spreadsheet. Each engineer took the time to address and respond to comments received.

Examples of issues found during these reviews include improper naming conventions of boundary conditions, failure to add channel burnlines at crossings where necessary, and improper recording of tidal still water elevations. For these issues, the engineers reopened their modified models and either renamed boundary conditions, added channel burnlines, or corrected the recorded tidal elevations as necessary. These modifications were then back checked for confirmation of completion by the reviewer. Following the conclusion of initial production, an automated quality review was conducted as a final quality check.

The goal of the automated quality review was to provide a review of model parameters using scripts to read the relevant HEC-RAS files and confirm if the model input matched the expected values based on the workflow provided. Details of the automated checks are explained later in this document.

5.4 AUTOMATED UNSTEADY SIMULATIONS AND POSTPROCESSING

Following model development and review, an automated process was executed in the cloud to prepare files and execute simulations for all scoped RAS plans. The steps taken for each basin were as follows:

1. *.g01 and terrain/terrain.hdf, which had been edited by engineers, were uploaded to S3. The g01 file contained edits to the mesh and to the boundary conditions. The terrain.hdf file contained edits to the burnlines. No other files from the hand-edited RAS model were uploaded.
2. For each tidal model, one static tide elevation value per epoch was uploaded to the Postgres database.
3. For all 63 plans, a Plan file and an Unsteady file (*.pNN and *.uNN extensions) were generated by a script. For tidal models, all five epochs were set up this way in parallel (315 total plans), and the static tide elevation for each was recorded in the *.uNN file.
4. For each plan:
 - a. Minimum required inputs for the [RAS Linux v.6.1](#) Unsteady routine were generated: for example, *.pNN.hdf.tmp and others as described in the official documentation.
 - b. The RAS Linux v.6.1 Unsteady routine was executed using AWS Batch, and the resulting Unsteady output files were uploaded to S3: *.pNN.hdf, *.dss, and *.log.
 - c. RAS Mapper (Windows, v.6.1) was invoked to extract a maximum depth grid (10 feet resolution) from the *.pNN.hdf file that had been written by RAS

Linux. During this step, the raw TIF from RAS Mapper was also reprojected into EPSG:3857 (Web Mercator) prior to being uploaded to S3.

5.5 AUTOMATED QUALITY CONTROL

The following quality control checks were performed against the files on S3.

5.5.1 INPUT CHECKS

1. ***.g01** file:
 - a. Boundary Condition (BC) line names match one of two patterns:
 - i. "BoundLine001", "BoundLine002", etc. (implies BC type normal depth), or
 - ii. "static1", "static2", etc. (implies BC type static tide WSE).
 - b. Storage Area name equals "FlowArea_0".
2. **Terrain/terrain.hdf** file:
 - a. Each burnline's bottom width is less than its top width.
 - b. Each burnline's Elevation Point Tolerance is 50.0 (a default).
 - c. Each burnline's Elevation Type is "SetIfLower" (a default).
 - d. Each burnline's left slope is -1.0 and right slope is 1.0 (45-degree angle on both sides).
 - e. When a burnline's bottom width was less than 5 feet or top width was greater than 100 feet, the model was flagged and an engineer re-reviewed it to confirm that the unusual value was appropriate.

5.5.2 OUTPUT CHECKS

1. **File chronology** – The various sets of files on S3 all have the expected chronology, meaning that for each plan:
 - a. All manually-edited files (*.g01 and terrain/terrain.hdf) are older than all RAS Linux inputs,
 - b. All RAS Linux inputs are older than all RAS Linux outputs, and

- c. All RAS Linux outputs are older than the depth grid TIF.
- 2. **Progress in *.log file** – The final “progress” statement is 1.0 (100%).
- 3. **Volume Error in *.log file** – The volume accounting error (as a percentage) was parsed from all simulations. Some models had surprisingly high-volume error. These were investigated, and it was found that high volume error in RAS 6.1 does not necessarily indicate that there is a problem with the model when a static WSE boundary condition is used. Details are given in a later section.

5.6 KNOWN LIMITATIONS

This section addresses known limitations that are generally associated with boundary conditions, stormwater conveyance, and fluvial processes.

5.6.1 BOUNDARY CONDITIONS

The non-tidal boundary condition was a preset uniform normal depth of 0.01 ft/ft. This may not represent the true slope at any given location along the boundary. However, as previously discussed, the sensitivity for the default boundary condition indicates the results are not significantly influenced by the assigned normal depth.

The tidal boundary was entered as a constant over time where tidal influence would ebb and flow during the run. At times, the actual tidal condition would be less conservative or more conservative than the selected boundary condition. However, a value must be selected, and it was proposed that the mean high water stillwater elevation was sufficiently conservative without being overly conservative.

5.6.2 STORMWATER CONVEYANCE

Stormwater conveyance features such as inlets, piping, and culverts were not incorporated into the models. The collection and implementation of stormwater data at this scale was not considered feasible. Drainage patterns reflect the natural overland flow process and may not accurately reflect drainage patterns based on functioning stormwater conveyance systems. Burnlines representing culvert locations were incorporated at intersections of major waterways and roadways to ensure conveyance downstream in the models. Additional burnlines were added where significant ponding was exhibited, and it was reasonable to assume through terrain data or aerial mapping that a culvert or other conveyance was present.

5.6.3 FLUVIAL PROCESSES

Several models contain velocities exceeding 25 fps and may occur at specific locations and time steps. Resulting high velocities may indicate inaccurate results at these locations. Additional detail was not added to the model and reduced time steps were not evaluated

to reduce or eliminate high velocities. However, these results occur largely within fluvial channelized areas, stream flow restrictions, or steep embankments. These areas are not considered to be impactful for developing large-scale pluvial models. Examples of areas with high velocities are provided in the following figures below (Figure 40, Figure 41, and Figure 42).

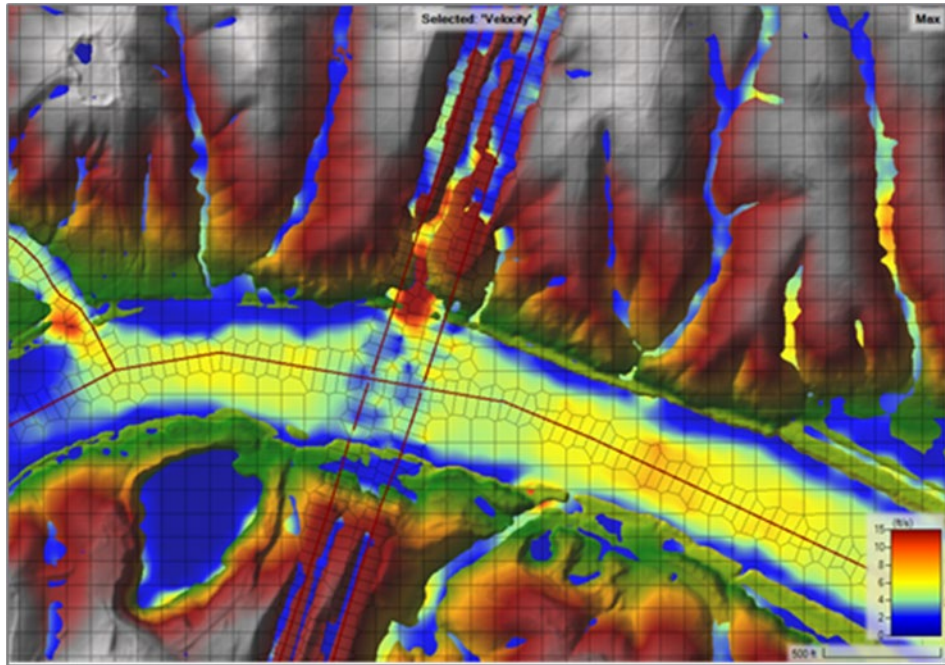


Figure 40. High velocities where there was steep flow from terrain into the channel (reference HUC 020801040102_4).

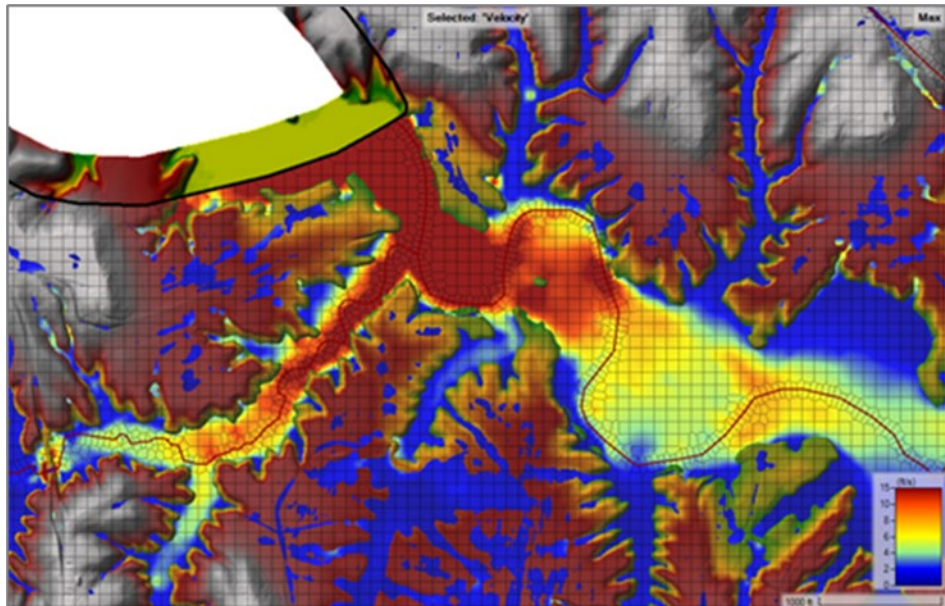


Figure 41. Higher velocities are being forced upstream by the tidal boundary (reference HUC 020700110601_1).

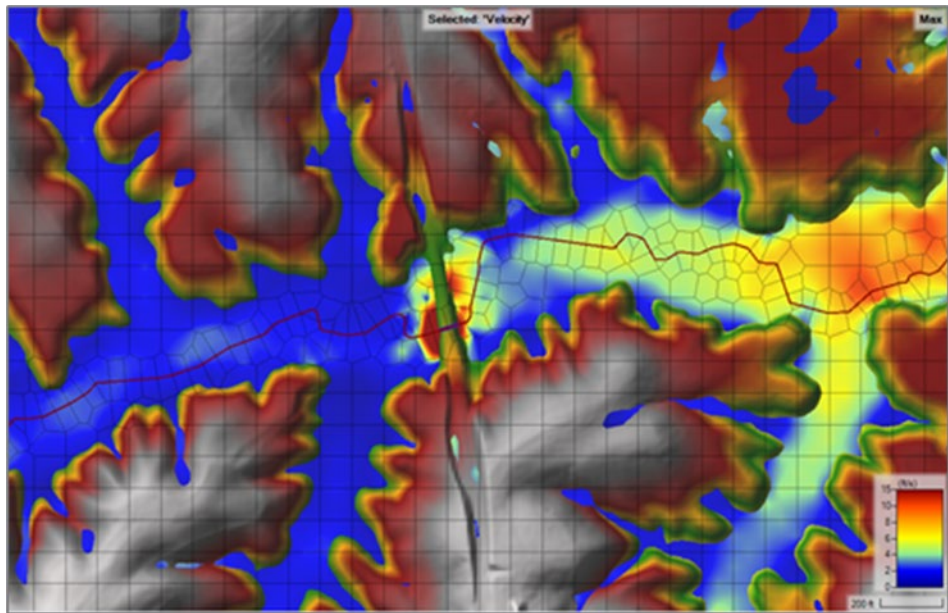


Figure 42. The constriction of flow through the burnline was causing higher velocities. This was within the fluvial channel (reference HUC 020700110601_1).

It is important that there was no routing of floodwaters between subbasins in this study. The study assumes that heavy rainfall occurs only in the modeled basin and has not received inflow from upstream basins, nor is the flow from a modeled basin sent downstream. As a result of this assumption, users may note discontinuities between water surface elevations at the boundaries between subbasins. In these cases, the stream in the upstream subbasin exhibits higher depths at the outlet compared to the inlet of the downstream subbasin. An example of this was demonstrated in Figure 43 below. This discontinuity was not considered to be relevant for the pluvial results.

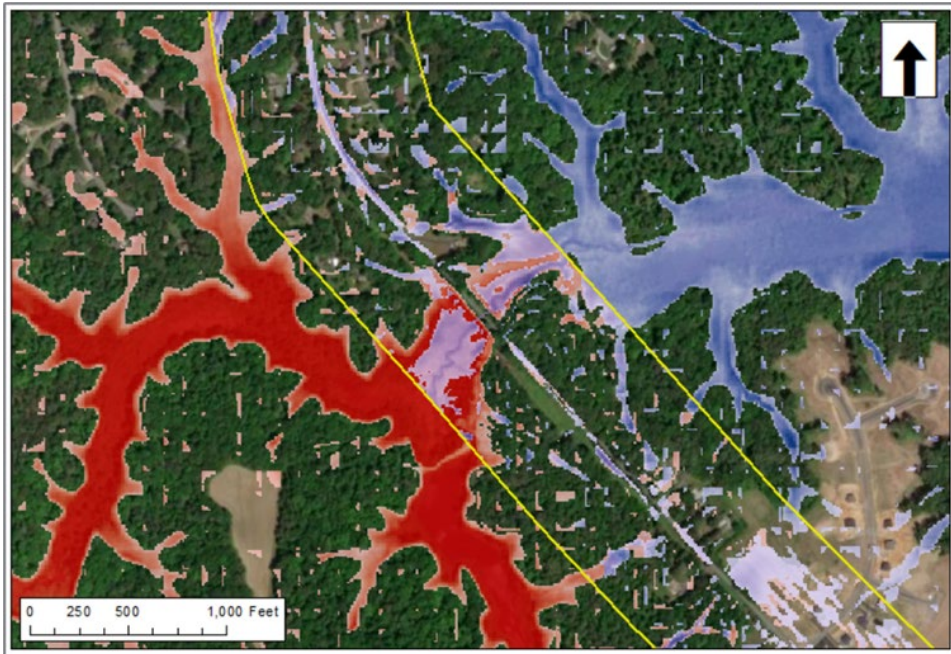


Figure 43. Fluvial results overlap in the boundary between upstream HUC 020700110601_4 and downstream HUC 020700110601_5 subbasin domains.

5.7 ANOMALY REVIEW

5.7.1 SUMMARY OF PRODUCTION NOTES

During production, engineers recorded anomalies that could not be rectified using standard modeling procedures. Such scenarios included low-lying tidal basins whose entire model domain was inundated for future tidal projections, urban areas that may show increased ponding due to the inability to account for underground stormwater conveyance infrastructure, basins with numerous small, privately owned dams, and terrain artifacts that were not consistent with available aerial imagery. Results for models that contain numerous dams and were completely inundated under future tidal projections were not affected by the anomalies noted as the simulations provide a reasonable estimation of pluvial and coastal flood inundation. Models with noted terrain artifacts not consistent with available imagery also provide reasonable estimates of flood inundation with best available data but can be improved as updated topographic data becomes available. Results for models in urban areas with high capacity of underground stormwater conveyance are valid but provide a more conservative estimate of pluvial flood inundation, accounting only for natural infiltration. See Appendix A for a table containing the models that were flagged for these issues.

5.7.2 HIGH VOLUME ACCOUNTING ERRORS

For models with a tidal (static WSE) downstream boundary condition, the reported volume error became very high when those static values happened to be lower than the RAS terrain. Engineers tested the behavior more thoroughly in RAS 6.1 by adding an artificial channel into the terrain near the tidal boundary condition such that the static WSE would be higher than some of the terrain. The testing showed that while artificially lowering the terrain in this way did resolve the volume accounting error as reported by RAS, it did not change the behavior of the boundary conditions (static or normal depth) and did not fundamentally change the resulting flood depth grids for the model, except in the immediate area of the terrain modification. Therefore, although volume accounting errors were logged globally for this project, attempts were not made to resolve them.

5.8 DATA DELIVERY AND DOCUMENTATION

Each simulation in this project is defined by four variables:

- A unique basin ID (and associated polygon),
- A tidal epoch (e.g. 2020),
- A storm duration (e.g. 2-hour), and
- A total precipitation depth (e.g., 1.0 inches).

For each simulation, a HEC-RAS model (zip file), a flood depth grid (TIF file), and a mosaic raster (VRT) was produced and uploaded to a publicly accessible [cloud storage service managed by DCR](#), referred to as the S3 bucket. Figure 44 and Figure 47 in this section show examples of the folder structure used for these products.

5.8.1 NOTES ON MOSAIC RASTER PRODUCTS

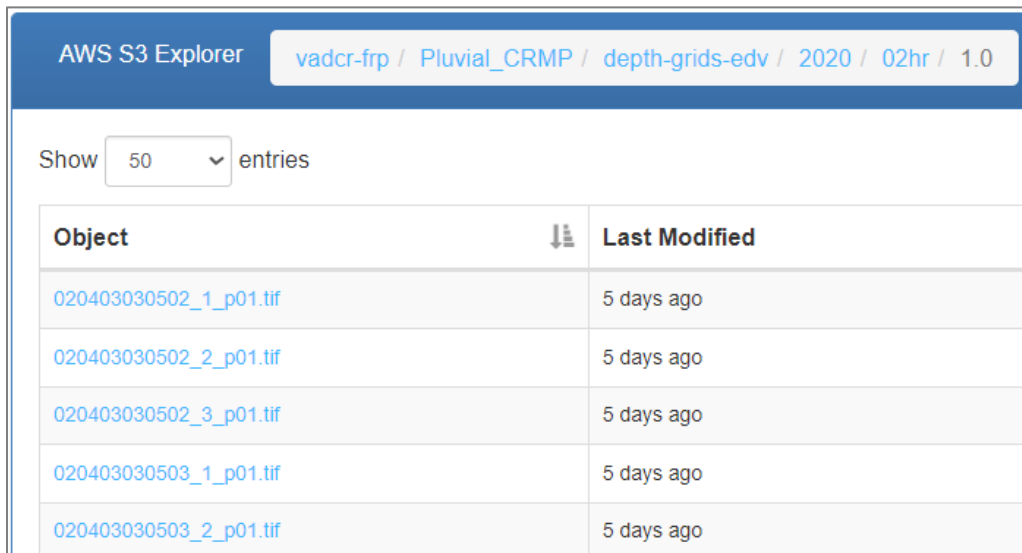
In addition to the individual model flood depth grid TIF files, raster mosaic products were produced. The mosaics were produced as VRT files, which are a type of “virtual” raster mosaic. It is a text file containing a spatially-indexed list of raster files (in this case TIFs). When GIS software reads a VRT, it loads only the data that affects the current view extent. In this case, since the TIFs are cloud-optimized, the VRTs also leverage “overviews” (sometimes called “pyramids”) and range-read techniques for an efficient and scalable experience.

In this project, a set of project-wide VRTs was produced using “absolute paths” to represent the underlying TIFs, and another set of VRTs was produced using “relative paths” to the same TIFs. These two paradigms support two different use cases. A typical user who wishes to stream data over the internet without downloading files to their drive would be advised to load the “absolute paths” version of the VRT. Another user who requires higher

performance would be advised to download the TIFs to their local drive and then load the “relative paths” VRT, which would cause their program to read from the local copy instead of streaming the data over the internet.

In this project, the basin polygons were designed to overlap one another at their edges to ensure full coverage and to allow for water to drain away from natural ridges in the topography. Therefore, for a particular simulation storm, areas of intended overlap may have more than one flood depth pixel value. By default, a VRT uses arbitrary ordering of its component rasters in areas of overlap. In this project, no effort was made to avoid this arbitrary ordering. Therefore, there is no guarantee that the VRT will display the “higher” depth value in areas of overlap. If a user of this data wants to ensure they are sampling the highest depth value in areas of overlap, they are encouraged to inspect the VRT index and to deliberately sample all component rasters that intersect the sampling point.

5.8.2 DELIVERED RASTERS



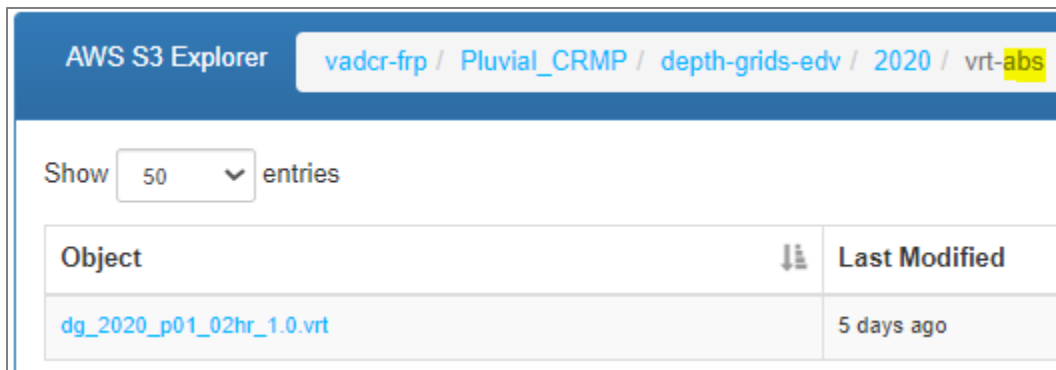
AWS S3 Explorer

vadcr-frp / Pluvial_CRMP / depth-grids-edv / 2020 / 02hr / 1.0

Show 50 entries

Object	Last Modified
020403030502_1_p01.tif	5 days ago
020403030502_2_p01.tif	5 days ago
020403030502_3_p01.tif	5 days ago
020403030503_1_p01.tif	5 days ago
020403030503_2_p01.tif	5 days ago

Figure 44. DCR bucket: Example of depth grids per-basin for RAS plan “p01” (1 inch of rain over 2 hours) at tide height associated with the 2020 CRMP epoch.



AWS S3 Explorer

vadcr-frp / Pluvial_CRMP / depth-grids-edv / 2020 / vrt-abs

Show 50 entries

Object	Last Modified
dg_2020_p01_02hr_1.0.vrt	5 days ago

Figure 45. DCR bucket: Example of global depth grid VRT for RAS plan “p01”, tide epoch 2020, with **absolute** paths stored for each TIF (for streaming).

AWS S3 Explorer		vadcr-frp / Pluvial_CRMP / depth-grids-edv / 2020 / vrt-rel		
Show		50 entries		
Object	Last Modified			
dg_2020_p01_02hr_1.0.vrt	5 days ago			

Figure 46. DCR bucket: Example of global depth grid VRT for RAS plan “p01”, tide epoch 2020, with **relative** paths stored for each TIF (for local download).

5.8.3 DELIVERED RAS MODELS

AWS S3 Explorer		vadcr-frp / Pluvial_CRMP / ras-models / 020403030504 / 020403030504_3		
		■ Hide folders?	▲ Folder	▼ Bucket
Show		50 entries	Search:	
Object	Last Modified	Timestamp	Size	
MHW2020/				
MHW2040/				
MHW2060/				
MHW2080/				
MHW2100/				
geometry.zip	19 days ago	2024-04-17 12:37:20	171 MB	
hyetographs.dss	8 days ago	2024-04-28 08:26:08	14 MB	

Figure 47. DCR bucket: Example of top-level RAS model files for one basin.

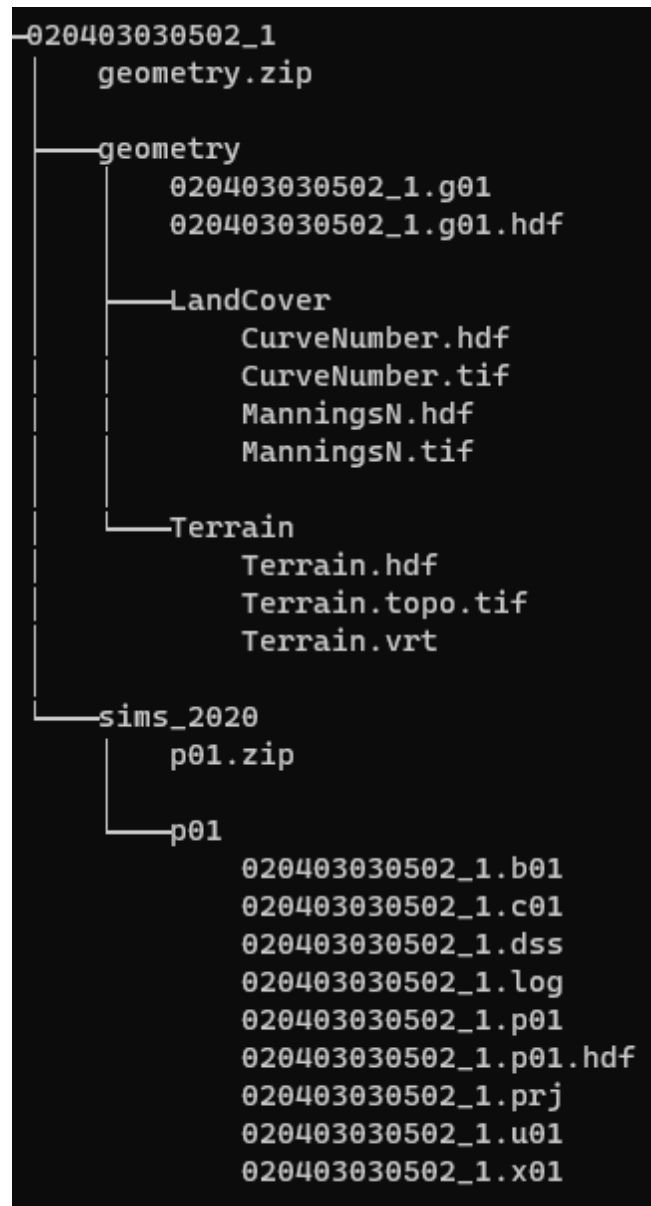


Figure 48. Example of the unzipped file tree for RAS model files for one basin, one plan, one epoch (one set of geometry data is shared among all plans and all epochs per basin).

5.8.4 METADATA AND DOCUMENTATION

5.8.4.1 *Metadata Catalog*

The SpatioTemporal Asset ([STAC](#)) specification was used to store metadata and provide access to input data (geometry), modeled data (HEC-RAS simulations), and output data (Depth Grids) for all models. A shapefile containing a record for each of the 1,830 subbasins modeled in this study was delivered with links for STAC Items and other information including tidal/non-tidal and HUC 12 reference included as attributes. A STAC Item was created for each suite of simulations (plans 1-63), with links to associated data listed under Assets.

For model simulations, a unique ID was created for each model using the pattern:

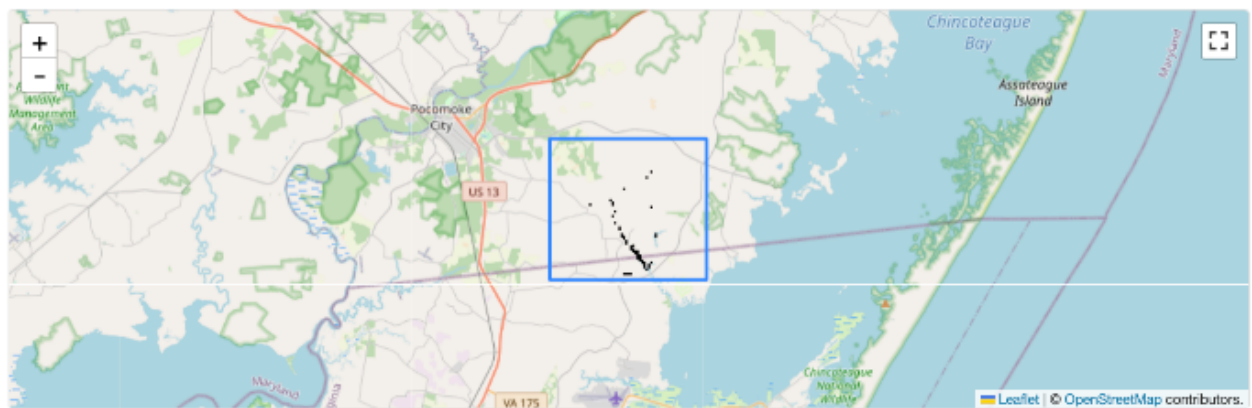
- Models including a tidal boundary:<HUC12_DomainID>-<MHW><epoch><sims>
 - Example: [020403030502_1-MHW2020-sims](#)
- Non-tidal models:<HUC12_DomainID>-<td>-<sims>
 - Example: [020700100503_3-NT-sims](#)

Assets for simulation items include the following:

1. Geometry (contents shown in Figure 49).
2. Precipitation (HEC-DSS containing precipitation time series for all simulations).
3. HEC-RAS Plans (for each simulation)

020403030502_1-MHW2020-dgs

[Browse](#)



Assets

> Simulation: 2 hour 1.0 inches (p01)	<input checked="" type="checkbox"/> SHOW	RAS-DEPTH-GRID	COG
> Simulation: 2 hour 1.5 inches (p02)		RAS-DEPTH-GRID	COG
> Simulation: 2 hour 2.0 inches (p03)		RAS-DEPTH-GRID	COG
> Simulation: 2 hour 2.5 inches (p04)		RAS-DEPTH-GRID	COG
> Simulation: 2 hour 3.0 inches (p05)		RAS-DEPTH-GRID	COG
> Simulation: 2 hour 3.5 inches (p06)		RAS-DEPTH-GRID	COG
> Simulation: 2 hour 4.0 inches (p07)		RAS-DEPTH-GRID	COG
> Simulation: 2 hour 4.5 inches (p08)		RAS-DEPTH-GRID	COG
> Simulation: 2 hour 5.0 inches (p09)		RAS-DEPTH-GRID	COG
> Simulation: 2 hour 5.5 inches (p10)		RAS-DEPTH-GRID	COG
> Simulation: 2 hour 6.0 inches (p11)		RAS-DEPTH-GRID	COG

Figure 49. Example STAC item on the left lists all depth grids output from HEC-RAS simulations in the MHW-2020 simulation.

020403030502_1-MHW2020-sims

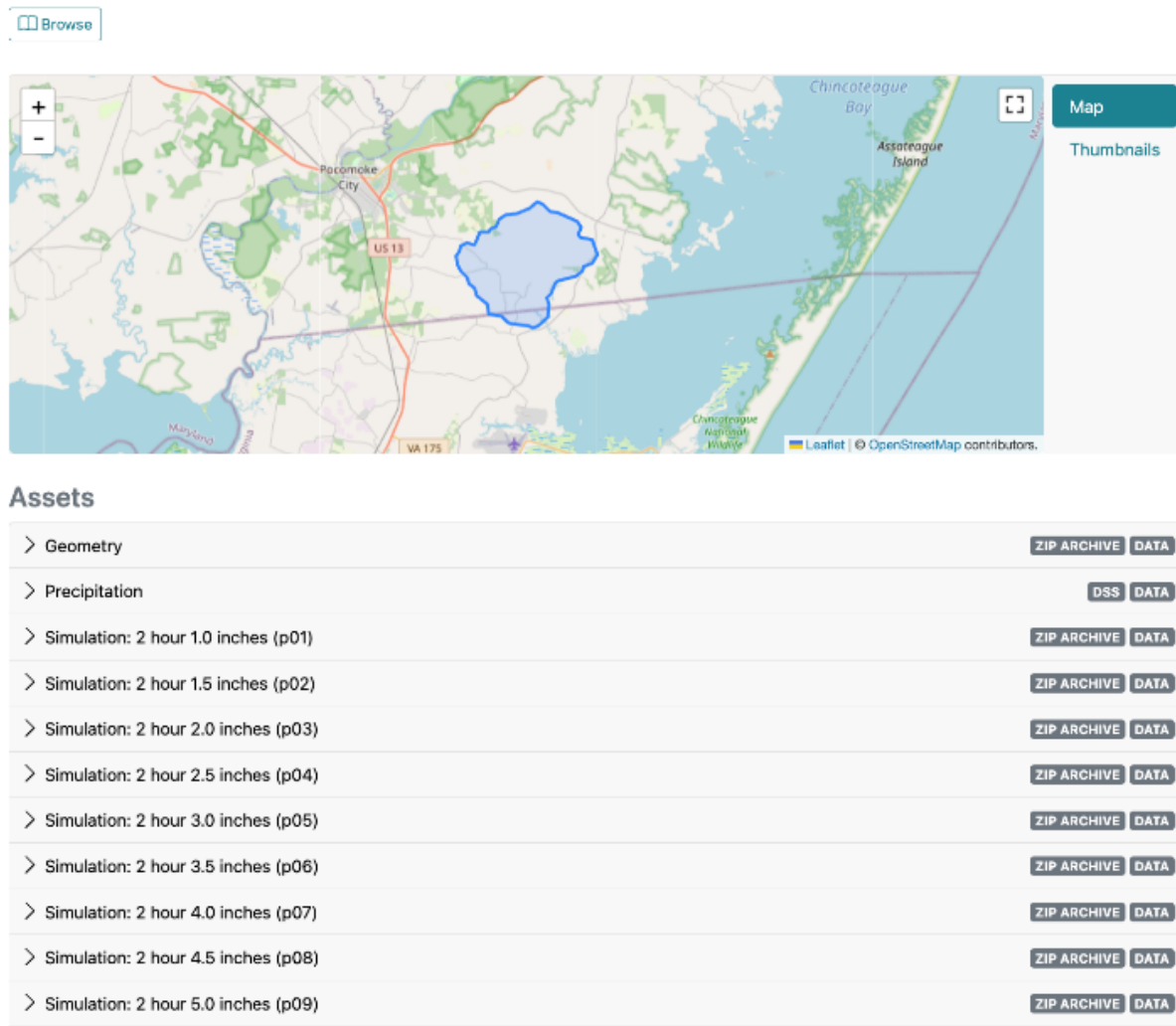


Figure 50. Example STAC item on the left lists HEC-RAS model data for all simulations in the MHW-2020 simulation. Links to the corresponding depth grids (not shown) are also included at the bottom of the item at the bottom.

For Depth simulations, a unique ID was created for each model using the pattern:

- Models including a tidal boundary:<HUC12_DomainID>-<MHW><epoch-dgs>
 - Example: [020403030502_1-MHW2020-dgs](#)
- Non-tidal models:<HUC12_DomainID>-<td>-<dgs>
 - Example: [020700100503_3-NT-dgs](#)

Assets for Depth Grid include the following datasets:

- Depth Grids (cloud optimized datasets for all simulations).

6 APPENDICES

6.1 APPENDIX A: ANOMALOUS ISSUES NOTED DURING PRODUCTION

Table 14. Summary of Anomalous Issues Noted During Production

Noted Model IDs	Issue
020403030504_5, 020801020303_4, 020801040704_3, 030102051303_8	Inundation of entire model domain under future tidal projections
020700100302_6, 020700100702_1, 020700100704_2, 020700100804_1, 020700100805_3, 020801040102_3, 020801040102_4, 020801040102_5, 020801040102_6, 020801040102_7, 020801040102_8, 020802050604_3, 020802071001_6, 020802071001_7	Ponding in urban areas due to inability to account for underground stormwater conveyance infrastructure
020700080403_5, 020700080701_2, 020700080701_4, 020700100701_1, 020700100701_2, 020700100701_4, 020700100702_1, 020700100704_2, 020700100801_3, 020700100804_1, 020700100805_3, 020700110602_2, 020801040102_3, 020801040102_4, 020801040102_5, 020801040102_6, 020801040102_7, 020801050104_1, 020801050104_2, 020801050105_2, 020801060701_1, 020801060802_4, 020802050503_2, 020802050503_3, 020802050503_4, 020802050503_5, 020802050504_1, 020802050504_2, 020802050505_4, 020802050601_1, 020802050601_2, 020802050601_3, 020802050601_4, 020802050602_1, 020802050603_3, 020802050604_3, 020802070405_2, 020802070801_1, 030102040702_3, 030102040703_5	Basins with numerous small, privately owned dams.

Noted Model IDs	Issue
020801020406_4, 020801020407_5, 020801040701_4, 030102040901_2, 030102040902_1, 020700080704_3, 020700100103_4, 020801040101_4, 030102050606_4, 030102051104_1, 020700100302_6	Terrain artifacts not consistent with available aerial imagery.

6.2 APPENDIX B: PRECIPITATION VOLUME

Table 15. Precipitation Volume Table

HEC-RAS Plan	Storm Duration (Hours)	Precipitation (Inches)
p01	2	1
p02	2	1.5
p03	2	2
p04	2	2.5
p05	2	3
p06	2	3.5
p07	2	4
p08	2	4.5
p09	2	5
p10	2	5.5
p11	2	6
p12	2	6.5
p13	2	7
p14	2	7.5
p15	2	8
p16	2	8.5
p17	2	9
p18	2	9.5
p19	2	10
p20	2	10.5
p21	2	11
p22	2	11.5
p23	2	12
p24	6	1
p25	6	2
p26	6	3
p27	6	4
p28	6	5
p29	6	6
p30	6	7
p31	6	8
p32	6	9
p33	6	10
p34	6	11
p35	6	12

HEC-RAS Plan	Storm Duration (Hours)	Precipitation (Inches)
p36	6	13
p37	6	14
p38	6	15
p39	6	16
p40	6	17
p41	24	2
p42	24	3
p43	24	4
p44	24	5
p45	24	6
p46	24	7
p47	24	8
p48	24	9
p49	24	10
p50	24	11
p51	24	12
p52	24	13
p53	24	14
p54	24	15
p55	24	16
p56	24	17
p57	24	18
p58	24	19
p59	24	20
p60	24	21
p61	24	22
p62	24	23
p63	24	24

6.3 APPENDIX C: QUALITY PLAN

Please see Quality Plan attached.